2014

Restraint Moments Due to Thermal Gradients in Continuous Prestressed Concrete Girder Bridges

Sushovan Ghimire
Louisiana State University and Agricultural and Mechanical College, sghimi2@tigers.lsu.edu

RESTRAINT MOMENTS DUE TO THERMAL GRADIENTS IN CONTINUOUS PRESTRESSED CONCRETE GIRDER BRIDGES

A Thesis

Submitted to the Graduate Faculty of the
Louisiana State University and
Agricultural and Mechanical College
in partial fulfillment of the
requirements for the degree of
Master of Science

in

The Department of Civil and Environmental Engineering

by
Sushovan Ghimire
B.S., Purbanchal University, 2009
August 2014

This work is sincerely dedicated to my parents.

`

ACKNOWLEDGEMENTS

First and foremost, I would like to thank Dr. Ayman Okeil, the chair of my research committee for making the completion of this research possible. Dr. Okeil has helped me a great deal throughout this research and has taught me lots of materials which were new to me through his understanding and steady patience. No words are enough to thank Dr. Okeil for what he has done for me.

I am very thankful to members of my advisory committee, Dr. Aly Moussad Aly and Dr. Michele Barbato, for taking time from their busy schedule and serving on my Advisory Committee. I would like to thank them for their support and guidance.

I am also very grateful for the chances and opportunities provided to me by LSU Department of Civil and Environmental Engineering. I came to LSU in pursuit of master's degree, but I am leaving with much more than just a diploma because of hard work of faculty and administrative staff. I would also like to thank Dr. Steve Cai and Dr. Suresh Moorthy for guiding and supporting me throughout this program.

I also like to thank my friends Shristi Shrestha, Amar Cumurovic, Tuna Ulger, Yogendra Prasad Subedi, Hem Raj Pant, Raju Thapa and Gyan Basyal for their support and friendship. I am truly grateful to my family for helping and supporting me to succeed in my life. I want to thank my parents for encouraging me. I wouldn't be what I am today without them.

Lastly, I want to thank everyone for being a part of my life.

TABLE OF CONTENTS

LIST OF TABLES

LIST OF FIGURES

ABSTRACT

This research is motivated by the need to develop new bridges, using new materials and construction details to achieve the goal of building longer span bridges that are safe and durable. The study of precast/prestressed concrete bridges made continuous started early in the 1960's. Continuous bridges have many advantages compared to simple span bridges such as reduction in structural depth, riding comfort and reserve load capacity under overload conditions. They also eliminate joints that require a lot of maintenance and cause deterioration in some cases. The design and construction of continuous bridges requires the consideration of many factors that are not considered in the design of simply supported bridges. For example positive restraining moment that can cause cracking near the bottom of the girders/continuity diaphragm at the supports develops in continuous bridges are caused by time dependent factors such as creep, shrinkage and thermal gradient. This research presents an analytical approach for calculating restraint moments in Prestressed Concrete continuous bridge girders. The RESTRAINT program, which is capable of predicting restraint moments due to creep and shrinkage, was modified to add a feature for calculating the restraining moment due to thermal gradient. A detailed parametric study was carried out using the modified version of mRESTRAINT to investigate the effect of various parameters on restraint moments in continuous girders. The results from the parametric study were then used to establish optimum girder age at time of establishing continuity such that an allowable restraining moment is not exceeded.

A reliability study was also conducted on two span continuous bridge with equal span lengths to estimate the probability of cracking at girder's ends due to positive restraint moments obtained from study. The reliability showed that prestressed girders have a high (68% - 93%) probability

of cracking if made continuous as a result of the combined effect of thermal gradient, creep and shrinkage.

1 INTRODUCTION

1.1 Background

Population growth in the United States and around the world puts a huge amount of pressure on the transportation infrastructure like roads and bridges. Therefore, it is very crucial to conduct a comprehensive research in these areas that leads to building safer, more economic and more durable structures. Bridge structures are built to serve the society for an extended period of time.

Developing new structural systems, employing modern construction materials and improving construction details are continuous efforts that bridge engineers adopt to design better bridges and it has been a continuous challenge for them. The study of continuous precast/prestressed concrete bridges started early in 1960. Continuous bridges have many advantages compared to the simple span ones like reduction in structural depth, riding comfort and reserve load capacity under overload conditions. Continuous structures can also help to improve the durability of the structure and improve the riding surface for the vehicles as the continuity will decrease impact damage due to tires hitting the joint.

These precast prestresssed bridge girders are built by placing them at the top of the abutments and then the deck is cast on site to form a composite structure. Continuity is introduced by constructing a diaphragm at the supports by pouring concrete between the girder ends. After the concrete hardens, the girders are structurally connected hence, the entire structure is continuous.

There are many factors that need to be considered in the design and construction of continuous bridges compared to simply supported bridges, one of which is the development of a positive restraining moment. Positive restraining moment causes cracking near the bottom of the girders/continuity diaphragm at the supports. Restraint moments in continuous bridges are

caused by time dependent factors such as creep, shrinkage and thermal gradient. This research is primarily focused on the restraint moments due to the thermal gradient.

Creep is defined as the physical property of material and is a time dependent deformation which results from the continuous sustained stress within the accepted elastic range. Shrinkage is also a physical property of material and is also a time dependent deformation but occurs in the absence of an applied load. Usually, evaporation of water from concrete makes shrinkage occur in the structure. Thermal stress can be defined as the mechanical stress induced in a body when some or all parts are not free to expand or contract in response to change in temperature. In most continuous bodies, expansion and contraction cannot occur freely because of the geometric constraints and thus thermal stresses are produced.

Creep, shrinkage and thermal gradients are those factors that cause an additional deflection in a continuous structure. These additional deflections are restrained by the continuity diaphragms resulting in the addition of the restrained moments and these restrained moments should be accounted while designing the bridges.

1.2 Research Objectives

In the past years, the effect of thermal gradient on the precast prestressed continuous bridge girders have been overlooked, but as recent studies have shown, it has been found that change in temperature results in inducement of thermal stress on the bridges that can be critical (Elbadry and Ghali 1986). Therefore, research on the effect of thermal gradient in the bridge girders was necessary, which motivated this research.

The primary objective of this research is to study the development of restraint moment due to thermal gradient in precast prestressed continuous girder bridges. For this research, the study was done using the modified version of RESTRAINT which is an analysis software developed as part

of NCHRP project 12-53 (Miller et al. 2004). Therefore, the study relies on the results obtained from the software. There were some limitations on the original RESTRAINT program and the modification was mandatory to obtain the result for this research. Some of the limitations of the restraint program are listed below.

1. Exclusion of Haunch in restraint moment calculations.
2. Exclusion of thermal gradient in calculation of the restraint moments.

After the required modifications were implemented, the program was ready for the research and for the general use as well. Now, using the modified RESTRAINT program, user can calculate the restraint moments due to creep, shrinkage and thermal gradient combined for bridges up to 5 spans with different strand data with and without the diaphragms.

1.3 Scope of Study

This research is primarily focused on precast prestressed girders which are composite in nature with a cast-in-place concrete deck and are made continuous using the diaphragms. The construction of these girders plays an important role in the development of new infrastructure.

This research also focuses on the calculation of restraint moments developed by the thermal gradients. Restraint moment developed due to positive thermal gradient and negative thermal gradient are presented in this study and the contribution of the thermal gradient on the development of the total restraint moment is also presented. The study focuses on the straight slab-on-girder bridges. This study does not consider the effects of horizontal curves or skews and also the effects of bearing movements will not be covered.

1.4 Thesis Outline

This thesis contains seven chapters. Chapter 1 presents an introduction and background information about the continuous prestressed concrete bridge girders. The time dependent effects like creep, shrinkage and thermal gradient which lead to development of restraint moments is also introduced in this chapter. The scope of the project, objectives and the thesis outline are given in this chapter.

Chapter 2 presents the literature review for relevant works that are done on the creep, shrinkage, restraint moment and thermal gradients. Some introduction and the history of development of the continuous prestressed concrete girder bridge system are also presented in this chapter. Time dependent effects that cause the development of the restraint moment are also discussed in this chapter. The literature on basic creep and shrinkage, development of restraint moment and the behavior of the continuous bridge when the restraint moment is developed are also presented. Finally, the literature on the works done on thermal gradient and its calculations are presented.

Chapter 3 presents the detailed discussion about the methodology used for this study. This chapter contains discussion about the methods that are used to calculate the restraint moments. This chapter also contains the discussion about the NCHRP project 12-53.

Chapter 4 contains a detailed discussion about the program named RESETRAINT, its limitations and the modifications that were done to RESTRAINT for this study to overcome its limitations. It also presents the previous modifications that were done by Dr. Ayman Okeil and his student and the modifications which were done for this study.

Chapter 5 presents the results that were obtained from a parametric study that included the effects of span-length ratios, diaphragm stiffness ratio and the age of continuity on the

development of the restraint moment is presented in this chapter. The optimum age of the girder for the allowable restraint moment is also presented in this chapter. Finally, the contribution of the thermal gradient and the creep and shrinkage individually on the total restraint moment is also discussed in this chapter.

Chapter 6 presents a reliability study done on two span bridges; one with AASHTO Type IV girder and the other with AASHTO BT-72 girder. The study was carried out using Monte-Carlo simulation and the probability of cracking was calculated based on the cracking moment of the girder and positive restraint moment developed due to creep, shrinkage and thermal gradient.

Finally, the conclusions drawn from this research are presented in Chapter 7 and recommendations for the future work and research are also summarized in this chapter.

2 LITERATURE REVIEW

2.1 Introduction

After the development of continuous prestressed concrete girder bridge system, its usage has seen a rapid increase and is now accepted worldwide in the construction industry. A continuous bridge can be defined as the type of the bridge in which two or more spans are connected end-to-end to form an integral superstructure. For prestressed concrete bridges, continuity is established with the help of a continuity diaphragm. It was around 1960 when some of the earliest continuous bridges were constructed including the Big Sandy River Bridge in Tennessee and the Los Penasquitos Bridge in California (Freyermuth 1969). These bridges were studied for a period of time, which revealed that their performance was more than satisfactory. As a result, many states began to research and design long span continuous bridges and because of their numerous advantages over the simple span bridges continuous prestressed concrete girder bridge system. According to National Bridge Inventory (NBI), there are 169,205 concrete bridges in United States and out of the total there are 77,550 concrete continuous bridges (NBI 2014). Therefore, 45.83% of the total concrete bridges are continuous bridges (NBI 2014)

2.1.1 History

In the late 1940s, after the end of World War II, post-war reconstruction started which was followed by rapid economic growth. In Europe, post-war reconstruction produced a rapid growth in bridge construction. The early years after the World War II were the most important years for the development of prestressed concrete because new design and construction techniques were developed, improved and tested. One of the most important research goals throughout the world at that time was the design and analysis of prestressed concrete. Although many researchers were

investigating various aspects of prestressed concrete, it took a long time to have a good understanding of behavior of the prestressed concrete. It was the book called *Spannbeton fur die Praxis* which was first published in 1954 and was later translated into English as *Prestrssed Concrete- Design and Construction* by Fritz Leonhardt which is considered as the first contribution to the field of prestressed concrete.

During the early days, the method of making a continuous bridge was to place the girders ends close to each other and post-tension them together (Menn 1986). Though the idea to make the bridge continuous was plain and simple, it was not considered efficient because the anchorages were relatively expensive. Furthermore, friction losses due to the severe curves necessary to make the post tensioning effective (Mattock et al. 1960) had to be accounted for. Therefore, a new technique that avoids the post-tensioning limitations was developed to make the bridge continuous. Instead of post-tensioning the strands, a small space between adjacent girder ends was allowed. Concrete would fill that space later at the time when the deck is poured. The small space between the girders where the concrete is poured to make the bridge continuous became known as continuity diaphragm.

The continuity diaphragm must be effective for transferring forces between girder ends. These forces can be due to negative as well as positive bending moments. Positive moment occurs because of the time dependent effects in the prestressed concrete like creep, shrinkage and thermal effects. In 2005, NCHRP sponsored Project 12-53 (Miller et al. 2004) to study the connection between simple-span precast concrete girders made continuous. From the study it was concluded that the cracking which occurs on the diaphragm due to the positive bending does not affect the continuity of the system. Even when the positive moment connection was cracked, the system maintained 70% continuity (Dimmerling et al. 2005). Like positive moments,

negative moments also occur in the continuity diaphragm due to loss in prestress, dead load and live loads. Reinforcement for the negative moment is placed in the deck while the reinforcement for the positive moment is placed in continuity diaphragms. There are two methods for providing positive moment reinforcement. The first utilizes prestressing strands by extending them from the girder's ends into the diaphragm at 90^{o} angle, while uses special reinforcing steel which embedded into the girder's end and extended into the diaphragm (Dimmerling et al. 2005).

2.2 Time-dependent Effects on Prestressed Concrete

It is a fact that the prestressing force applied initially to the concrete structure undergoes a process which involves its reduction in force over a period of approximately five years (Nawy 2009). Therefore, it is important for designers to accurately estimate the level of the prestressing force at each loading stage. The reduction of the prestressing force can be divided into two categories. The first one is the prestress loss due to the elastic loss during the construction process of the fabrication process. It also included the elastic shortening losses on the concrete like anchorage losses and frictional losses. The second one is the prestress loss due to the time-dependent losses such as creep, shrinkage and due to the temperature effects (Nawy 2009). The reduction of the prestressing force is essentially because of the time-dependent losses such as creep, shrinkage and those due to temperature effects. Creep, shrinkage in concrete member and the relaxation of prestressing strands, elastic shortening and immediate elastic loss are the main causes for the time-dependent changes in a prestressed concrete. Due to these time-dependent effects, stress levels in the prestressing reinforcement vary throughout the member which has a large impact on the structure and should be considered while designing the structure (Menn 1986).

In most of the cases, to determine prestress losses and the deflection of the member, time-dependent losses must be predicted accurately. It is not feasible for an exact determination of the magnitude of these losses because they fully depend upon a multiplicity of interrelated factors. There are many approaches for calculating these losses such as the code of practice provided by Prestressed Concrete Institute (PCI), the ACI-ASCE joint committee 423 approach and the AASHTO lump-sum approach (Nawy 2009). All the above mentioned approaches differ in various ways. In most of the calculation methods, elastic analysis is done to determine to forces acting and a lump-sum method is used to calculate the time-dependent effects at various stages. For pre-tensioned structures it is recommended that losses should be assumed in between of 15 and 20% and for the post-tension structures the losses should be assumed in between 10 and 15% of total prestressing force (ACI 209R-92).

Calculation of time-dependent effects in a real structure requires a more in depth analysis for continuous and composite structures. This analysis should account for various construction stages.

Due to these time-dependent effects, restraint moments occur in the girder and the continuity diaphragm which are difficult to compute because the continuous structure is statically indeterminate. Two types of restraint moments can develop in continuous structures; namely, negative restraint moment and positive restraint moment. Differential shrinkage between the deck and the girder concretes causes a negative moment and positive moment are caused by the creep in the girders and thermal gradients.

Since restraint moments develop due to time-dependent effects like creep and shrinkage and due to temperature changes, it is very important to account for these types of effects.

2.3 Creep

Creep is defined as the deformation of any concrete material under constant loading or controlled stress within the accepted elastic range (Nawy 2009). Applied loads cause an initial elastic strain while additional strains due to the same sustained load cause creep strains. At first creep causes strain to increase at a high rate but after a certain amount of time it will increase in at a slower rate (Nilson 1987). Deformations due to creep are the main cause for excessive deflection at the service load of a concrete member (Nilson 1987). One thing that should be noted while calculating the creep effects is that it cannot be calculated directly and it should be calculated only by deducting shrinkage and elastic strain from the total deformation (Nawy 2009). Concrete creep depends on different parameters like temperature, mix proportions, stress level, moisture level on the concrete material and temperature variation (MacGregor et al. 2005). Figure 2.1 shows the increase in creep strain with respect to time.

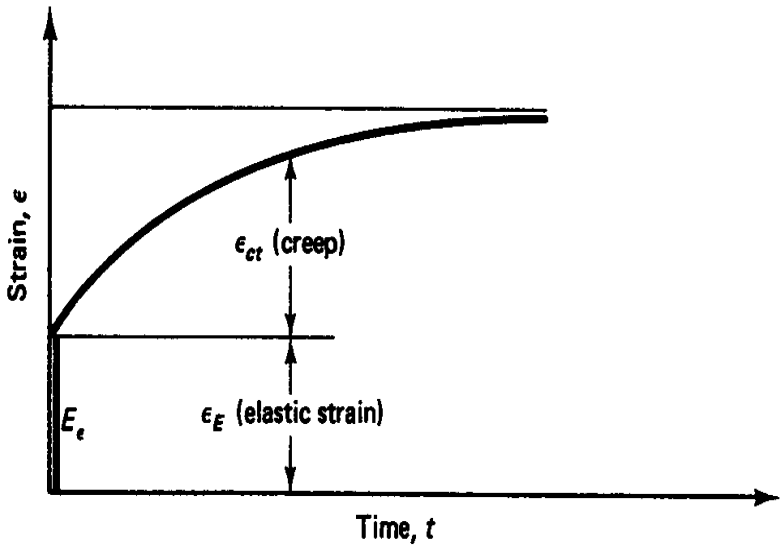

Figure 2.1 Strain-time curve (Nawy 2009)

There are two main types of creep. Creep strain consists of basic creep and drying creep. Basic creep can be defined as the change in strain due to a constant and sustained load when the loss due to the moisture is prevented therefore basic creep is independent of the member size (ACI 209R-05). Basic creep always occurs under the conditions where there is no moisture on the concrete materials. It has not been proven that the basic creep will approach asymptote although it always increases quickly at first and then slows over the time (Bazant 1975). On the other hand, drying creep can be defined as the additional creep caused by the drying; i.e., it is the type of the creep which occurs when the movement of the moisture is allowed. Drying creep is dependent on the size of the member.

One of the main adverse effects of creep is that it increases the deflections of slabs and beams and are known for causing loss of prestressing force (Nawy 2009). On a reinforced concrete, the initial eccentricity will increase with time due to creep and as a consequence the compressive load will transfer from the concrete to the steel and once the steel yields, concrete has to carry the additional load which may lead to the failure of the concrete.

Creep coefficient, Φ(t,to) is the most used common way to express creep in a mathematical form. It is basically a ratio of the creep strain at any time, *t,* for the stress applied at t_0 (initial time), to the elastic strain at the initial time (t_0). The equation for the creep coefficient can be written as:

$$\Phi(t,to)=\frac{\epsilon_{cp}(t,t_0)}{\epsilon_0}=\frac{\epsilon(t,t_0)-\epsilon_0}{\epsilon_0} \quad (2.1)$$

2.4 Shrinkage

Over time, a certain decrease in the volume of the concrete takes place which is defined as shrinkage. It is a material's property that causes concrete to change its volume regardless of the

existence of sustained load. Shrinkage occurs as a result of water evaporating from the concrete and hydration with time. Like creep, the rate at which shrinkage takes place is initially high which slows down as it approaches an asymptote after some time (Nilson 1987). The reason shrinkage is easy to compute unlike creep is that it is independent of the sustained loading by the concrete member.

There are two types of shrinkage in a concrete material; namely plastic shrinkage and drying shrinkage (Nawy 2009). Plastic shrinkage occurs after placing the fresh concrete in the forms and it usually occurs during the first few hours. Because of the larger contact surface of the floor slabs, they are more exposed to the dry air and in such case moisture evaporates quickly from the concrete surface thus causing shrinkage. On the other hand, drying shrinkage occurs after the concrete has hardened and attained its final set. Drying shrinkage usually occurs when moisture is allowed to enter and leave the member. It usually occurs because of the slow movement of water towards the surface of the concrete which is lost due to evaporation making other particles more compact (MacGregor et al. 2005). Drying shrinkage can also be defined as the decrease in the volume of concrete when it loses the moisture by evaporation. Figure 2.2 shows the nature of the shrinkage strain over time from initial t_0 to the final time t. Figure 2.2 illustrates that the increase in strain $\in_{sh}$ with respect to the time. Since the concretes which are old in age are more resistant to stress and undergo less shrinkage, the rate will decrease with respect to time.

There are several factors in the concrete material that affect the magnitude of the drying shrinkage. These are aggregate type, size of the concrete element, medium ambient conditions, amount of reinforcement, water/cement ratio, admixtures, type of cement and carbonation (Nawy 2009). The most important factor among the factors mentioned above is the aggregates because it restrains shrinkage (ACI 209R-05). If the water to cement ratio in concrete is increased, then

more shrinkage will occur because the increase in water content will reduce the volume of aggregates (ACI 209R-05). Shrinkage in concrete will also increase if the ratio of the volume of the cement to the volume of the concrete is significantly high (MacGregor et al. 2005). The type of the cement used in the concrete material will also have an impact on shrinkage, more shrinkage are generally shown by the cement which have low quantities of sulfate (ACI 209R-05).

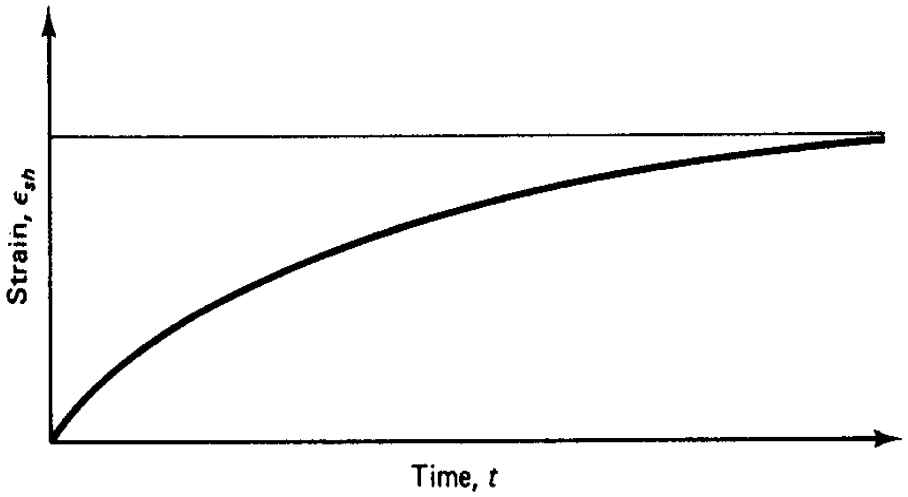

Figure 2.2 Shrinkage-time curve (Nawy 2009)

Shrinkage is also influenced by the shape and size of the concrete member. If all the other factors are identical, a long member would shrink more and quicker than a short one. This is due to the fact that when the moisture has to travel through more material to reach the environment (air), the shrinkage will at occur at slower rate (ACI 209R-05).

The surrounding atmosphere or environment also affects the shrinkage of the concrete material. The curing process of the concrete and the drying period will have an effect on the material. The humidity of the environment also affects concrete shrinkage; lower the humidity leads to higher then the shrinkage.

2.5 Review on creep and shrinkage

Bellevue and Towell (2000) conducted a study on a bridge to understand creep and shrinkage effects on the final stresses in a structure. A parametric study was conducted on a segmental bridge with the creep and shrinkage effects which was then repeated without the creep and shrinkage effects. The results from the both methods were then compared. To get the results, structural analyses was carried out using TANGO, commercially available software. From the results, it was analyzed that the creep and shrinkage effects are substantial.

Benboudjema et al. (2001) proposed a creep model for the concrete structures that was subjected to the multi-axial compressive stresses. The model was considered as the result of two process which are driven by the spherical and deviatoric components. The model was validated using experimental results from Gopalakrishnan (Gopalakrishnan et al. 1969). The model does not underestimate the creep strains in both uniaxial and biaxial tests (Benboudjema et al. 2001). Figure 2.3 shows the results analyzed by Gopalakrishnan et al. (1969), which depicts the creep poisson's ratio with respect to time.

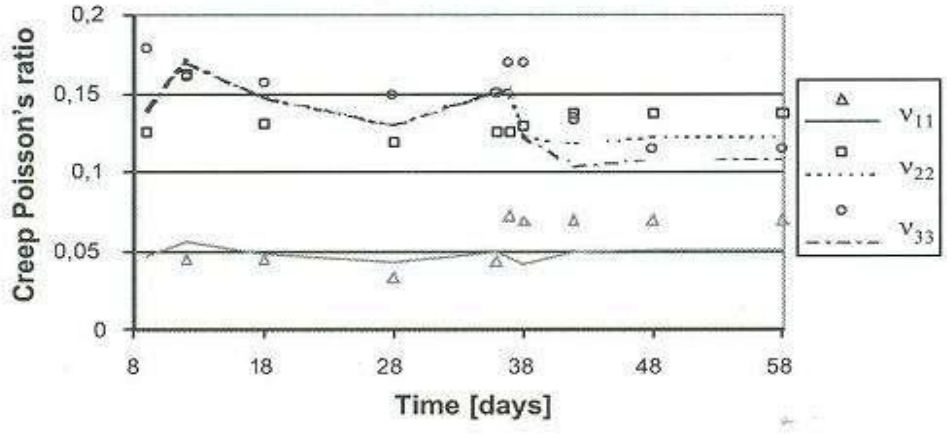

Figure 2.3 Evolution of the basic creep Poisson's ratio (Gopalakrishnan et al. 1969)

Fanourakis and Ballim (2006) conducted an experiment to review the suitability of nine design models for predicting creep in concrete. The concrete used in the experiments incorporated three types of aggregate and for each aggregate types there were two strength grades. The total creep strain was determined by subtracting the results from the shrinkage measurement from the total time dependent strain. Based on the results, it was found that there was no correlation between the specific total creep and the elastic moduli.

The coefficient of variation of errors was used to identify the most suitable model that provides accurate predictions over all the concretes, the. The study concluded that CEB-FIP model (1970) and BS 8110 (1985) methods with a coefficients of variations of 18% and 24%, respectively, provide the most suitable accurate predictions over all the concretes. CEP-FIP (1978) was the least accurate method with a coefficient of variation of 96%.

Ozbolt and Reinhardt (2001) conducted an experiment to study the effect of creep-cracking interaction using the microplane model for concrete which is couple in series with the Maxwell Chain model. The microplane model is a 3-d macroscopic constitutive law based on the relaxed kinematic constraint concept. Results from numerical analysis showed that the model is able to forecast the effects of non-linear creep, i.e. decrease of concrete strength for sustained load and the increase of creep deformations at higher stress levels (Ozbolt and Reinhardt 2001).

2.6 Thermal Effects

Thermal effect on bridge construction materials lead to the development of positive restraint moments in continuous bridges. If the bridge is allowed to deform freely due to thermal effects, translational movements will occur as a result of uniform temperature changes in the structure throughout the cross section. If the bridge is restrained, thermal stresses are introduced in the structure. These thermal stresses may lead to adverse effects in concrete bridges. Thermal

cracking of the deck and deformation of the bridge itself are some of the adverse effects induced by thermal stresses.

Throughout the cross-section of the bridge temperature variations can exist, which may lead to rotational distortions of the bridge girders if they are unrestrained. If the bridges are continuous then the temperature variation lead to bending moments. It is very important to analyze the effect of the temperature gradient on the precast/prestressed continuous girder bridges since it leads to the development of the positive restraint moment.

2.6.1 Background

Thermal stress can be defined as the mechanical stress induced in a body when some or all parts are not free to expand or contract in response to change in temperature. Continuous bridges are restricted from expanding and contracting freely because of the geometric constraints. Hence, thermal stresses develop in continuous bridges.

Heat can be transferred in any material by convection, radiation and conduction. Since the contributions of the heat transfer from the convection and conduction are so small, a single coefficient can be used to account for these effects (Imbsen et al. 1985). Significant amount of thermal changes is caused by heat transfers by radiation due to sunlight falling on exposed parts of the structure.

Before 1980, effects of thermal gradients in structures were not fully understood. There were different opinions about how thermal stresses should be calculated. There were not many reported cases where change in temperature caused significant damage to continuous bridges (Imbsen et al. 1985). The main reason of the occurrence of the temperature gradient is because of the temperature difference between the top and bottom member of the concrete member while the middle portion is being insulated from the effects because of the relatively non-conductive

nature of concrete. A negative thermal gradient occurs when the deck is cooler than the girder. Conversely, when the deck is warmer than the girder, a positive thermal gradient occurs.

Generally, temperature changes cause two types of thermal stresses; a primary thermal stress and a secondary thermal stress. Primary thermal stress is the stress that develops due to the nonlinear distribution of temperature across the height of structure. This stress is calculated by removing the redundancies on the structure; thus allowing it to deform freely and eliminating the development of secondary straining actions. Secondary thermal stresses develop in statically indeterminate structures as a result of the compatibility to maintain the boundary conditions. The total thermal stress acting on the concrete member is the combined effect of both primary and secondary thermal stresses.

For this study, to calculate the primary thermal stress, secondary thermal stress and restrained moment due to thermal gradient, an analytical approach presented by M.J.N. Priestley at the RILEM LTO-45 Technical Committee Meeting in 1984 is used. The equation presented by Priestley (1978) is used and coded in the modified version of mRESTRAINT program. These equations are used to calculate final curvature, strain, primary thermal stress, secondary thermal stress and restrained moment due to thermal gradient. The temperature gradient used for this study is the one proposed by AASHTO in AASHTO LRFD bridge design specifications 2007. A detailed discussion of analytical approach proposed by Priestly (1978) and the AASHTO temperature gradient is presented in Chapter 3 (Methodology).

2.6.2 Studies on prediction of thermal stresses

The prediction of thermal stresses in structures constructed from high-strength concrete is a very important aspect in structural design. Thermal stress can degrade the structures serviceability, water tightness, and durability. Previously, several case study have been

conducted for the calculation of the thermal stresses and to assess the problems associated with it. This section summarizes a few of these studies.

Priestley (1978) presented an analytical method for predicting thermal stresses in concrete bridges. A 5th-order polynomial was assumed to represent the temperature distribution across the section's height as can be seen in Figure 2.4. Priestley's analysis was done on concrete box girder; however the method could be adapted for any geometric shape

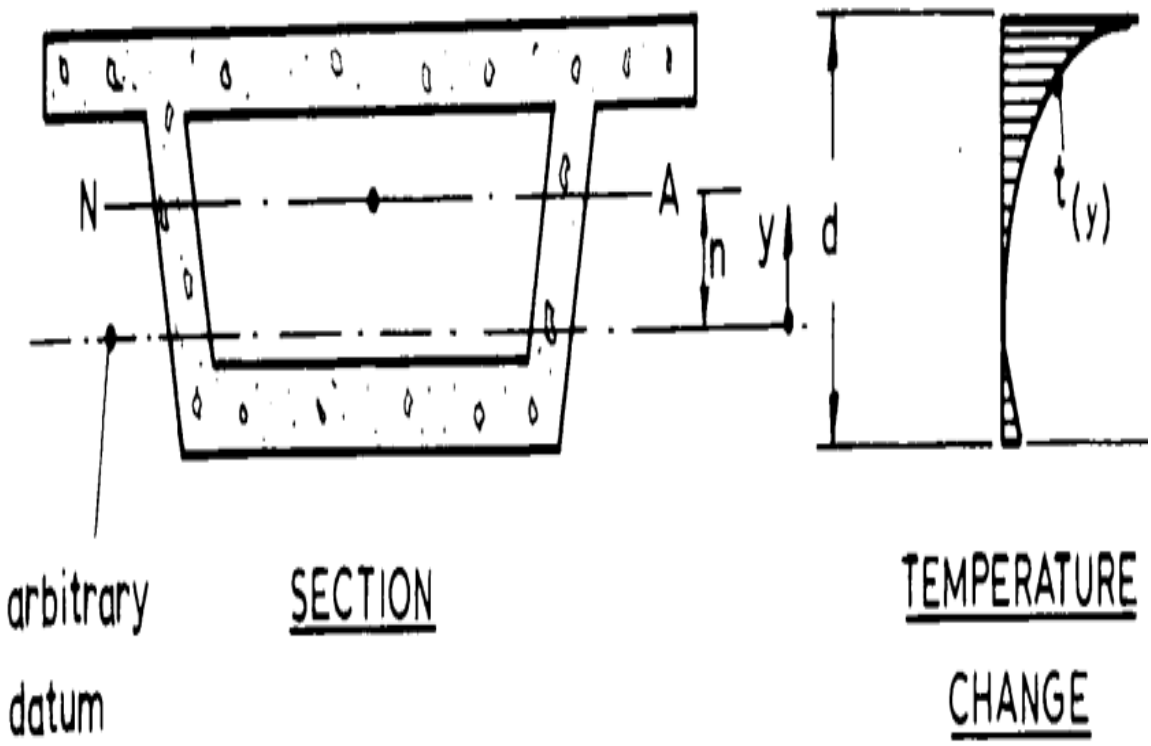

Figure 2.4 Box girder and temperature gradient (Priestley 1978)

. Figure 2.5 presents the stress profile that Priestley (1978) calculated for both primary and secondary thermal stress developed in a continuous bridge.

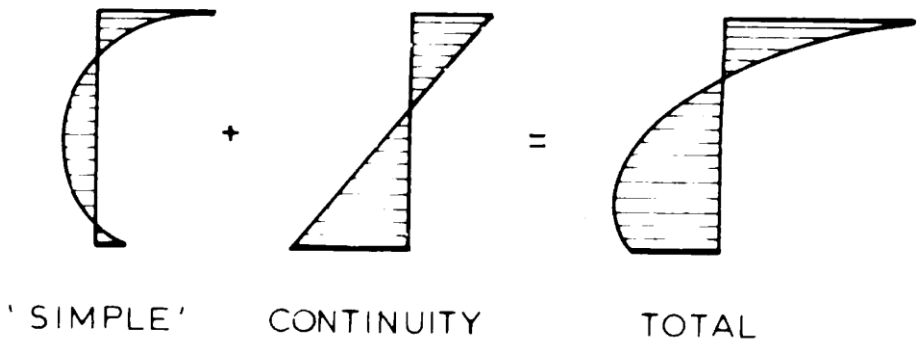

Figure 2.5 Result of Priestly approach (Priestley 1978)

Elbadry and Ghali (1986) conducted an experiment to find out how the thermal stresses are produced and their effects. From their experiment it was concluded that

1) Temperature variations over the cross section of a bridge structure are generally nonlinear and can induce stresses of substantial magnitude in both the longitudinal and transverse directions.

2) The cracking of the concrete in different parts of a box girder are primarily due to tensile stresses produced by the change in temperature.

It was also recommended using partial prestressing in concrete bridges will help in reduce thermal stresses and thermal cracking.

Krauss and Rogalla (1996) investigated the consequences of thermal stresses on concrete bridge decks by examining stresses on 18,000 hypothetical bridges. It was concluded that there are normally three main factors that affect the thermal stress; namely, concrete material, geometry and geographic location of the bridge. Thermal stresses in bridges can develop because the girders restrain natural thermal movement of the bridge deck; however thermal stresses can be developed even without restraints because temperatures are rarely uniform or linearly distributed in bridges. Thermal stresses can develop in a bridge because of diurnal temperature

change or seasonal temperature change. Out of the two, diurnal temperature change produces larger thermal stresses especially over the interior supports of a continuous span structure.

Shushkewich et al. (1998) conducted a study on a prestressed concrete segmental bridge and compared the positive and negative temperature gradients that were observed from the experiment with AASHTO specifications. From the results it was concluded that, the proposed temperature gradients in the 1998 AASHTO Segmental Guide Specifications (AASHTO Guide Specifications for Design and Construction of Segmental Concrete Bridges 1998) and the 1994 AASHTO LRFD Bridge Design Specifications were satisfactory (AASHTO LRFD Bridge Design Specifications 1994). It was also postulated that the prestressing of the concrete is needed for segmental bridges in order to help reduce thermal stresses produced by the temperature gradient.

Roberts-Wollman et al. (2002) studied the measurements of thermal gradients and their effect on segmental concrete bridges. Based on the research, the following conclusions were drawn:

1) The positive thermal gradient recommended in the AASHTO LRFD are too conservative for untopped structures, but appropriate for asphalt topping of at least 50mm.

2) They also concluded that the fifth-order parabola developed by Priestley (1978) is an adequate approximation for a typical positive and negative temperature gradient.

Fu et al. (2006) conducted several case studies to investigate how thermal stresses in concrete structures were affected by the heating rate. Two cases were considered for the research where heating rates of 10°C/min and 20°/min were used. From the research, it was determined that:

1) The temperature gradient is dependent on the heating rate and thermal conductivity of the material.

2) The temperature profile reaches a uniform value with increasing heating rate.

Several studies were conducted at LSU on the effect of thermal stresses on the behavior of concrete bridges.

Segura (2011) implemented an analytical method for thermal stress calculation (Priestly 1978) in a spreadsheet program. A case study was then analyzed to demonstrate how thermal stresses can be predicted for one of the segments of the John James Audubon Bridge. It was concluded that thermal stresses induced by positive temperature gradients may be of a magnitude that may exceed allowable service loads in continuous concrete bridge structures.

Hossain (2012) conducted a study on the temperature effects at a bridge segment of John James Audubon Bridge. Analytical method and field study were used for this research. Installed sensors which are based on the vibrating wire technology and are capable of measuring temperature and physical strain at each monitored point were used (Okeil et al. 2011). The temperature readings from the sensors were used and compared with the results obtained using analytical method. A computer program named *RadTherm* was used to predict the temperature at different locations of girder and the predicted temperature were compared with the observed temperatures from installed sensors. Finally, the temperature gradient across the superstructure was studied and thermally induced stresses were calculated. Based on the results from the research, it was concluded that:

1) Analytical and field temperature data were in good agreement, hence, analytical methods can be used to calculate the thermal stresses on complex structures.

2) AASHTO LFRD design temperature gradient is accurate enough for design of girder bridges

3) Temperature effects should be considered in the design of continuous bridges.

2.7 Restraint moments

A continuous bridge is structurally advantageous over simple-span bridges. Compared to a simple-span design, a continuous bridge can have longer spans and fewer lines of girder which results in lower overall cost (McDonaugh and Hinkey 2003). Continuous bridge construction improves the durability of the bridge, improves the riding surface for the vehicles and reduces the overall cost by increasing the span lengths of the girders (Mirmiran et al. 2001).

Although there are many advantages of continuous bridge compared to the simple span bridges, there are many important factors that need to be considered in their design. More factors should be considered for the continuous bridge in comparison with simply supported bridge (Ma et al. 1998a). Since there will be different continuity methods and construction sequences, there will be different time dependent effects on the bridge. On a typical prestressed concrete continuous bridge system, time dependent effects include creep, shrinkage, and relaxation of steel (Mirmiran et al. 2001). Another time dependent effect in the continuous bridges is thermal effects. All of these time dependent effects will cause restraint moments in continuous bridges.

Oesterle et al. (1989) performed analytical studies on restraint moments that develop due to time dependent effects. To predict the time-dependent restraint moment the computer software called BRIDGERM was developed under a National Cooperative Highway Research Program (NCHRP) along with Construction Technology Laboratories (CTL). From the study, it was concluded that without any structural benefit, positive moment connections are time-consuming, difficult and expensive to install.

Ma et al. (1998a) conducted an analytical study using a computer program called CREEP3 which was developed in 1970's and illustrated a variety of continuity methods and construction sequences required for constructing the bridge system (see Figure 2.6). Three cases were

considered which are dependent on the time when the deck and diaphragm are cast to investigate the time-dependent effects due to the construction sequence. The cases are diaphragm only, diaphragm and deck cast simultaneously and deck cast after the diaphragm is cast. It was concluded that when the deck is cast after the diaphragm, smaller positive restraint moment develop and when the diaphragm and deck are cast simultaneously negative moments developed due to creep and differential shrinkage.

Ma et al. (1998) also conducted an experimental analysis. From the analysis, it was concluded that it is not recommended to include all of the continuity reinforcement in the deck slab. It was also concluded that in determining the maximum length of the span of the girder, the cross-sectional area of the bottom flange of the girder play an important role. The concrete diaphragm joint may crack if a diaphragm is cast before the deck.

Figure 2.6 Finished Connection (Ma et al. 1998)

Peterman and Ramirez (1998) conducted an experimental study to understand the restraint moment developed at interior piers of bridges. Study was conducted on bridges constructed with full-span prestressed concrete form panels. From the study it was concluded that the orthodox design methods like PCA and CTL used for designing the bridges overestimated negative moments because of the restraint in bridges due to time-dependent deformations.

Mirmiran et al. (2001) conducted an analytical study to determine the performance of the continuity for precast, prestressed concrete girders continuity connections. For this analytical study, a flexibility based model was developed and from the model the study was conducted on the time-dependent behavior of continuity connections. The model that was used for this study considers the change in the girder/deck's change in stiffness under time dependent effects and loads. It also considers the nonlinear response of the diaphragm and girder/deck's stress-strain. It was concluded that restraint moments due to the time dependent effects are highly dependent on the girder age at time of establishing continuity. Restraint moments are highly effected by the positive moment reinforcement which is in the continuity diaphragm. It was also concluded that restraint moments are not affected by the continuity diaphragm's width. The behavior of the continuous bridge is usually better when the continuity is established at the later ages compared to the behaviors of the continuity bridge whose continuity is established at the early ages.

McDonaugh and Hinkley (2003) studied on the design for continuity using WSDOT standard precast, prestressed concrete bridge girders. From the analytical studies, the relationship between the size of the girders and the positive restraint moments was found. It was indicated that the girders which have longer spans generally do not develop large positive restraint moments due to creep and shrinkage. The result also indicated the possibility of designing the girders for full continuity without the development of large positive restraint moments. From the study, it was

concluded that girder age at the time continuity is established should be 90 days or more than 90 days to achieve near full continuity.

Miller et al. (2004) performed an investigation on the serviceability, strength and the continuity of connections of the continuous precast/prestressed girders. Due to the time-dependent effects like creep, shrinkage and temperature effects, the connected girders camber upward. Consequently, positive restraint moments develop at the diaphragm. Six positive moment connections were tested. It was concluded that each of the connections had pros and cons. It was also recommended that the selection of the connections should be given to the engineer because all of the connection performed satisfactorily..

Chebole (2011) conducted a research to study the development of restraint moments in precast/prestressed continuous girder bridges due to creep and shrinkage. RESTRAINT program developed by Miller et al. (2004) was used and modified in order to eliminate many of the limitations in the original RESTRAINT program. A detailed parametric study was carried out to investigate the effect of different parameters on restraint moments in continuous bridges. From the parametric study, it was concluded that the restraint moment values are affected by girder-age, span length ratio, and ratio of diaphragm to girder stiffness. The results were then used to determine the optimum girder ages that will result in targeted restraint moments.

3 METHODOLOGY

3.1 Introduction

In this chapter, a detailed discussion of the methodology used for the research and the modified RESTRAINT is presented. There are few methods for calculating the restraint moments in a continuity diaphragm, namely Portland Cement Association Method (PCA), P-method, BRIDGERM, RMCalc and RESTRAINT. PCA and P-method are analytical methods and BRIDGERM, RMCalc and RESTRAINT are computer based programs. For this research, mRESTRAINT was used to calculate the restraint moments in continuous bridges. There were some limitations on the original program for which it had to be modified. The modifications that were done to the mRESTRAINT program are discussed later in this chapter.

For this research, the mRESTRAINT program was modified according to the needs of the study. mRESTRAINT which is a modified version of the program RESTRAINT was again modified. The time-dependent effects on the calculation of the restraint moments were added. The original mRESTRAINT is only capable of accounting for creep and shrinkage effects on the development of restraint moments in continuous bridges. Now, after the modification, mRESTRAINT-TG is capable of calculating calculate the mRESTRAINT with including the effect of thermal gradient as well.

Visual Basic for application (VBA) was used to code the new module for inclusion of the thermal gradient and few of the modifications were made on the input, analysis and output section of the mRESTRAINT program. Detailed discussion of the modified mRESTRAINT program will be discussed later in Chapter 4. After modifying mRESTRAINT, the detailed parametric studies were carried out to study the effect of different parameters on restraint moments. The parameters considered in the study were span ratio, age of continuity and

diaphragm stiffness ratio. It was found that all of those parameters effect the total restraint moment. Results from the parametric study were then used to establish optimum girder age at time of establishing continuity such that an allowable restraining moment is not exceeded. Details of the results will be discussed later in the Chapter 5.

Since the mRESTRAINT-TG program was used to calculate the restraint moment for this research and was the most important part of the research, the details of the RESTRAINT program are discussed later in this chapter

3.2 Restraint Moment Calculation

As discussed earlier, mRESTRAINT-TG program was used to calculate the restraint moment in the continuous bridges. RESTRANT, the original version of the program, was developed for the study conducted by National Cooperative Highway Research Program (NCHRP) Project 12-53 (Miller et al. 2004).

3.2.1 NCHRP Project 12-53 (RESTRAINT Program)

After the development and implementation of the PCA method, almost all of the bridges construction and design changed in early 1980's. Because of the PCA method, bridges finally could have the longer span and have larger spacing between the girders. Although, the PCA method was used in that time and was performing well, a new method had to be developed because the of the fact that the studies conducted on the continuous structures using the PCA method showed that negative moments over piers can be resisted by deck using reinforcement. However, the studies also showed that there were cracking on the diaphragms and the cause of the cracking positive moments caused by time dependent effects like creep, shrinkage and the thermal gradient (Miller et al. 2004). Therefore, new method had to be developed.

NCHRP Project 12-53 was funded to study the connections between precast/prestressed concrete girders made continuous. Investigation on the strength, serviceability, and continuity between precast/prestressed concrete girders made continuous were carried out (Miller et al. 2004).

The main reason behind the development of the positive moment on the diaphragms is that whenever the girders are connected to each other at their ends to make the bridge continuous, upward movement camber due to the time-dependent effects like creep, shrinkage and temperature gradient occur, which leads to the development of a positive moment at the diaphragm (Miller et al. 2004). Therefore, positive moment connection must be provided to resist these positive moments at the diaphragm. Positive moment connections are built by using either the prestressing strands or additional reinforcing bars which extend from girder ends into the continuity diaphragms (Miller et al. 2004). The positive moment connections used for the project are shown in Figures 3.1 and 3.2 respectively.

Figure 3.1 Bent-bar positive moment connection (Miller et al. 2004)

Figure 3.2 Bent-strand positive moment connnection (Miller et al. 2004)

Miller et al. (2004) started their research by conduction a survey as their first phase as a part of the NCHRP Project 12-53. The survey was conducted to study the number of connections for the positive and negative moments. The type of positive and negative moment connection, sequence of the construction, details of the connections, the age at which the continuity is established and methodologies for design were surveyed. After the survey was conducted, a detailed parametric study was done for the continuous system. A program called RESTRAINT was developed to conduct this parametric study. RESTRAINT is a spreadsheet based program which was coded on the visual basic for application environment.

After the surveys were conducted, analytical studies were performed. The purpose of this study was to propose the configurations for the specimen which was required for the experimental work. An analytical model was created for this task and this model was later used to conduct the parametric studies on the continuous system having different moment connections.

For this analytical model, the two-span continuous structure assumes that there is a fixed support and the end of each girder which can be seen in Figure 3.3. For the analytical model a new version of existing software BRIDGERM was developed and was named as RESTRAINT.

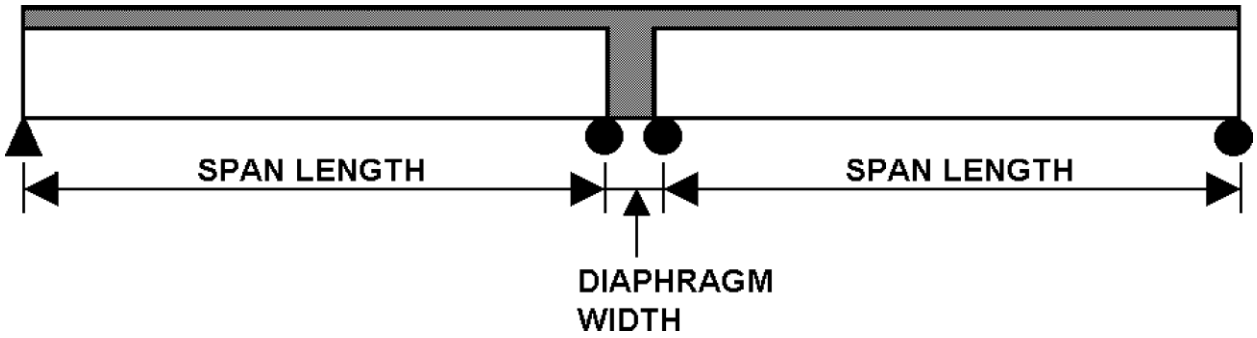

Figure 3.3 RESTRAINT model (Miller et al. 2004)

RESTRAINT was designed in VBA environment and works within a standard spreadsheet program. Initially, this program was designed to model a two-span continuous structure but it was later revised and re-coded to add many new features which will be discussed later in this chapter. The program is coded in a way that it discretizes the span and the diaphragm into several elements. RESTRAINT is a flexibility-based tool for the purpose of determining the time-dependent effects on precast/prestressed continuous girders. Time-dependent effects like creep, shrinkage, prestress loss, sequence of construction, age at loading was taken into account.

On the model, different types of nonlinear stress-strain responses shown by continuity diaphragm and the girder/deck composite sections and the changes in the stiffness of the structure under time-dependent effects were considered (Mirmiran et al. 2001).

Before using the RESTRAINT program for the analytical studies, it was important to develop the moment curvature relationship as the data from the relationship are input into the RESTRAINT program. For determining the moment curvature relationship, any convenient method (computer program, finite element analysis, experimental data and hand calculations)

can be used. To determine the moment curvature relationship, RESPONSE program (Collins et al. 1991) was used. RESTRAINT calculates the internal moment that is the results of the time-dependent effects from creep and shrinkage of the prestressed girder and the deck. From the relationships given in the American Concrete Institute Report (ACI 209), creep and shrinkage strains are found.

RESTRAINT takes the time of casting of the diaphragm and the deck as the input which the assumption that the release of the pretensioning forces is time=0 (based on the age of the girder, this can be different; but the reference is taken as the time after the release of the post-tensioning) and it allows the time of casting for the diaphragm and the deck to be different. Other basic material properties are also taken as input by the program. RESTRAINT program also accounts for the loss of the presstressing force. The loss of the prestressing force is calculated using the method provided by the Precast/Prestressed Concrete Institute (PCI) handbook. Shrinkage of the deck and the girder is assumed to be uniform in the span and creep which is caused by the dead load plus the prestressing force is assumed to be parabolic. Creep in the diaphragm was ignored due to the lack of prestressing and the differential shrinkage between the slab and the diaphragm is assumed to be zero because they are usually cast together.

The program adds the dead-load moments once the internal moments are known and the moment due to a point load (live load) at midspan can also be included if desired by the user. After calculating the total internal moment, the program divides each girder's span into 10 or more than 10 numbers of slices as defined by the user but for the diaphragm, only one single element is used. For each element of the girder and the diaphragm, the program now calculates the curvature from the moment-curvature relationship. After calculating the curvature, using consistent deformation analysis, the program calculates the deflection at the center supports. For

the consistent deformation analysis, the center reactions are removed to make the structure statically determinate. The remaining reactions are also calculated from the equilibrium and are used to calculate the continuity moments. The calculated continuity moments are then added to the other moments. The program loops the entire analysis until the answers converges.

After the parametric studies were conducted, six positive moment connection details were developed and were tested on various AASHTO girders. The girders used for the experimental study were Type II and Type III AASHTO girders.

The results from the survey, parametric studies and the experimental work were used to propose the changes for AASHTO Load Resistance Factor Design Specifications (Miller et al. 2004). The findings from the NCHRP Project 12-53 were summarized in NCHRP 519 report. In the report, it was mentioned that the time-dependent effects and the sequences of the construction must be considered on the design. The combinations of the girder age at time and placement for the diaphragm were suggested. It was also mentioned that the temperature effects on the system are significant and the daily temperature changes causes the reactions to vary by $\pm 20\,\%$ (Miller et al. 2004). The behavior of the bridge is also affected by the seasonal temperature changes.

3.3 Analytical approach

Thermally induced stresses can be calculated as the superposition of primary and secondary effects. The formulas/equations presented in this section are adapted from Priestley's (1984). In this approach, thermal stress can be calculated by the principal of structural mechanics and the following assumptions were made.

- Material properties are temperature independent.
- Initially plane sections remain plane after thermal loading.

• Homogeneous behavior is assumed.

The primary thermal stress is calculated using the following equation

$$f_{p(y)} = E_c(\epsilon_y - \alpha_c\theta_{(y)}) \quad (3.1)$$

where E_c is the modulus of elasticity of concrete, ε_y is the linear strain distribution, α_c is thermal expansion coefficient of concrete, and $\theta_{(y)}$ is the temperature change.

Above mentioned equation can be used to calculate the axial force if it is integrated over the section depth "*d*". Therefore, the equation becomes

$$P = E_c \int \left(\epsilon_y - \alpha_c\theta_{(y)}\right) b_{(y)} dy \quad (3.2)$$

where $b_{(y)}$ is the net section width at height *y*. Also by taking the moments of the primary stress distribution about the neutral axis will yield the internal moment induced by $\theta_{(y)}$. The moment is represented by the following equation:

$$M = E_c \int \left(\epsilon_y - \alpha_c\theta_{(y)}\right) b_{(y)} (y - n) dy \quad (3.3)$$

where *n* is the distance between the neutral axis and the arbitrary datum and *y* is height at which the net section width is taken at.

The calculation of primary stress is done by making the structure statically determinate by the removal of sufficient internal redundancies in such a way that restrained moment and forces given by 3.2 and 3.3 cannot develop.

Therefore, P=M=0

The linear strain ϵ_y can be calculated by using the following equation.

$$\epsilon_y = \epsilon_o + \psi y \quad (3.4)$$

where, ε_o is the final strain at *y*=0 and ψ is the final curvature.

Now, we can substitute Equation 3.4 into the moment and force equations and setting them equal to zero, the curvature and strain equations can be calculated and the generated equations are

$$\psi = \frac{\alpha_c}{I} \int \theta_{(y)} b_{(y)} (y - n) dy \tag{3.5}$$

$$\varepsilon_o = \frac{\alpha_c}{A} \int \theta_{(y)} b_{(y)} dy - n\psi \tag{3.6}$$

Rewriting the equation 3.5 and 3.6 in the summation form we get,

$$\psi = \frac{\alpha_c}{I} \sum_{i=1}^{n} \theta_i (y_i - n) dA_i \tag{3.7}$$

$$\varepsilon_o = \frac{\alpha_c}{A} \sum_{i=1}^{n} \theta_i dA_i - n\psi \tag{3.8}$$

where the section is divided into n elements and θ_i and y_i are the average temperature change of the i^{th} element of area dA_i and centroid located a height y above the datum respectively.

Therefore, the final equation to calculate the primary stress is as follows.

$$f_{p(y)} = E_c(\epsilon_o + \psi y - \alpha_c \theta_{(y)}) \tag{3.9}$$

The temperature change $\theta_{(y)}$ can be calculated by the use of AASHTO temperature gradient profile.

Figure 3.4 displays the AASHTO temperature gradient profile used in this research to calculate the change in temperature. The values of T_1 and T_2 are determined from Table 3.1. The value for the T_3 should be no more than 5^oF depending on site-specific study. The temperature that are shown in Table 3.1 are the different solar radiation zones on the map of the United States which can be seen in Figure 3.5. To calculate the negative temperature gradient, the values in Table 3.1 must be multiplied by -0.30. The dimension of A should be determined by the following criteria:

- 12 in. if the concrete structure is more than 16 in. in depth
- 4 in. less than the actual depth if the depth is less than 16 in.
- 12 in. for steel superstructures and t shall be taken as the depth of the concrete deck

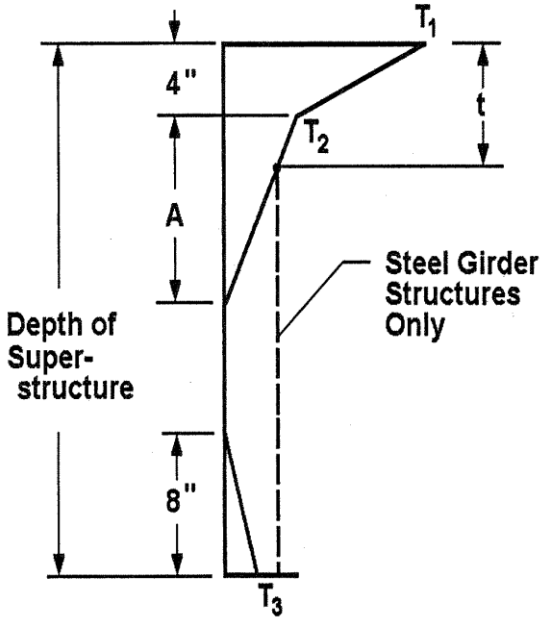

Figure 3.4 AASHTO LRFD Bridge Design Specifications 2007

Table 3.1 Basis for Temperature Gradient-AASHTO LRFD Bridge Design Specifications 2007

Zone	T_1 (^{0}F)	T_2 (^{0}F)
1	54	14
2	46	12
3	41	11
4	38	9

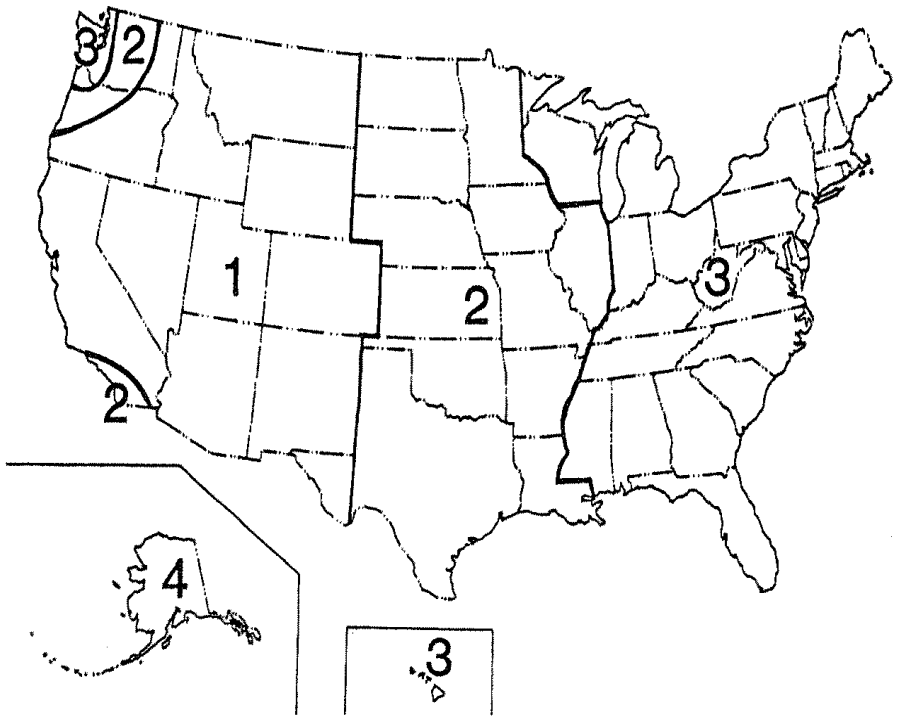

Figure 3.5 Solar Radiation Zones – AASHTO LRFD Bridge Design Specifications 2007

For example, if we want to calculate the values of T_1 and T_2 from the AASHTO LRFD Bridge Design Specifications then from Figure 3.4, we can say that Louisiana is in the number 2 of solar radiation zone and from Table 3.1 for zone 2 T_1 is 46°F and T_2 is 12°F.

For continuous beams, it is very important to calculate the secondary stress developed by the curvature calculated in Equation 3.7. First, the calculation of the fixed end moment produced by the curvature is needed. This is done by cutting the beam at each support to remove redundant reactions. Figure 3.6 shows two possible approaches to achieve this condition; namely removing vertical translational constraints or removing rotational constraints at continuous piers. Equation 3.10 represents the formula for determining fixed end moments, *M*, in the released structure. The restraint moment can either be positive or negative.

$$M = E_c I \psi \tag{3.10}$$

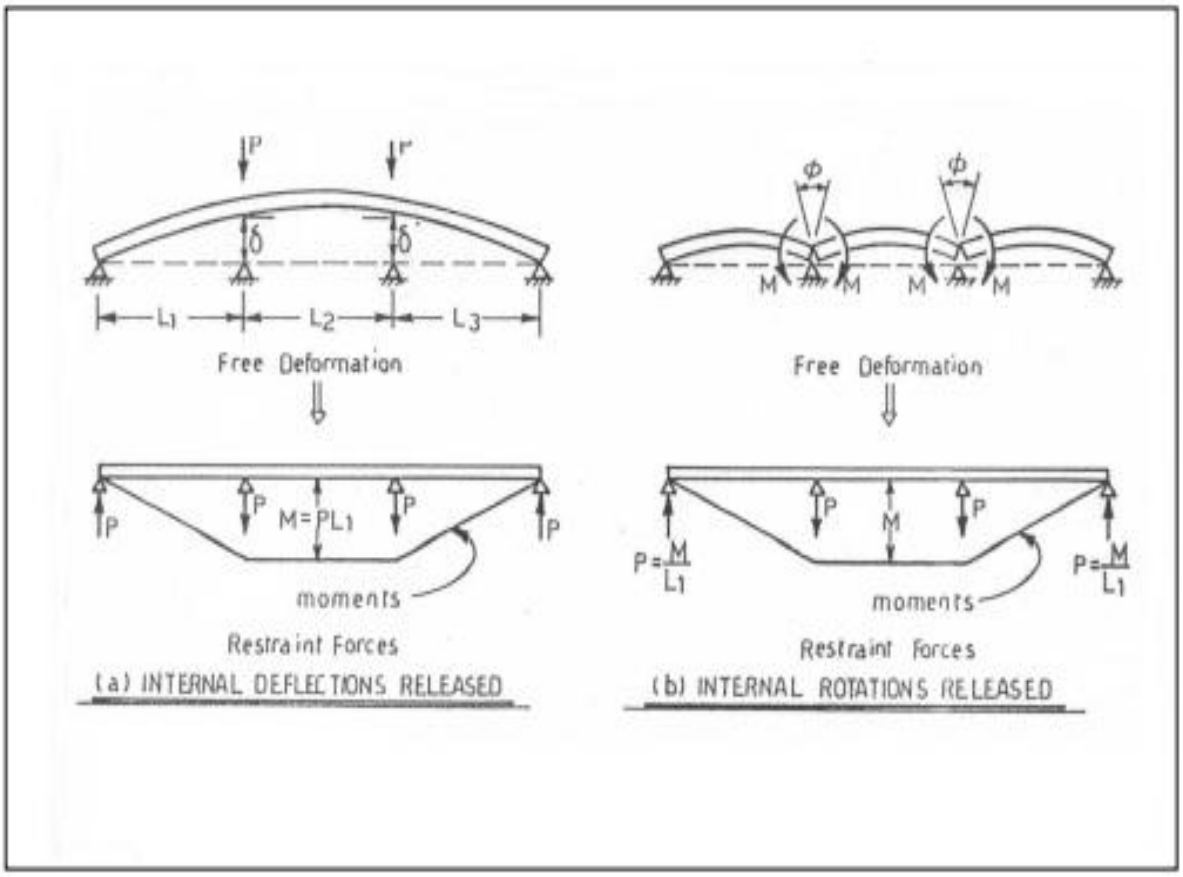

Figure 3.6 Redundancy release for continuous bridges subjected to thermal hogging (Priestley 1978)

The final moment values, *M'*, are then calculated by means of moment distribution. After M' is calculated, the secondary stress can be calculated as seen in Equation 3.11.

$$f_{s(y)} = \frac{M'(y-n)}{I} \tag{3.11}$$

Now the total thermal stresses can be calculated using the following equations.

$$f_{t(y)} = E_c\left(\epsilon_o + \psi y - \alpha_c \theta_{(y)}\right) + \frac{M'(y-n)}{I} \tag{3.12}$$

3.4 Summary

In this chapter, the methodologies used in this research were discussed and the method used for calculating the restraint moment was presented in detail. Different types of method used for calculating restraint moment were identified and computer-based program RESTRAINT which was used for this research was discussed in detail. NCHRP project 12-53 was discussed in detail as it was the project which designed the program RESTRAINT.

4 MODIFIED RESTRAINT PROGRAM

4.1 Introduction

This chapter presents the computational tool used for estimating restraint moments in continuous concrete girder bridges that was developed by the research team for NCHRP Project 12-53. This chapter also presents comparisons and previous modifications carried out at Louisiana State University (LSU) by Veeravenkata Chebole to overcome some of the limitations on the original RESTRAINT program. The modified program is called as mRESTRAINT. The modifications which were needed for this research are also presented in this chapter.

4.2 Comparison of RESTRAINT program by Chebole

Chebole (2011) had previously modified the original RESTRAINT program for his research on continuity moments in prestressed concrete girder bridges. For the research, the comparisons between the methods for calculating the restraint moments were carried out at first. Using PCA method (Mattock et al. 1961), RMCalc program (McDonagh and Hinkley 2003) and RESTRAINT program (Miller et al. 2004) restraint moments were calculated and compared for a selected bridge configuration.

For the comparison of the available methods, two span bridges with identical span lengths were considered. The other bridge parameters are listed in Table 4.1. All prestressing strands were assumed to be straight low-relaxation strands and their centroids was assumed to be 3 inches from the girder's soffit.

Restraint moments were calculated using PCA, RMCalc and RESTRAINT methods. For PCA method, restraint moments were calculated manually, while the computer programs were used for RMCalc and RESTRAINT program. Restraint moments from all of the three methods

were analyzed by creating a plot in which the x-axis was age of girder and the y-axis was restraint moment values. Figure 4.1 shows the plots.

Table 4.1 Input Values (Assumed) for Comparing Restraint Models (Chebole 2011)

Section Type	AASHTO Type - VI
Span Length(ft)	70
Girder Spacing(ft)	8.0
Deck Thickness (in)	7.5
Intial Strand Stress (psi)	202500
Girder Compressive Strength (psi)	5000 at transfer; 6000 at 28 days
Deck Compressive Strength (psi)	4000
No. of Strands	20
Strand Diameter (in)	0.5
Age of Continuity (Days)	90
Unit Weight of Concrete (pcf)	150
Creep Coefficient	2.3
Ultimate Shrinkage	600μ
Relative Humidity	50%

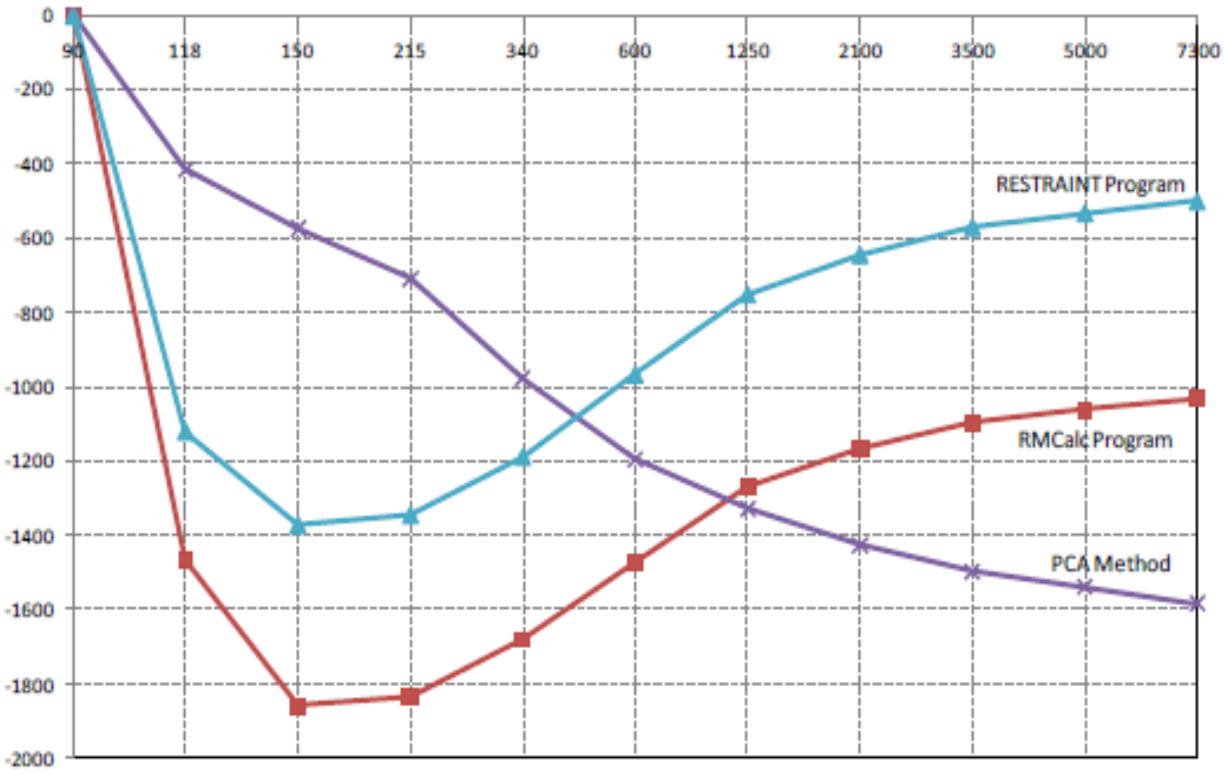

Figure 4.1 Restraint Moment Values vs. Age of Girder (Chebole 2011)

From Figure 4.1, it can be seen that trend of the plot between the RESTRAINT program and the RMCalc Program is same but the PCA method is different. This may be due to the fact that, restraint moment is calculated at the end of specified times of interest in one step in the PCA method, whereas an incremental approach as in RESTRAINT program and the RMCalc program updates the bridge conditions at every intermediate step.

The RESTRAINT program was chosen for the study to calculate the restraint moments because restraint moment predictions were more in line with expected patterns based on literature review due to the time step analysis approach for calculating the restraint moments. Modification of RESTRAINT program by Chebole (2011)

Due to the limitations that existed on the original RESTRAINT program, Chebole et al. (2011) modified the program. The limitations on the program were as follows:

1) Only span ratio with value of 1 was allowed for symmetry.
2) Program only supported AASHTO TYPE I – VI girders.
3) One strand configuration was allowed regardless of the span-lengths.
4) Diaphragms were not considered.
5) Restraint moments calculations extended for 20 years only.

The modification of the RESTRAINT program was done in such a way that it supports bridges up to 5 unequal spans and the diaphragm can be modeled as a link between the two adjacent girders. Modified RESTRAINT (mRESTRAINT) can also calculate the moment for more than 50 years (20,000 days) of bridge life.

Modifications were divided into three categories which are modifications in input, analysis calculations and output. For the input part of the modifications, changes were made on the section of the program where user inputs their desired data. The first change was made on the "Input data form" because the modified program needed to calculate the restraint moments 5 unequal spans with or without diaphragm whereas the original RESTRAINT program only supported the 5 equal spans without the diaphragms. The next change was made of the textbox where the user can choose the girder type. A new form (input window) was created for the choosing the type of girders from AASHTOO Type I to VI for I-section girders, in addition to allowing the user to enter custom girder sections. The strand configuration needed to change as well since the new program was meant to calculate the restraint moments for the five unequal span lengths with and without the diaphragms. In the modified RESTRAINT program, the users are allowed to enter the different strand configuration for each span. Changes were also made on the "Number spans form" because the effect of the diaphragm in restraint moment calculations was to be added since the original programs not include the diaphragm's effect. After including

the diaphragm effect, the new form was introduced to input the length of the diaphragm and the ratio of the moment of inertia of the diaphragm and the moment of inertia of the girder and it was named as “Diaphragm Length”. Another new form added to the program was “Strand data Diaphragm”, which was meant to enter the strand data for the diaphragm. Another major modification in input was the change of days. The new RESTRAINT program was meant to calculate the restraint moments for little more than the 50 years where as the original RESTRAINT program calculates the restraint moment up to 20 years. Hence “Time data” form was modified.

For analysis new spreadsheets on the program named 2spanswd, 3spanswd, 4spanswd and 5spanswd were added to the modified program to allow for considering the diaphragm’s effect. The spreadsheets with the name such as “2spans” are meant to contain the user defined inputs and the calculations for the 2-span bridge and the spreadsheets with the name such as “2spanswd” are meant to contain the user defined inputs and the calculations for the 2-spans bridge with the effects of diaphragm. The original RESTRAINT program also had some limitations calculating the prestress loss because it was programmed in such a way that it only takes a value from the exterior span length for the loss due to elastic shortening. Therefore, changes were made in the modified RESTRAINT program in such a way that loss due to elastic shortening is calculated for all spans based on each span’s strand configuration. Changes were also made on each of the spreadsheets to calculate the deal-load moments since the span lengths are unsymmetrical and the diaphragm was added. “Moment Distribution” module was modified to calculate the fixed end restraint moments for all configurations covered in the modified version.

The final modification to the original RESTRAINT program was on its output module. On the “output” form, extra textboxes were added because of the fact that the restraint moment may

not be same on the unequal span lengths. A macro named “chart module” was also changed in such a way that it now plots restraint moment values for all of the continuity joints.

4.3 Modification of mRESTRAINT for this research

After analyzing the original RESTRAINT program and the modified RESTRAINT program also known as the mRESTRAINT, it was concluded that mRESTRAINT should be modified to conduct this research as it did not offer any thermal analysis. The main purpose of this research is to understand the effect of the temperature gradient on continuous precast/prestressed girder bridges, which was beyond the scope of the original RESTRAINT program and the mRESTRAINT. In addition to the lack of thermal analysis capabilities, it was also determined that girder hauches were not considered in the cross-section of the I-section girders.

The modifications done to the mRESTRAINT program are divided into three categories for the clarity. The three categories are modifications in Input, analysis and Output.

4.3.1 Modifications in Input

This part of the chapter discusses the modifications made to the input part of the mRESTRAINT program. Since haunch was not included in the section properties of the I – section girders, the first modifications made to the program was the addition of the new textbox named “haunch” on the user form “ISectionDimensions” as shown in the Figure 4.2. Now, the user can enter the desired value for the haunch’s thickness. The program is coded in such a way that it will take the value of haunch from the textbox and will include it in the cross section of the I-section girders. Therefore, the new cross-section of the I-section girders on the modified mRESTRAINT program will be different but accurate than the old mRESTRAINT.

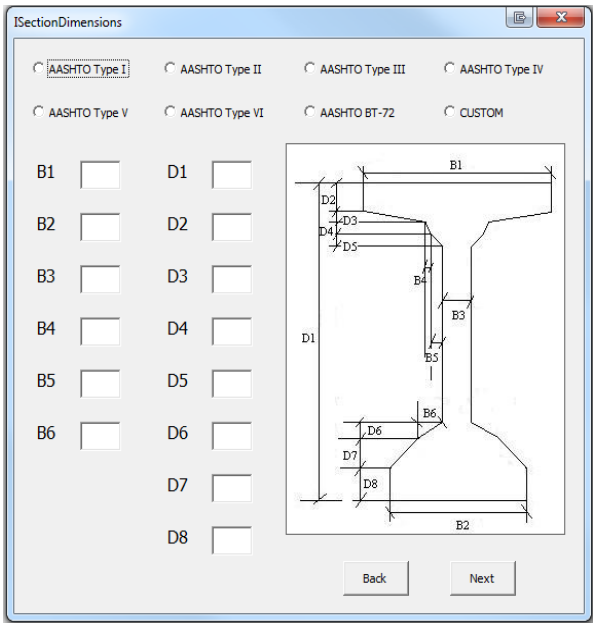

Originat mRESTRAINT

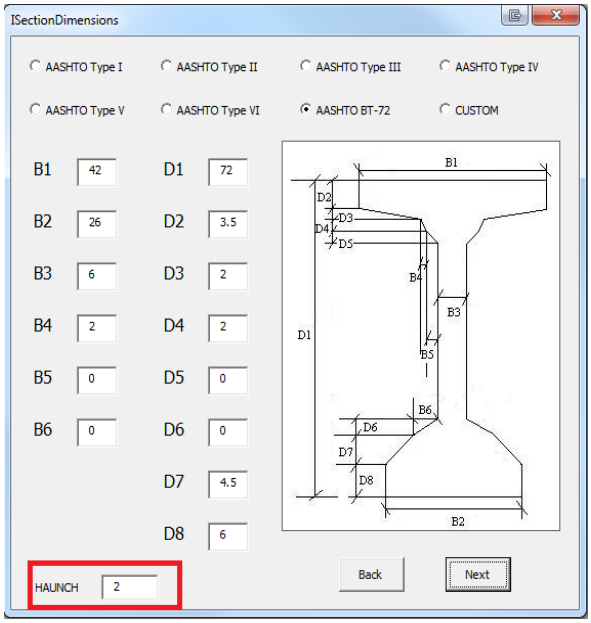

Modified mRESTRAINT

Figure 4.2 Addition of Haunch on the ISectionDimesnions form.

The more important modification for mRESTRAINT was the addition of the new form called "THERMAL STRESS" as shown in Figure 4.3. This form was introduced for few reasons and they are as follows:

1) To include the effect of the temperature change on the restraint moment calculations.
2) Users can have the full idea that the new mRESTRAINT have thermal gradient effect included.
3) This user form lets the user to choose if they want to include the effect of temperature gradient on the calculations or not.

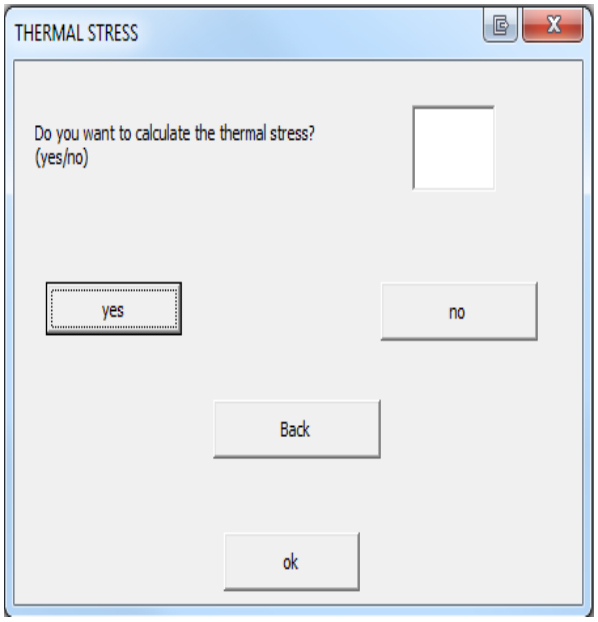

Modified mRESTRAINT

Figure 4.3 Introducing the new user form "THERMAL STRESS"

This user form "THERMAL STRESS" contains the code that was written to calculate the restraint moments including the effect of the thermal gradient in it. This form lets the user to choose if they want to include the effect of thermal gradient or not, by clicking the "yes" or "no" buttons, then "OK" to proceed. The program will then include the effect of the thermal gradient

or not based on the users input. This freedom for users to choose if they want to include the thermal gradient effects or not was given because some users might want to calculate the restraint moments just due to the creep and shrinkage effects, while others might want to include the effect of the thermal gradient along with creep and shrinkage. The “THERMAL STRESS” form appears to the user right after the form “Select” because it takes lot of values from other user forms till “Select” and therefore it was determined to be the right spot for “THERMAL STRESS”. This user form is only available if the user wants to perform the linear analysis because this research is not concerned with the non-linear analysis. Therefore if the user wants to do the non-linear analysis, the thermal gradient analysis will not be available.

After introducing this new form it was important to introduce the message box which asks the user to enter the number of slices. Calculations of restraint moments due to the effect of the thermal gradient require discretizing the section into layers or fibers. This message box only appears if the user chooses to perform thermal analysis and asks for the number of slices they want to discretize the composite structure. Figure 4.4 shows the message box for the pop up that asks the users for the number of slices. On the text box of the message box users are supposed to enter their value and press “ok” then the program will discretize the composite structure according to the value the users entered.

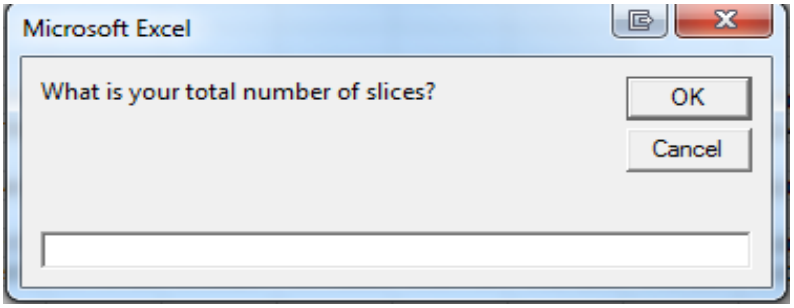

Figure 4.4 Message box for the number of slices

With these modifications, mRESTRAINT is now capable of calculating restraint moments due to creep, shrinkage and thermal gradient effects. For thermal gradient effects, primary and secondary stresses are calculated and the final moment is given due to the effect of the thermal gradient including both positive and negative thermal gradient.

4.3.2 Modifications in Analysis Calculations

This part of the modifications deals with the changes that were made on the existing spreadsheets on the program, the changes that were made on the codes and the new codes that were written to include the thermal gradient effect.

The number of the rows depends upon the number of slices entered by the user for the discretization of the composite structure as discussed above. This program is coded in such a robust way that it will automatically count the number of the rows and columns needed for the calculation without taking extra space depending on the number of the spans and the diaphragm.

Another important part for analysis modification was addition of the code which calculates the restraint moment due to thermal gradient. For this research, this code is the most important part because the primary objective of this research is to study the effect of the thermal gradient on the continuous precast/prestressed girders. This code was written in Visual Basic for Application (VBA) environment and it was started by writing the function called “CncSegslc”, whose purpose is to discretize the girders into layers of fibers of slices entered based on the number entered by the user. Other functions and routines were written to calculate the variables and restraint moment.

The “Chartmodule” was also modified. This module is responsible for presenting the output of the result in graphical form. The output graph plots the Restraint moment values on the y-axis and the Girder age on x-axis. The changes were necessary because the old mRESTRAINT only

calculated the restraint moments due to the creep and shrinkage but the modified mRESTRAINT has thermal gradient capabilities. This code is written in such a way that it will give the output based on the user's choice. For example if the user does not want to include the thermal gradient effect then the program will give the output the same way that the old mRESTRAINT did and if the user wants to include the effect of the thermal gradient then the program will give the output including the effect of the thermal gradient as shown in Figure 4.5.

4.3.3 Modifications in Output

After completing the modification of the input and the analysis stages, it was necessary to modify the program's output. Since there were many variables to be shown as output to the user many rows and columns were added on the spreadsheet as discussed above in this chapter. Variables like primary stress, secondary stress, final moments and restraint moments due to both positive and negative thermal gradients can be seen by the users as the output on the spreadsheets based on the number of spans and diaphragms they chose. Another modification that was done for output was on the chart for the restraining moments. This modification was necessary as the old mRESTRAINT only showed the output of restraint moments due to the creep and shrinkage but the new mRESTRAINT shows the output of restraint moment due to the thermal gradient as well.

5 RESULTS AND ANALYSIS

5.1 Introduction

This chapter presents the results from parametric study that was conducted to investigate the effect on the development of restraint moments of various parameters in continuous prestressed girder bridges. The parameters considered in the parametric study and effects on restraint moments due to thermal gradients are presented in this chapter. The restraint moment due to the effect of creep and shrinkage is also calculated and presented graphically to assess its values in relation to restraint moments due to thermal gradients. In all, 120 different cases were analyzed and then the results that were calculated from the 120 cases were analyzed. Parameters considered were: span lengths ratio, diaphragm to girder stiffness ratio and age of the continuity. More details about the considered parameters will be presented later in this chapter.

The parametric study was also used to calculate the age of continuity days for all 120 cases such that the restraint moments do not exceed an acceptable limit, which was taken equal to the 25%, 50%, 75% and 90% of cracking moment for each case. The cracking moment of the girder and the restraint moment due to all of the time-dependent effects were compared to determine the optimum age of girder. The results from the parametric studies were also used study the proportions of restraint moments caused by the thermal gradient and the creep and shrinkage with respect to the total restraint moment.

5.2 Parameters

This section presents the details of the parameters covered by the parametric study. As stated earlier, different combinations of the parameters were used and 120 different cases were analyzed. The three major parameters used for this study are the span lengths ratio, the

diaphragm stiffness ratio and the age of continuity for the girders. Although mRESTRAINT is capable of computing the restraint moments due to creep, shrinkage and the thermal gradient for continuous bridge up to 5 spans with or without the diaphragm, only 2 and 3 spans bridges were considered in this study. This is due to the fact that the bridges with more spans are repetitive and they do not hugely affect the restraint moment values. Sixty of the cases used for this study include 2 spans bridges and the other sixty include 3 spans bridges. The other parameters are:

1. Girder age at continuity.
2. Spans lengths ratio.
3. Ratio of diaphragm to girder (I_d/I_g) stiffness.

The age at continuity for the girders is the age of the girder at which the deck and the diaphragm are poured which is the time after which the bridge can be considered continuous. Girder's span lengths ratio is the ratio of the length of different spans which effects the relative stiffness between spans and hence the restraint moments. For example, if there are 2 spans continuous bridge with 50 ft. and 100 ft., then the span length ratio of the girder is 0.5. Three spans lengths ratios were considered in this study. Finally, the ratio of the diaphragm to girder stiffness was considered since it affects the ability of the system to redistribute girder end moments. Five different stiffness ratios were considered.

Table 5.1 lists the details of the parameters used for this research. Each analyzed case is given a designation to help in presenting the results. The designation represents the parameters in Table 5.1. For example "2S" and "3S" are given as designations for the 2-span and 3-span cases respectively. Similarly, each parameter has its own designation. For example, a case of two spans whose girder age at time of establishing continuity is 28 days with span lengths ratio of 0.75:1 and diaphragm stiffness equal to girder stiffness is called case 2S-0.75R-1D-28C. Similarly, 3S-

1R-0.25D-180C denotes the case with three equal spans lengths and the diaphragm stiffness equal to 25% of girder stiffness and the age of the girder when the continuity is established is 180 days.

Table 5.1 Parameter Values for the Parametric Studies

Parameter						
No. of Span (2)	2-Spans(2S)			3-Spans(3S)		
Spans Lengths Ratio (3)	1:1 (1R)	0.75:1 (0.75R)	0.5:1 (0.5R)	1:1:1 (1R)	1:1.5:1 (1.5R)	1:2:1 (2R)
Girder Age at Continuity (4)	28 days (28C)	60 days (60C)		90 days (90C)	180 days (180C)	
Stiffness Ratio (5)	$I_{dia}=I_g$ (1D)	$I_{dia}=0.5*I_g$ (0.5D)	$I_{dia}=0.25I_g$ (0.25D)	$I_{dia}=0.125*I_g$ (0.125D)	$I_{dia}=0.05*I_g$ (0.05D)	

The physical values for the input parameters are given in Table 5.2. Design aids were used to choose girder sections and strand configurations based on the chosen span lengths.

Table 5.2 Input Values for Parametric Study

Parameter	2-Span Case	3-Span Case
Type of Section	AASHTO Type- III;III;IV	AASHTO Type- III;IV;V
Span Length (ft)	70,70;66,88;50,100	70,70,70;62,93,62;60,120,60
Girder Spacing (ft)	8	8
Deck Thickness (in)	7.5	7.5
Initial Strand Stress (psi)	202765	202765
Girder Compressive Strength (psi)	8000	8000
Deck Compressive Strength (psi)	4000	4000
No. of Strands	16; 18; 20	16; 18; 22

Table 5.2 continued

Parameter	2-Span Case	3-Span Case
Strand Diameter (in)	0.6	0.6
Diaphragm Span-length (ft)	2	2

5.3 Results from Parametric Study

Using the input values shown in Table 5.2, the restraint moment were calculated for all 120 cases using the modified version of the mRESTRAINT program. First, the inputs were entered on the modified mRESTRAINT program and the restraint moments were calculated up to 20000 days of girder age after establishing continuity. The calculated restraint moment for each case were plotted for the combinations of the age of continuity, span length ratios and stiffness ratios as shown below on Figure 5.1 and Figure 5.2 respectively. The horizontal axis in these plots represents the girder age and the vertical axis represents the restraint moment values.

Figure 5.1 Restraint Moment vs. Age of Continuity for 2-Span Bridge

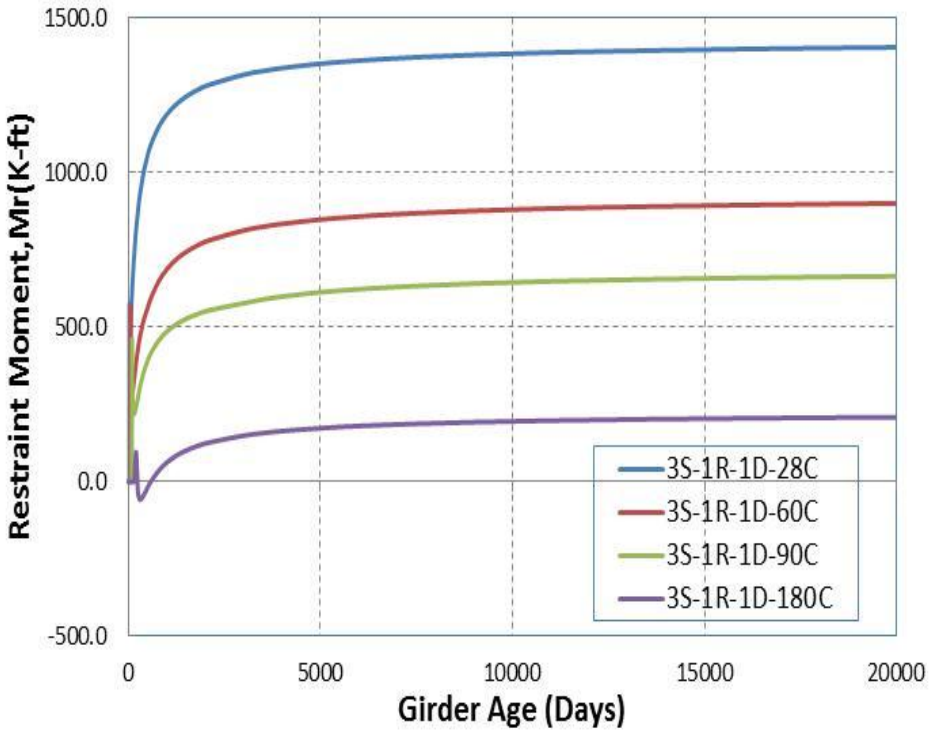

Figure 5.2 Restraint Moment vs. Age of Continuity for 3-span girder

Figure 5.1 shows the development of restraint moments with time for four cases of bridge with 2spans. The span lengths ratio for the plot is $L_1/L_2 = 1$ and a diaphragm stiffness $I_d/I_g = 1$ thus, the only variable is the girder age at continuity; 28, 60, 90 and 180 days.

Figure 5.2 is a similar plot for the corresponding four cases of 3-span girders with span lengths ratio of 2.0 and diaphragm to girder stiffness ratio of 1.0. The only variable for this plot is the girder age at continuity.

Figures 5.3 through 5.5 are similar plots corresponding to the other cases of parameters for the 2-span cases and Figure 5.6 to Figure 5.8 represent all the plots corresponding to the each case of the parameter for the 3-span cases.

It should be noted that the restraint moments in all these plots are due to the effect of creep, shrinkage and thermal gradient together.

5.3.1 Effect of Age of Continuity on 2-Spans Bridges

Figures 5.3(a) – 5.3(o) can be used to study the effect of age of continuity on the restraint moment values for the 2-span bridges. The plots are grouped by the similar span lengths ratio and diaphragm to girder stiffness thus these four plots represent the different girder ages at continuity.

From all the plots in Figures 5.3(a) – 5.3(o) it is clear that the age of continuity affects the magnitude of the restraint moment. It can be noted from the figures that if the age of girder is early like 28 days when the continuity is established then, higher positive restraint moment will develop, while smaller positive restraint moments develop when the age of girder when the continuity is established is 180 days and these restraint moments can be negative for some cases as well.

The age of the continuity can be studied more if there are any desired values for the final restraint moment value. From these plots, one can calculate the optimum age of the girder depending upon the desired restraint moment value which is done and presented later in this chapter.

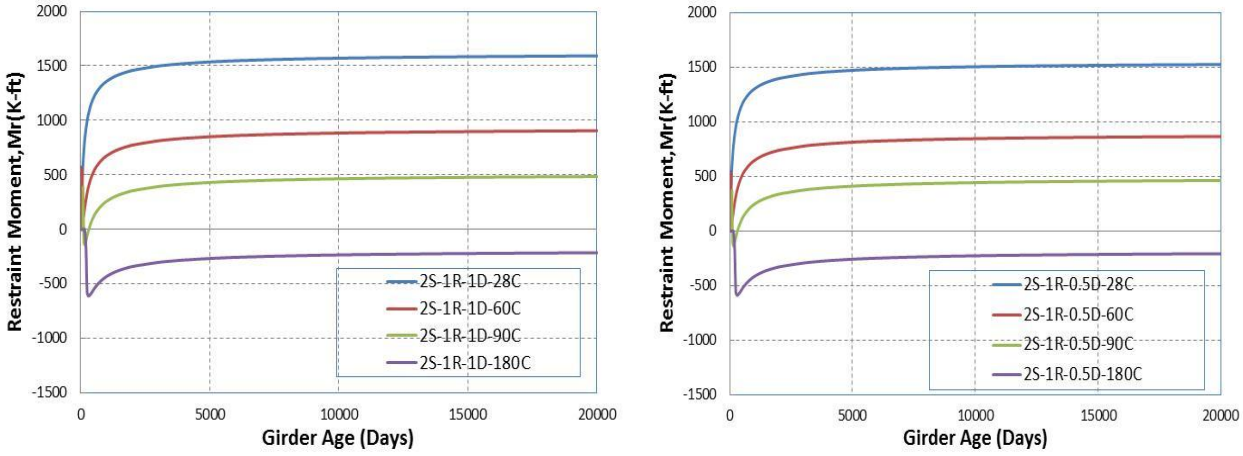

(a) $L_1 = L_2$ and $I_{dia} = I_g$ (b) $L_1 = L_2$ and $I_{dia} = 0.5 * I_g$

Figure 5.3 Effect of Age of Coninuity on Restraint Moment (2-Span)

Figure 5.3 Continued

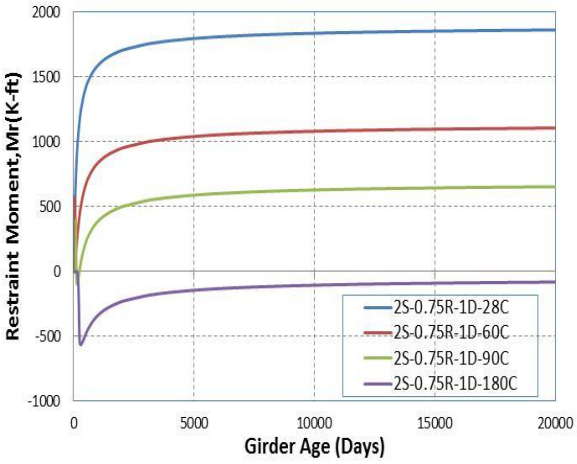

(c) $L_1=0.75*L_2$ and $I_{dia}=I_g$

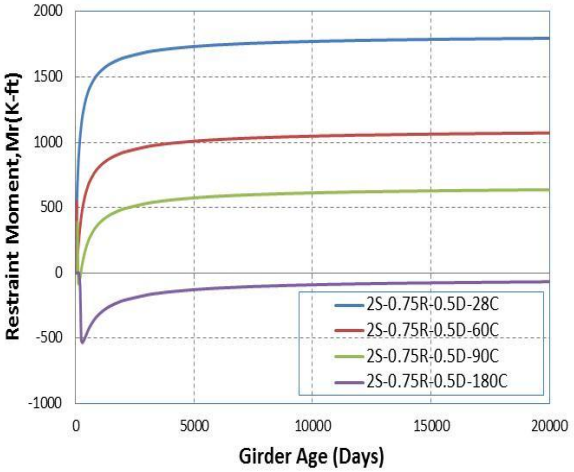

(d) $L_1=0.75*L_2$ and $I_{dia}=0.5*I_g$

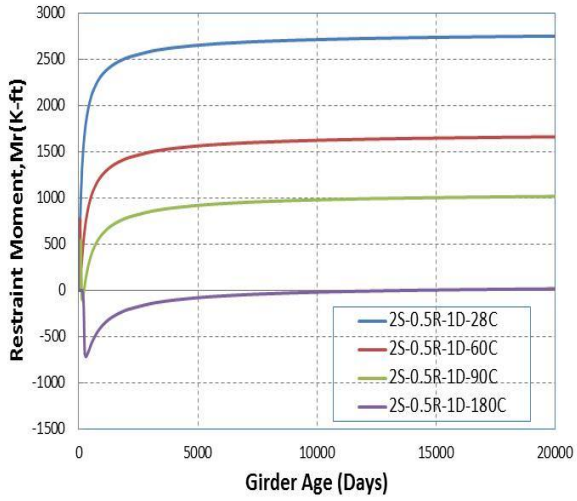

(e) $L_1=0.5*L_2$ and $I_{dia}=I_g$

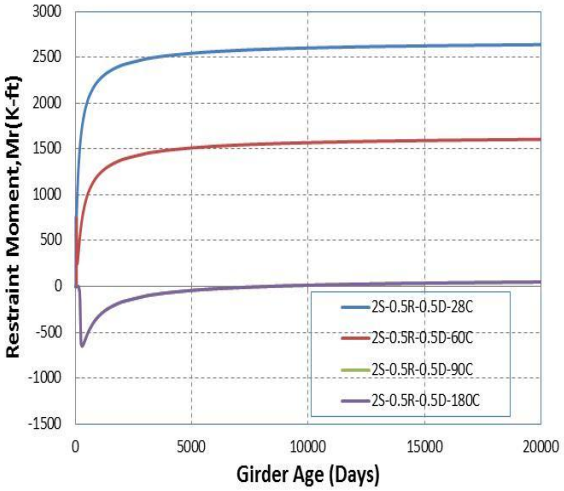

(f) $L_1=0.5*L_2$ and $I_{dia}=0.5*I_g$

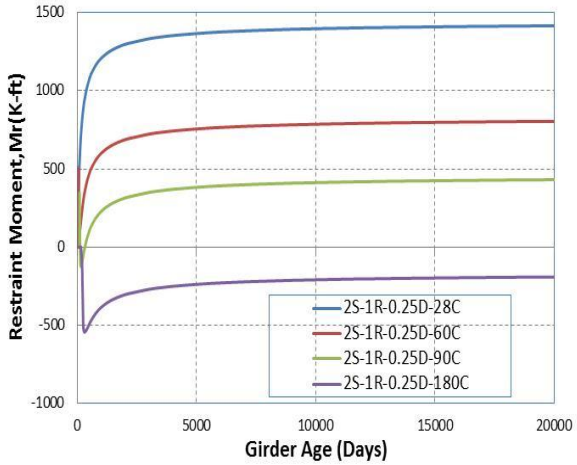

(g) $L_1=L_2$ and $I_{dia}=0.25*I_g$

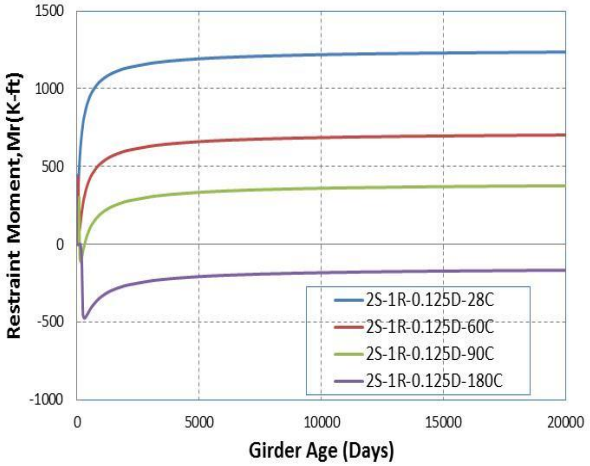

(h) $L_1=L_2$ and $I_{dia}=0.125*I_g$

Figure 5.3 continued

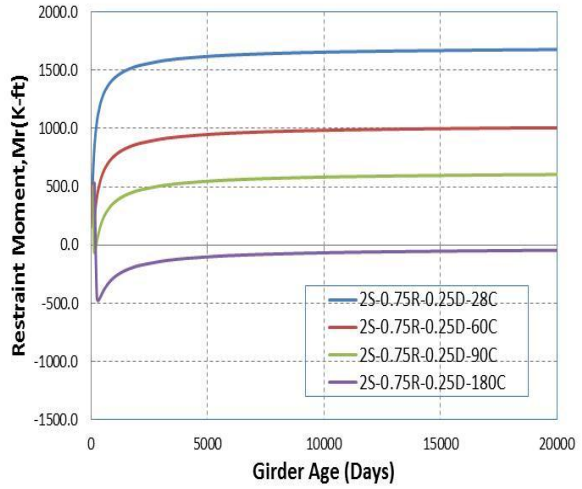

(i) L_1= 0.75*L_2 and I_{dia} =0.25*I_g

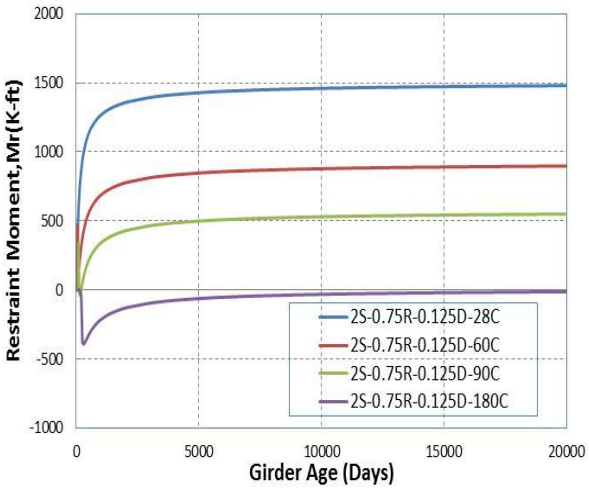

(j) L_1 =0.75*L_2 and I_{dia} =0.125*I_g

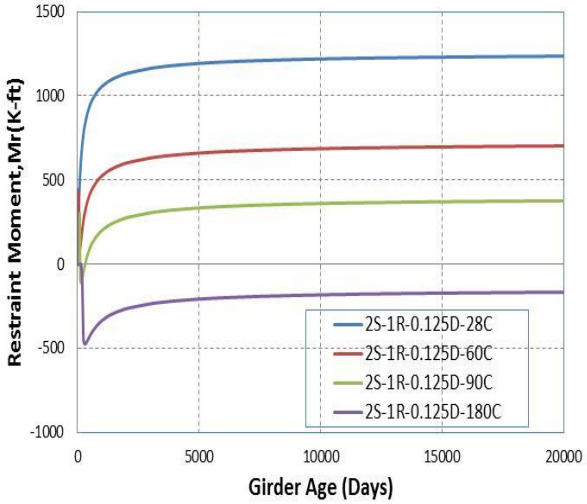

(k L_1 =0.5*L_2 and I_{dia} =.25*I_g

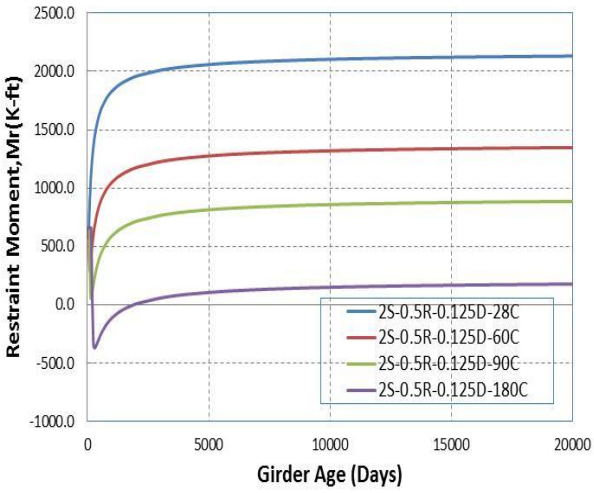

(l) L_1 =0.5*L_2 and I_{dia} =0.125*I_g

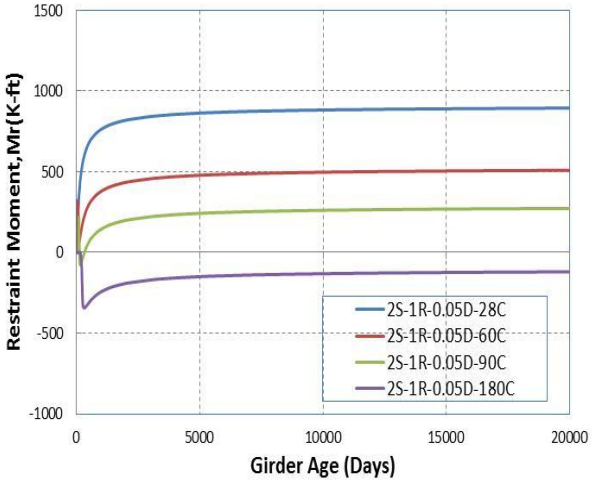

(m) L_1 =L_2 and I_{dia} =0.05*I_g

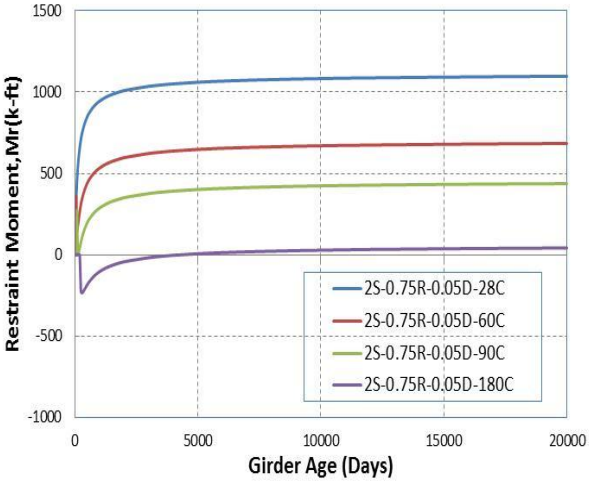

(n) L_1 =0.75*L_2 and I_{dia}=0.05*I_g

Figure 5.3 continued

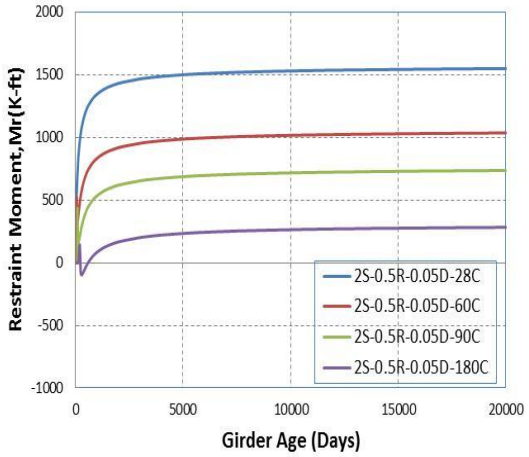

(o) $L_1 = 0.5 * L_2$ and $I_{dia} = 0.05 * I_g$

5.3.2 Effect of span length ratio on 2-Span Bridge

This section presents the effect of the span lengths ratio on the magnitude of the restraint moment for 2-spans bridges. Figures 5.4(a) – 5.4(t) are presented in this section to illustrate the effect of the span length ratios parameter. The plots are grouped by the age of continuity and diaphragm to girder stiffness ratio; hence, three different cases can be seen in each plot, each represents a different spans length ratio. As mentioned earlier, the span length ratios for all the cases for 2-span bridges are 0.5:1, 0.75:1 and 1:1.

(a) Age = 180 days and $I_{dia} = I_g$

(b) Age = 180 days and $I_{dia} = 0.5 * I_g$

Figure 5.4 Effect of Span Length Ratio on Restraint Moment (2-Span)

Figure 5.4 continued

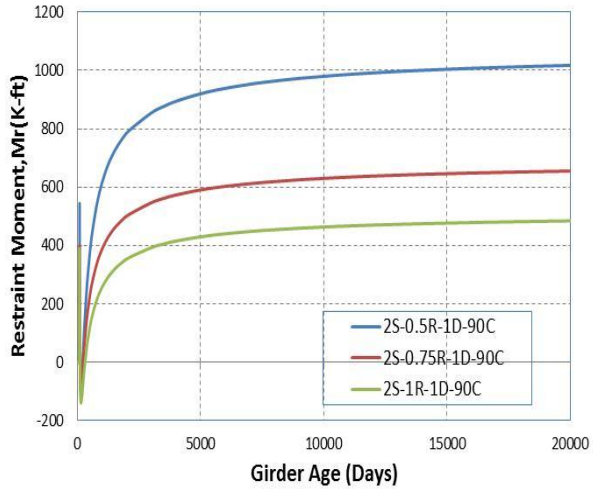

(c) Age = 90 days and $I_{dia} = I_g$

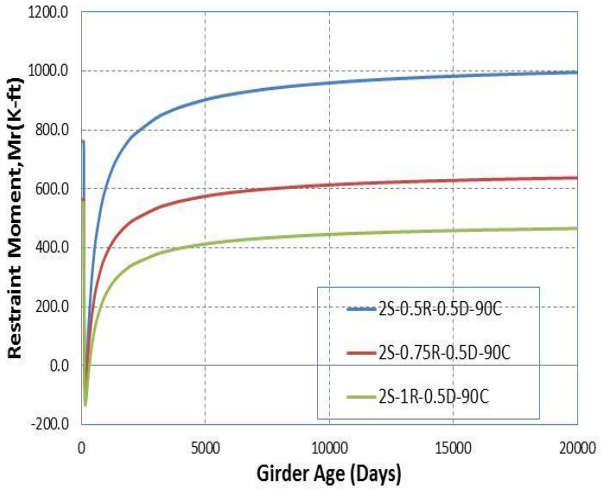

(d) Age = 90 days and $I_{dia} = 0.5* I_g$

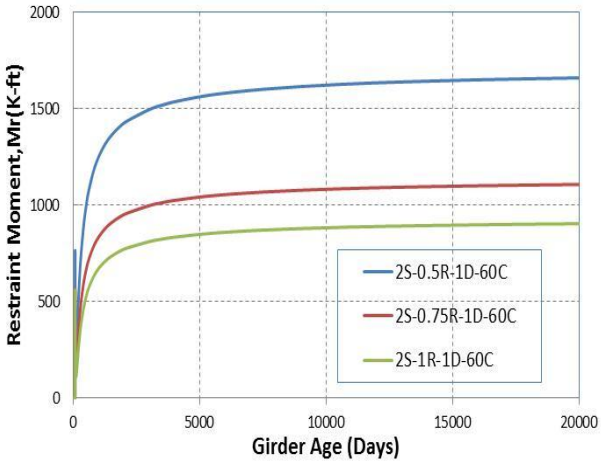

(e) Age = 60 days and $I_{dia} = I_g$

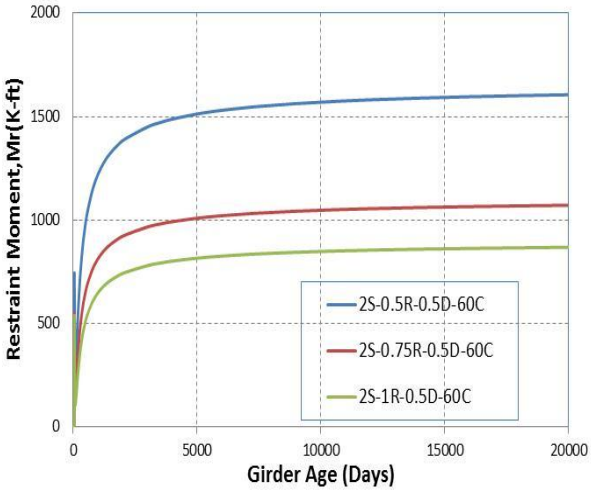

(f) Age = 60 days and $I_{dia} = 0.5* I_g$

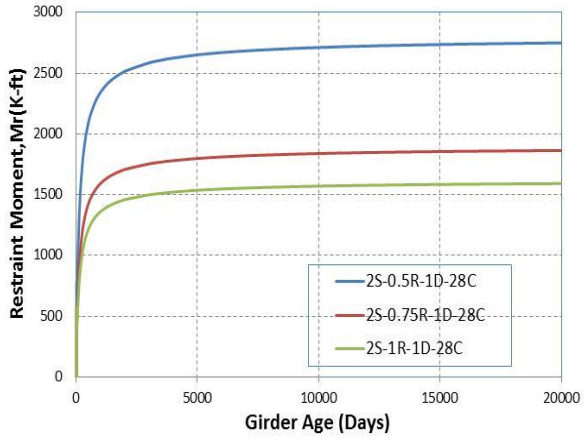

(g) Age = 28 days and $I_{dia} = I_g$

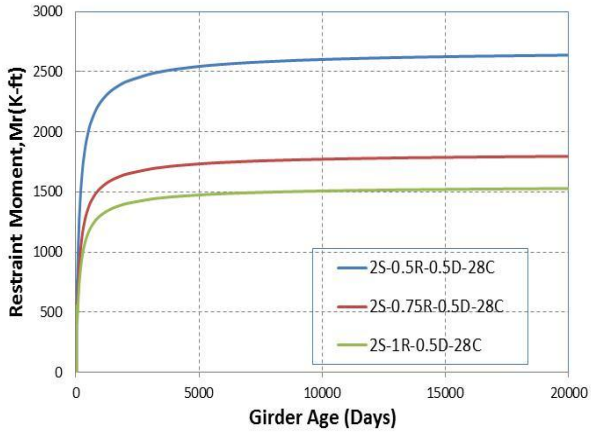

(h) Age = 28 days and $I_{dia} = 0.5* I_g$

Figure 5.4 Continued

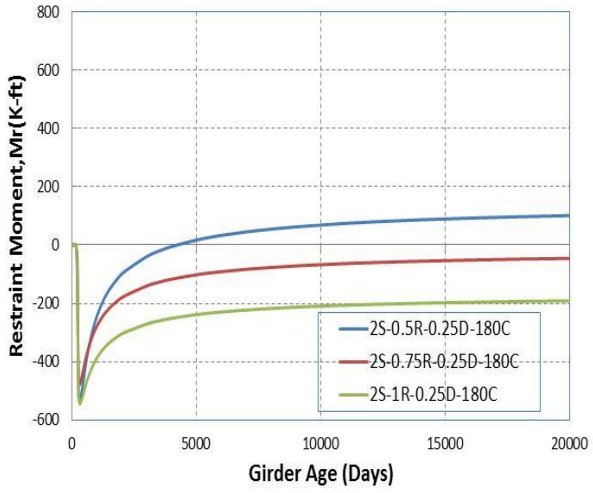

(i) Age = 180 days and I_{dia} = 0.25* I_g

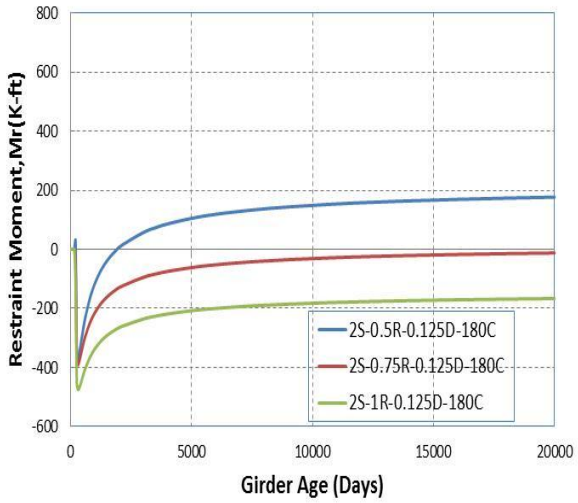

(j) Age = 180 days and I_{dia} = 0.125* I_g

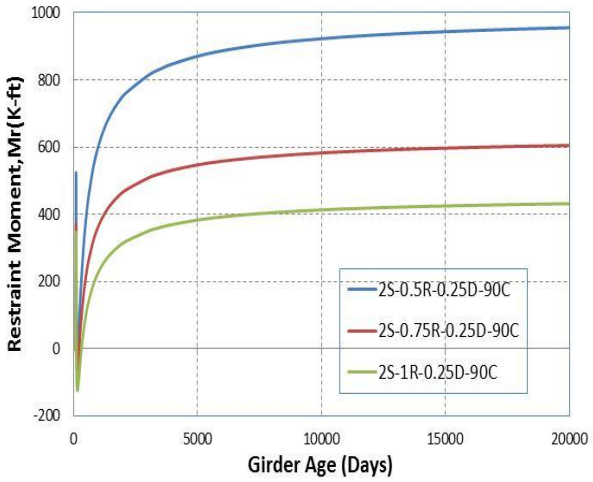

(k) Age = 90 days and I_{dia} = 0.25* I_g

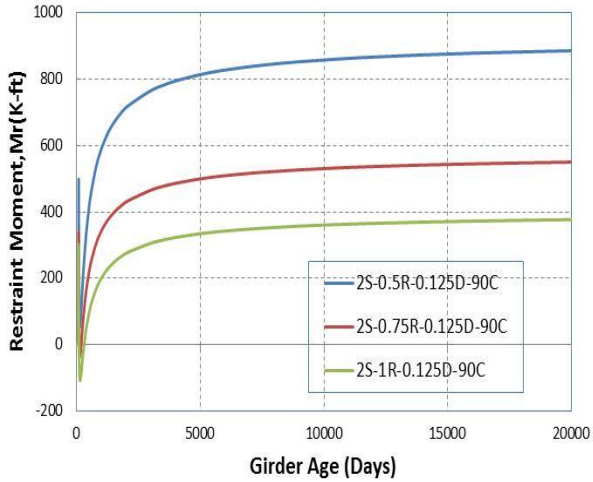

(l) Age = 90 days and I_{dia} = 0.125* I_g

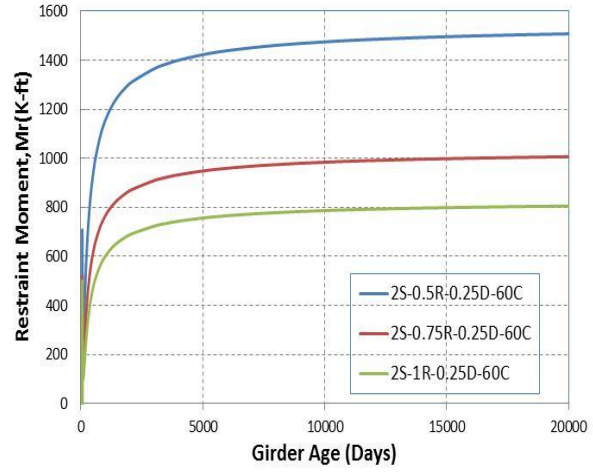

(m) Age = 60 days and I_{dia} = 0.25* I_g

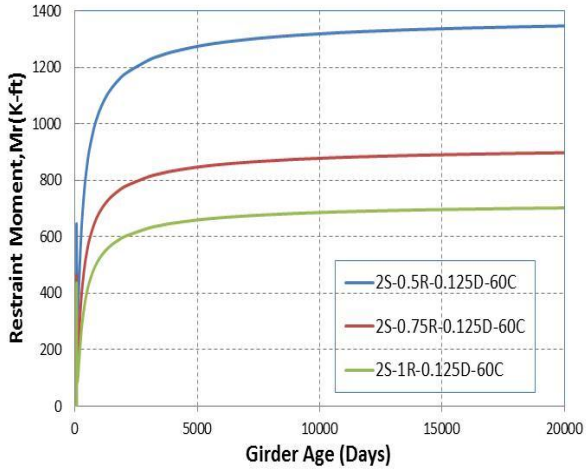

(n) Age = 60 days and I_{dia} = 0.125* I_g

Figure 5.4 continued

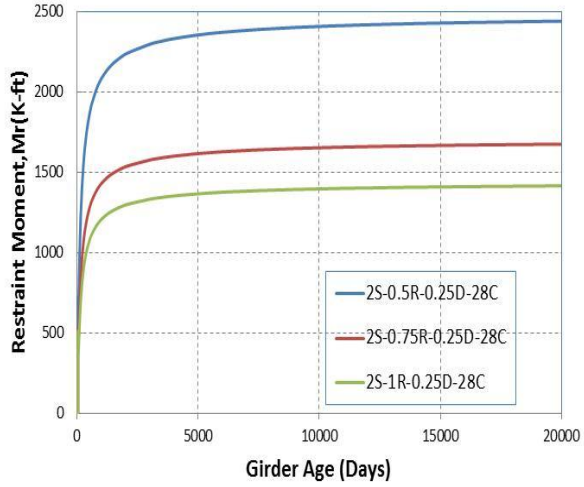

(o) Age = 28 days and $I_{dia} = 0.25*I_g$

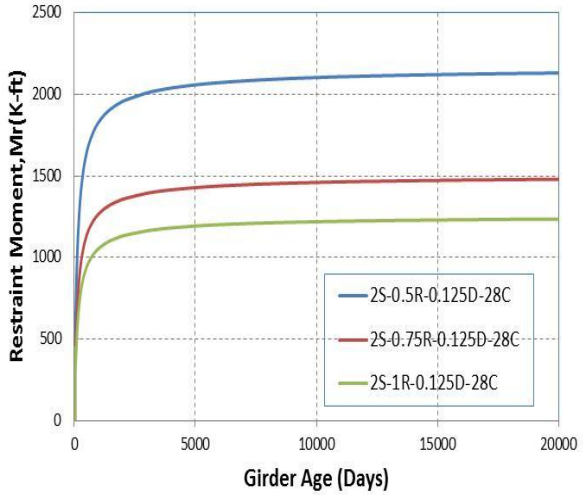

(p) Age = 28 days and $I_{dia} = 0.125* I_g$

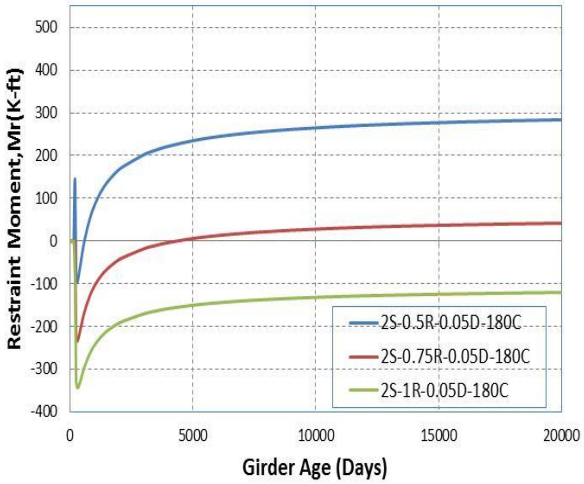

(q) Age = 180 days and $I_{dia} = 0.05* I_g$

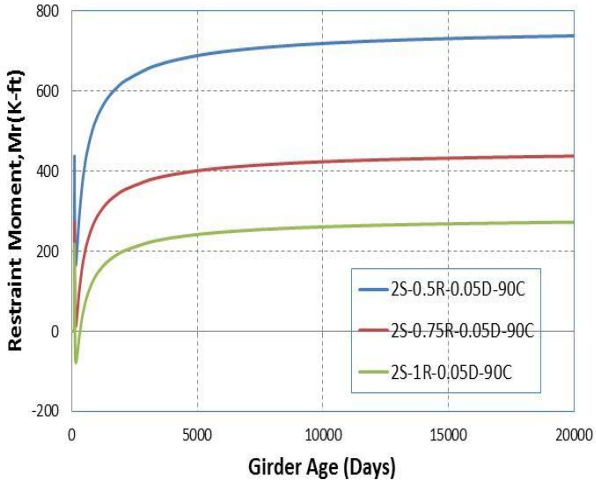

(r) Age = 90 days and $I_{dia} = 0.05* I_g$

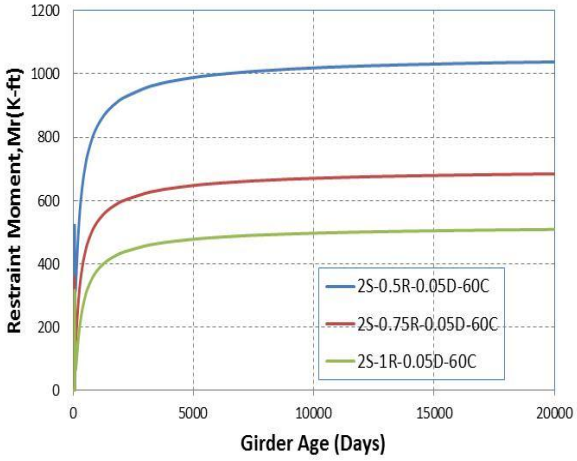

(s) Age = 60 days and $I_{dia} = 0.05* I_g$

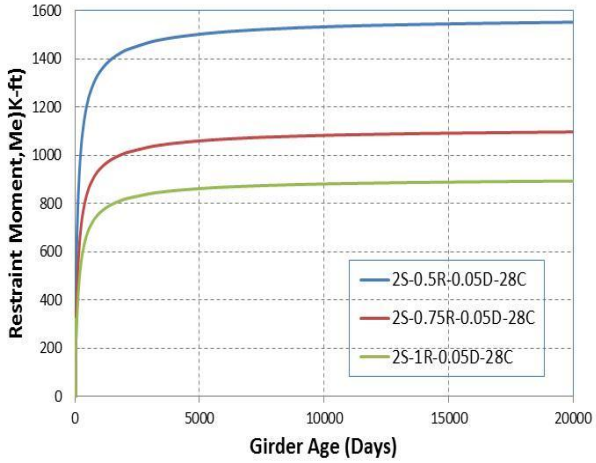

(t) Age = 28 days and $I_{dia} = 0.05* I_g$

From the plots in Figure 5.4, it can be said that higher positive restraint moment develop when the span length ratios are the combination of the short and long span lengths. In other words, the magnitudes of the restraint moment are affected by the span lengths ratios and its value increases or decreases depending upon the age of girder at continuity with the asymmetry of the span lengths ratios. It can also be seen in Figure 5.4 that depending upon the bridge configuration the final restraint moment value can be either positive or negative as a results of the girder age.

5.3.3 Effect of Diaphragm Stiffness Ratio for 2-spans

This section presents the effect of the diaphragm stiffness to the magnitude of the final restraint moment. There are twelve plots (Figures 5.5(a) – 5.5(l)) presented to understand the way how the diaphragm stiffness ratio affects the restraint moment value. The plots are grouped by the other parameters span length ratio and girder age at continuity thus; five plots can be seen in each figure corresponding to the five diaphragm stiffness ratios considered in this study.

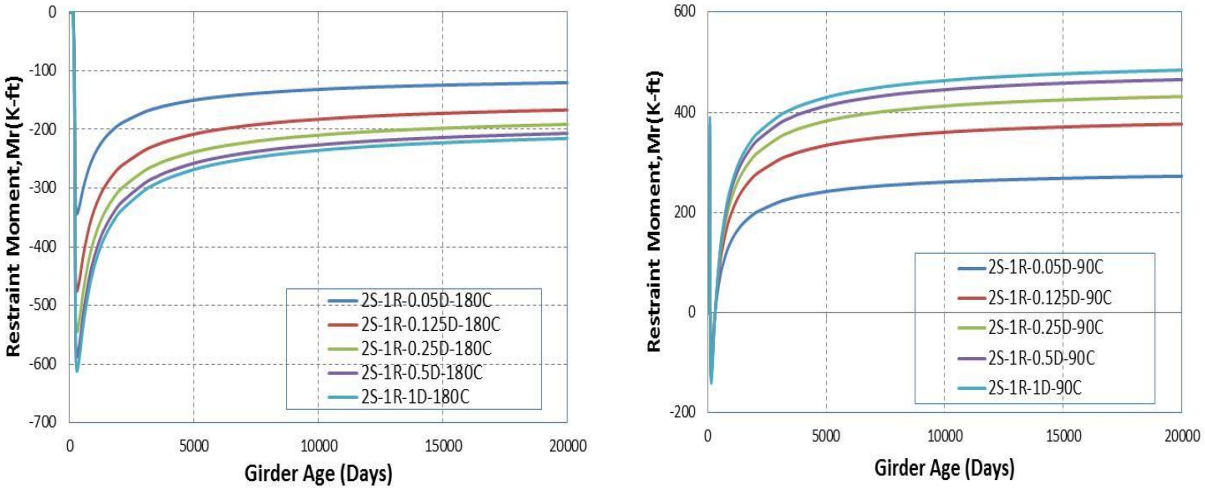

(a) $L_1 = L_2$ and Age = 180 days (b) $L_1 = L_2$ and Age = 90 days

Figure 5.5 Effect of Diaphram Stiffness Ratio on Restraint Moment (2-Span)

Figure 5.5 continued

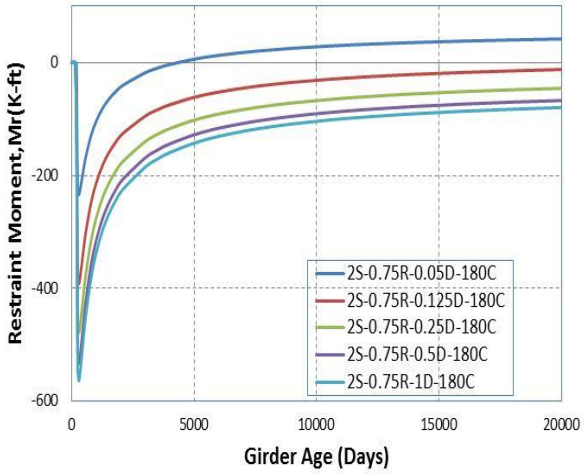

(c) $L_1 = 0.75*L_2$ and Age = 180 days

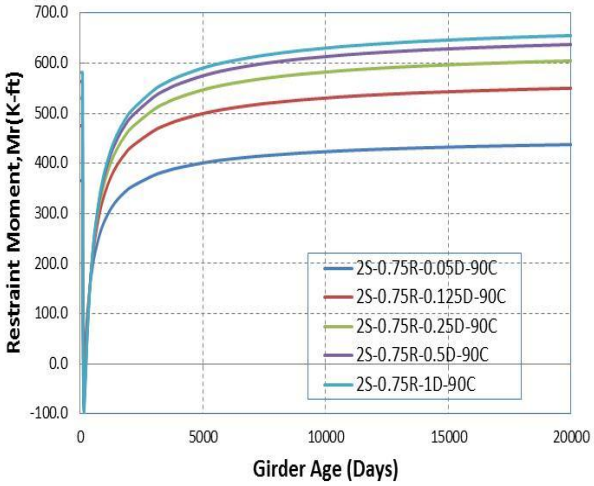

(d) $L_1 = 0.75*L_2$ and Age = 90 days

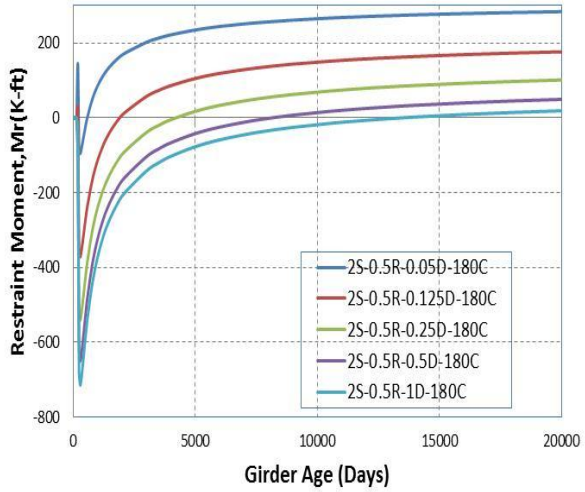

(e) $L_1 = 0.5*L_2$ and Age = 180 days

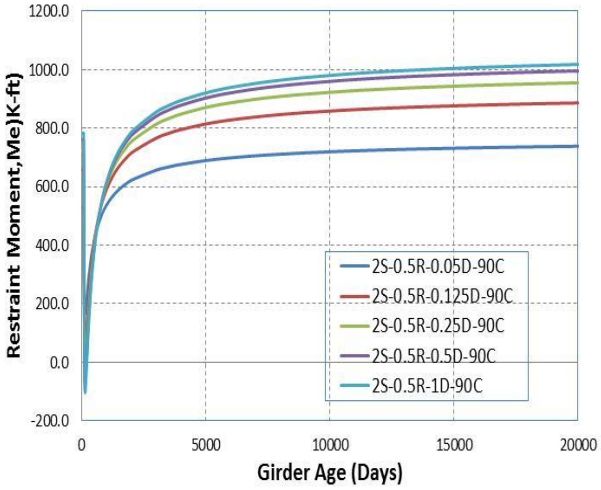

(f) $L_1 = 0.5*L_2$ and Age = 90 days

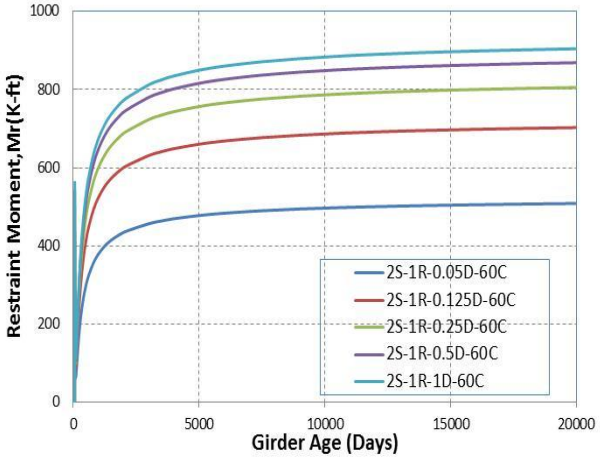

(g) $L_1 = L_2$ and Age = 60 days

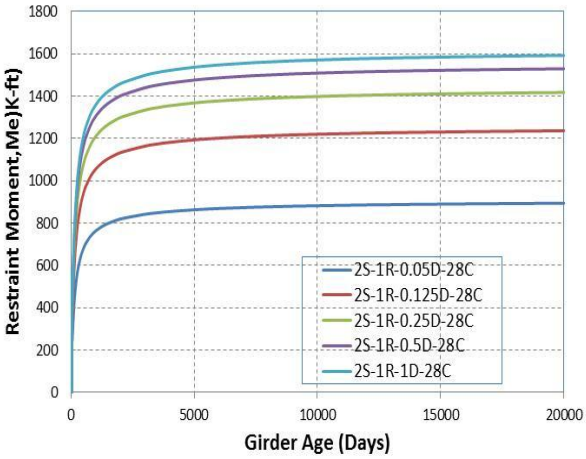

(h) $L_1 = L_2$ and Age = 28 days

Figure 5.5 continued

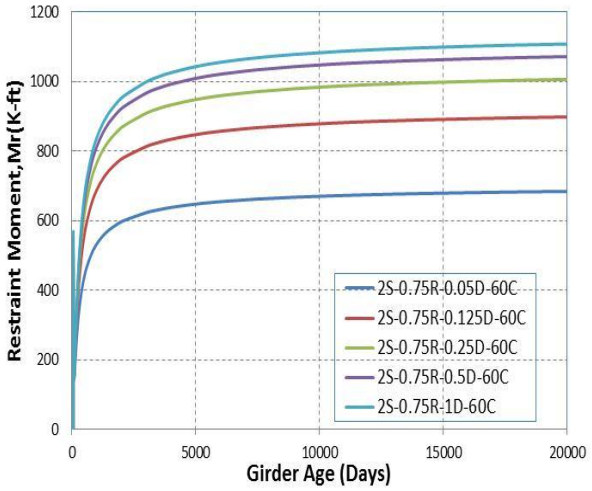

(i) $L_1 = 0.75*L_2$ and Age = 60 days

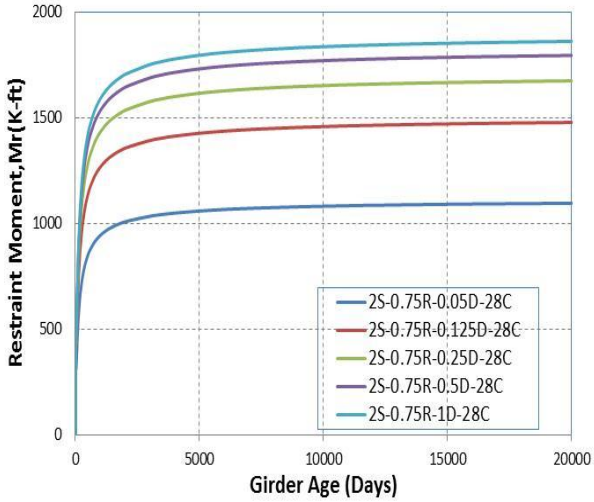

(j) $L_1 = 0.75*L_2$ and Age = 28 days

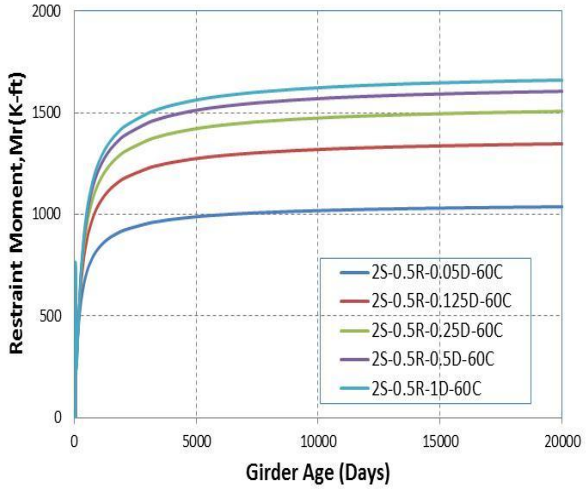

(k) $L_1 = 0.5*L_2$ and Age = 60 days

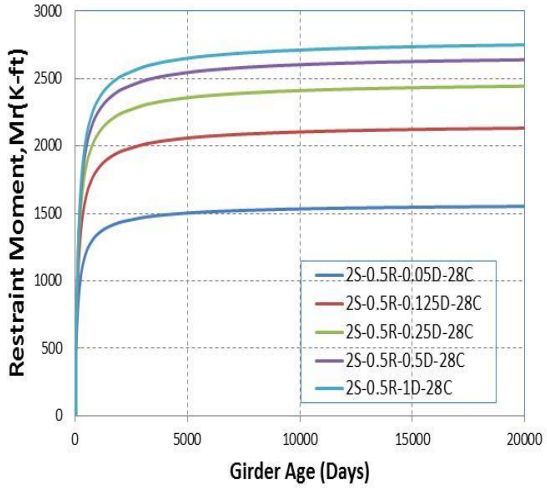

(l) $L_1 = 0.5*L_2$ and Age = 28 days

From the plots presented on Figures 5.5, it can be concluded that diaphragm stiffness ratio affects the total magnitude of final restraint moment values. It can be seen that lower negative final restraint moment values are achieved when the diaphragm to girder stiffness ratio is high when the girder age at continuity is established at later ages. However, when the girder age at continuity is established at early ages then the higher positive final restraint moment values can be achieved for the same diaphragm to girder ratios. For example in Figure 5.5(a), it can be seen

that the lower negative restraint moment values can be seen when the diaphragm to girder stiffness ratio is 1 when the girder age at continuity is 180 days.

Likewise, if figure 5.5(l) is analyzed then it can be noticed that the higher positive restraint moment values are achieved when the diaphragm to girder stiffness ratio is equal to 1.00 and the lower positive restraint moments are achieved when the diaphragm to girder stiffness ratio is low like 0.05 and 0.125. Therefore, it can be concluded that restraint moment increases when the diaphragm stiffness is increased.

In summary, the parameters age of continuity, span lengths ratio and the diaphragm stiffness ratio affects the total magnitude of the final restraint moment values.

5.3.4 Effect of Age at Continuity on 3-Spans Bridges

This section presents the effect of the age of continuity on 3-span bridges. Total numbers of 15 figures from Figures 5.6(a) – 5.6(o) are presented. The plots are grouped by span lengths ratio and diaphragm stiffness ratio, thus the four different plots represent the different girder ages at continuity.

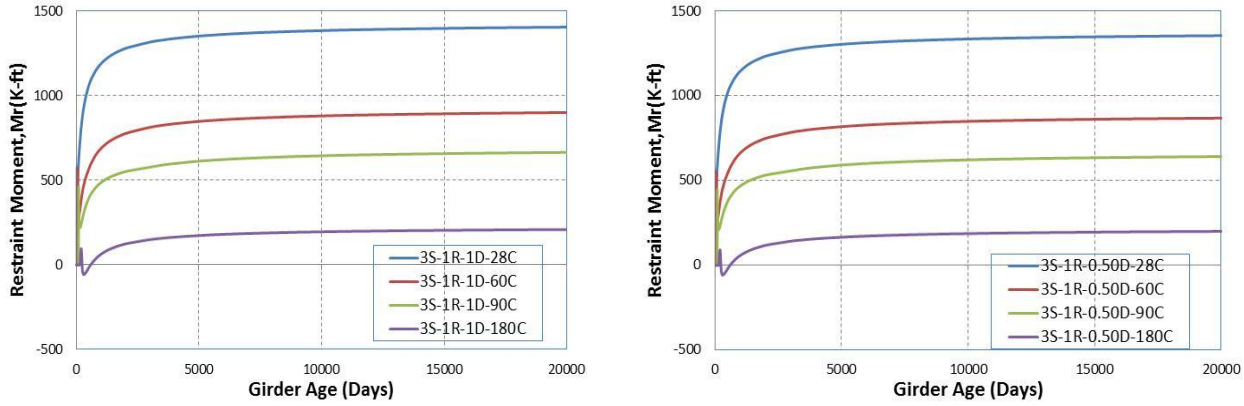

(a) $L_1 = L_2 = L_3$ and $I_{dia} = I_g$ (b) $L_1 = L_2 = L_3$ and $I_{dia} = 0.5*I_g$

Figure 5.6 Effect of Age of Continuity on Restraint Moment (3-Span)

Figure 5.6 continued

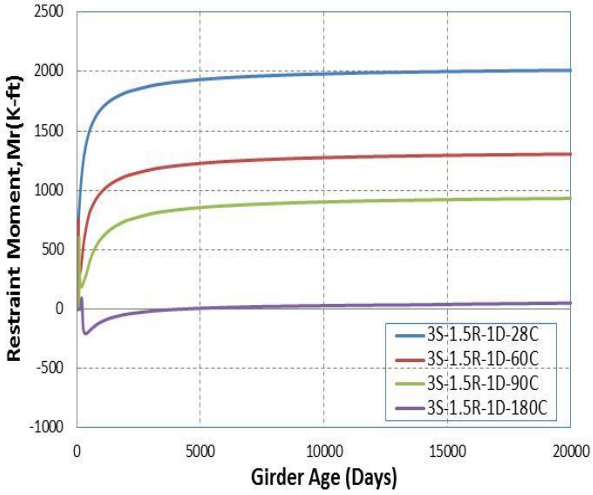

(c) $L_2 = 1.5* L_1 = 1.5*L_3$ and $I_{dia} = I_g$

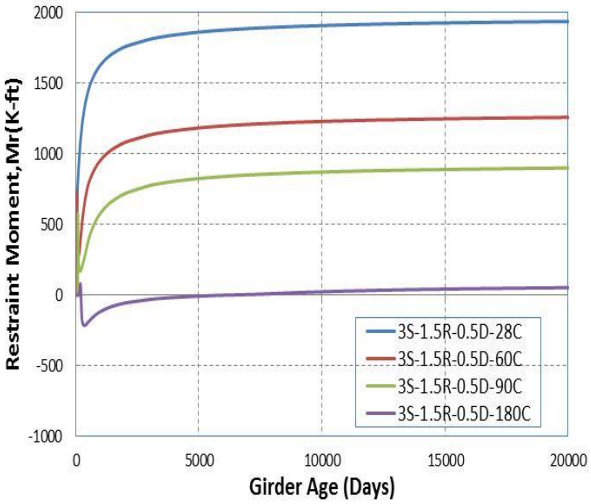

(d) $L_2 = 1.5* L_1 = 1.5*L_3$ and $I_{dia} = 0.5*I_g$

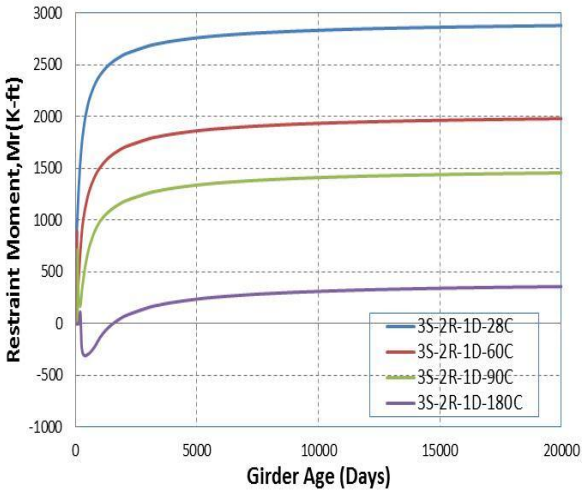

(e) $L_2 = 2.0* L_1 = 2.0*L_3$ and $I_{dia} = I_g$

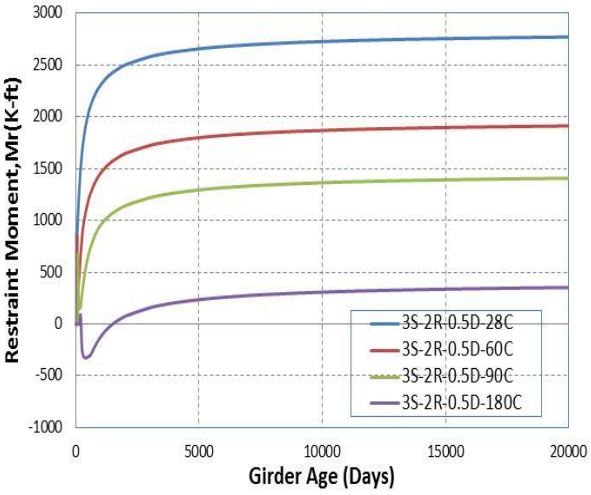

(f) $L_2 = 2.0* L_1 = 2.0*L_3$ and $I_{dia} = I_g$

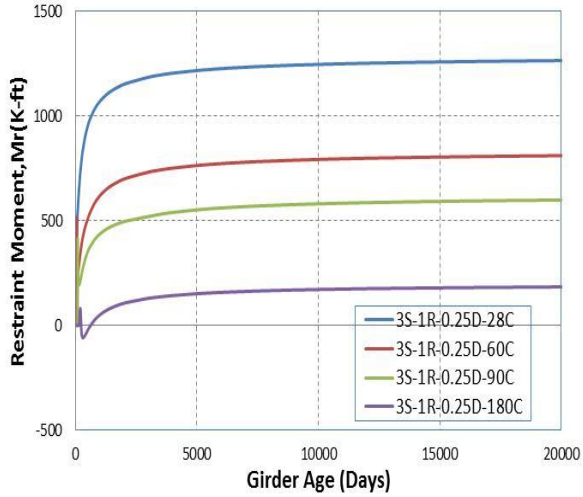

(g) $L_1 = L_2 = L_3$ and $I_{dia} = I_g$

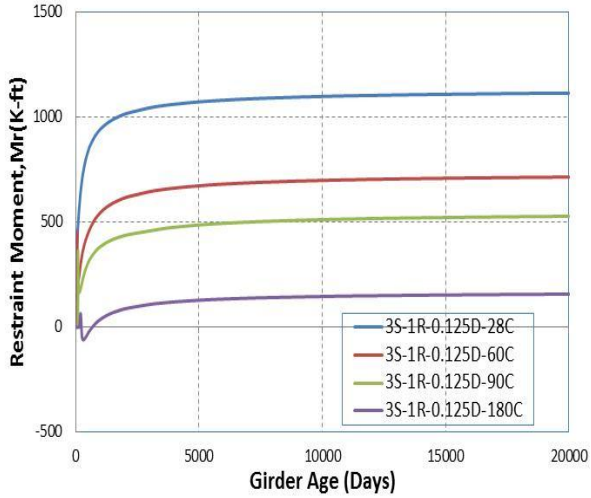

(h) $L_1 = L_2 = L_3$ and $I_{dia} = I_g$

Figure 5.6 continued

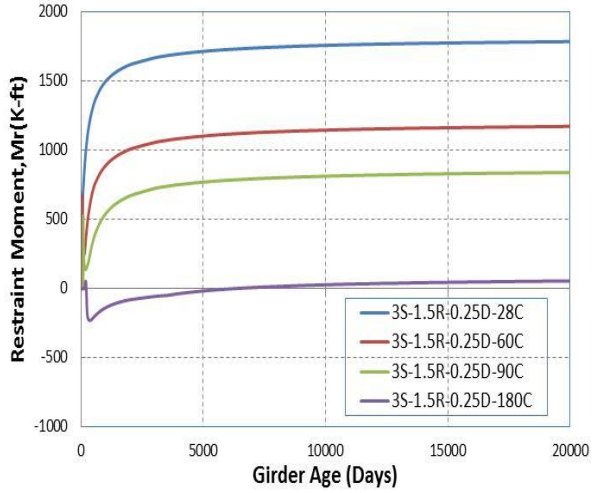

(i) $L_2 = 1.5*L_1 = 1.5*L_3$ and $I_{dia} = 0.25*I_g$

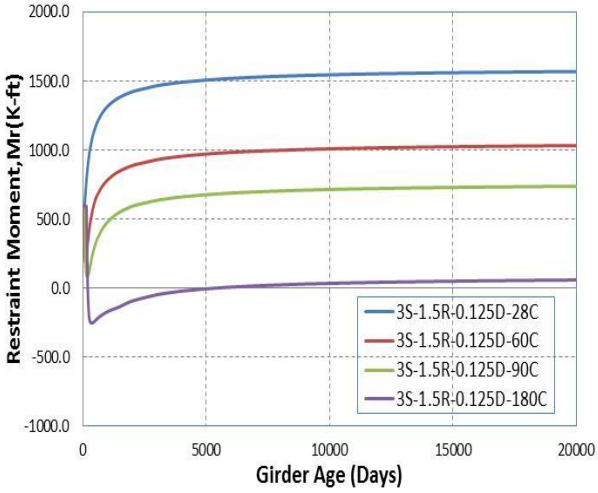

(j) $L_2 = 1.5*L_1 = 1.5*L_3$ and $I_{dia} = 0.125*I_g$

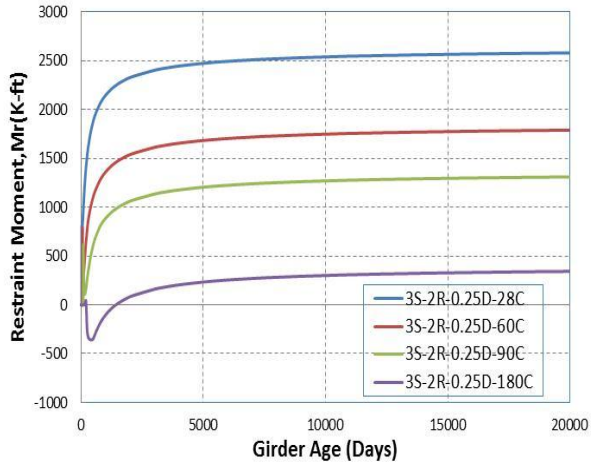

(k) $L_2 = 2.0*L_1 = 2.0*L_3$ and $I_{dia} = 0.25*I_g$

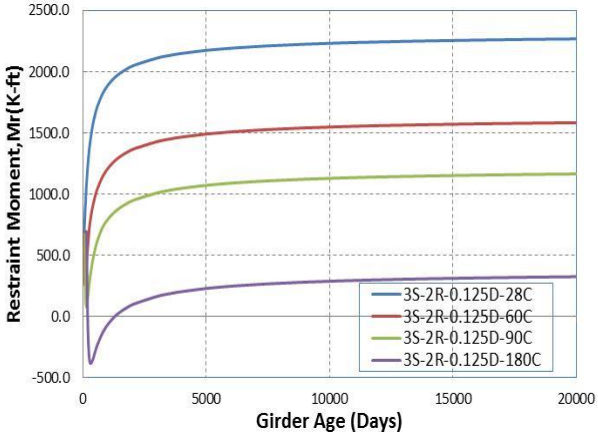

(l) $L_2 = 2.0*L_1 = 2.0*L_3$ and $I_{dia} = 0.125*I_g$

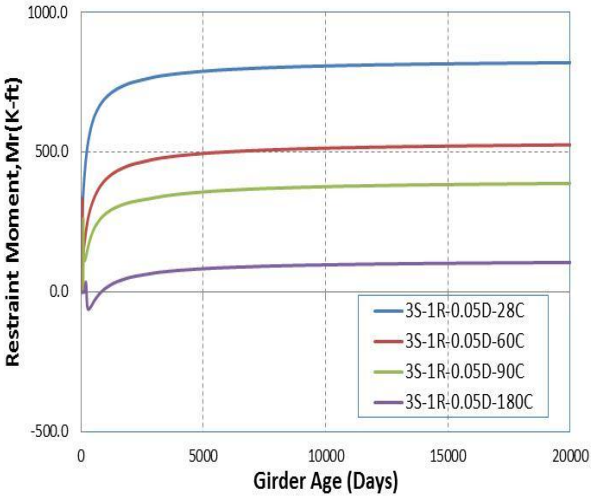

(m) $L_1 = L_2 = L_3$ and $I_{dia} = 0.05*I_g$

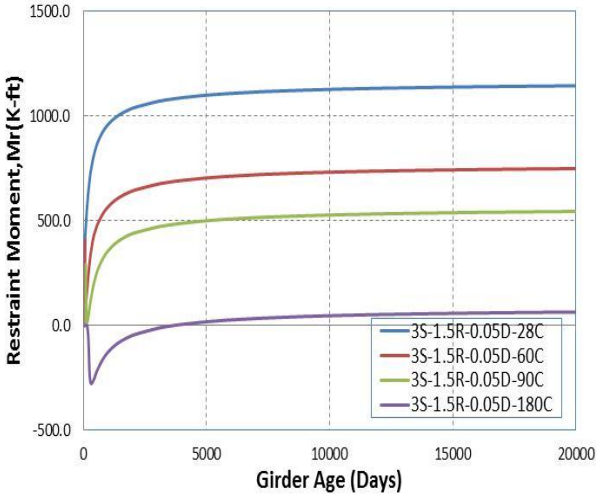

(n) $L_2 = 1.5*L_1 = 1.5*L_3$ and $I_{dia} = 0.05*I_g$

Figure 5.6 continued

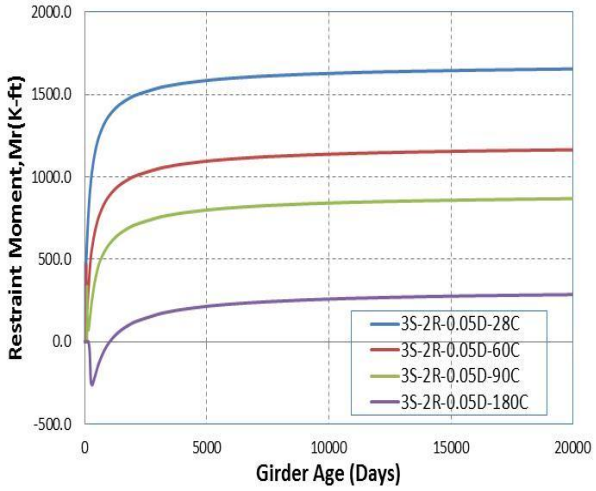

(o) $L_2 = 2.0*L_1 = 2.0*L_3$ and $I_{dia} = 0.05*I_g$

From the above plots, it is clear that the age of continuity affects the magnitude of the restraint moment. It can be noted from the figures that the higher positive restraint moment values are developed when the girder age at continuity is at early days and when the age of girder at continuity is at the later ages the lower negative restraint moment values are achieved. Therefore, it can be deduced that the age of continuity affects the final magnitude of the restraint moments.

If the girder age when the continuity is established is early like 28 days then the final restraint moment value was found to be positive but when the continuity is established at later ages like 90 and 180 days then the magnitude of the restraint moment values can be positive or negative and it depends upon the bridge's configuration. Furthermore, the age of girder when the continuity is established can be studied for the case when the desired final restraint moment value is known. Ages of continuity for the girders are studied and presented in detail later in this chapter for the 3-span girders.

5.3.5 Effect of Span Length Ratio (3-Spans)

This section presents the effect of the span lengths ratio on the magnitude of the restraint moment for 3 spans bridges. Twenty figures (Figures 5.7(a) – 5.7(t)) are presented in this section to illustrate the effect of the span lengths ratio parameter. The plots are grouped by the age of continuity and diaphragm to girder stiffness ratio; hence, three cases can be seen in each plot, each represents a different span lengths ratio. As mentioned earlier, the span length ratios for all the cases for 3-span bridges are 1:1:1, 1:1.5:1 and 1:2:1.

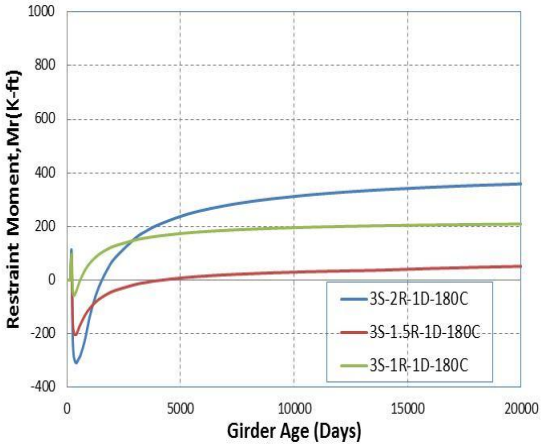

(a) Age = 180 days and $I_{dia} = I_g$

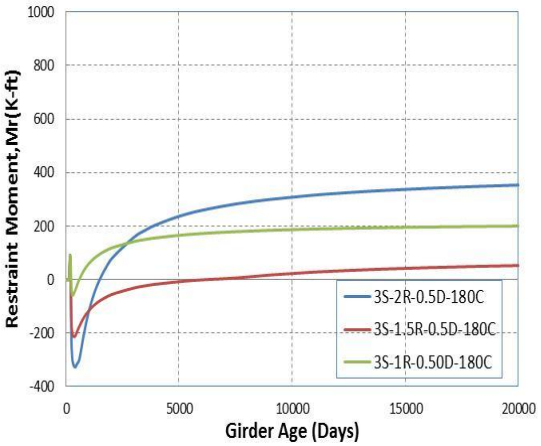

(e) Age = 180 days and $I_{dia} = 0.5*I_g$

(b) Age = 90 days and $I_{dia} = I_g$

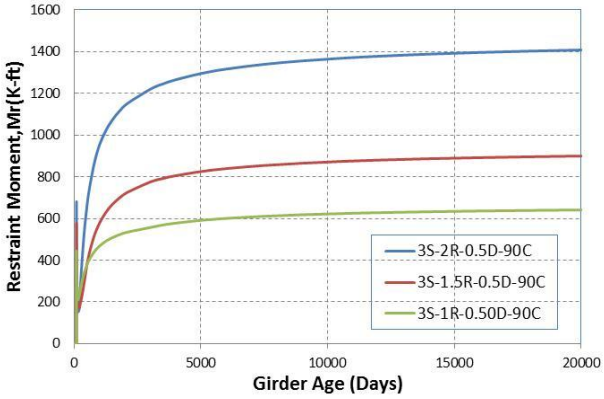

(f) Age = 90 days and $I_{dia} = 0.5*I_g$

Figure 5.7 Effect of Span Length Ratio on Restraint Moment (3-Span)

Figure 5.7 continued

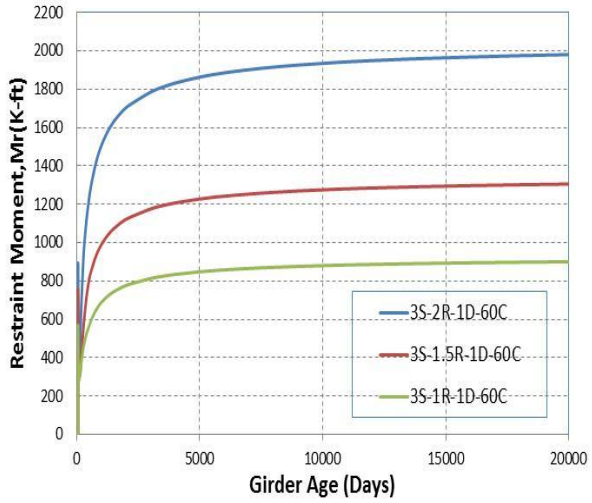

(c) Age = 60 days and $I_{dia} = I_g$

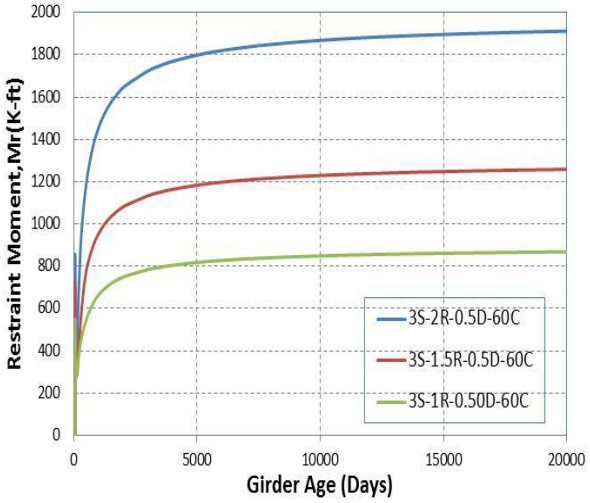

(g) Age = 60 days and $I_{dia} = 0.5*I_g$

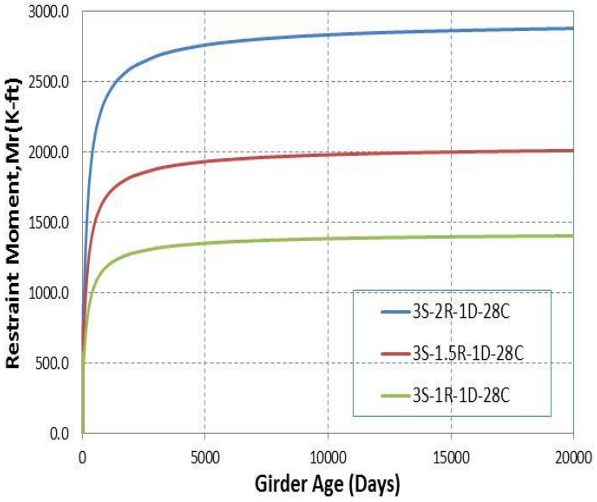

(d) Age = 28 days and $I_{dia} = I_g$

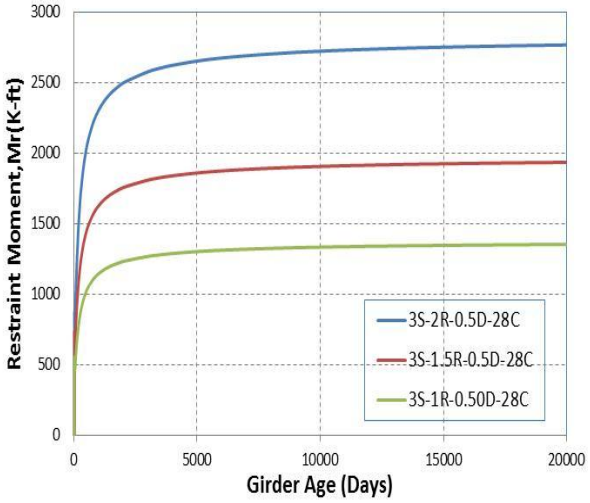

(h) Age = 28 days and $I_{dia} = 0.5*I_g$

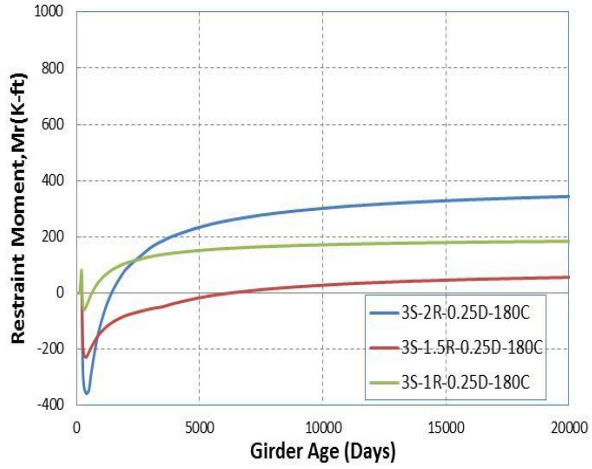

(i) Age = 180 days and $I_{dia} = 0.25*I_g$

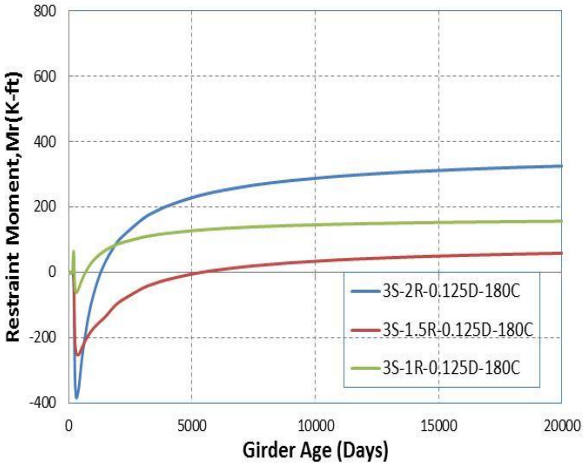

(m) Age = 180 days and $I_{dia} = 0.125*I_g$

Figure 5.7 continued

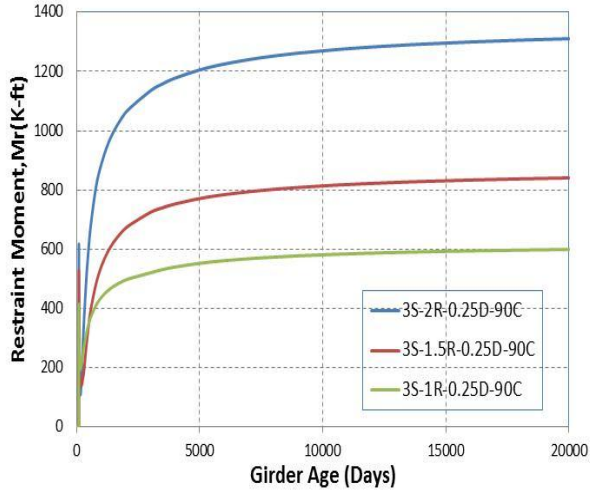

(j) Age = 90 days and $I_{dia} = 0.25*I_g$

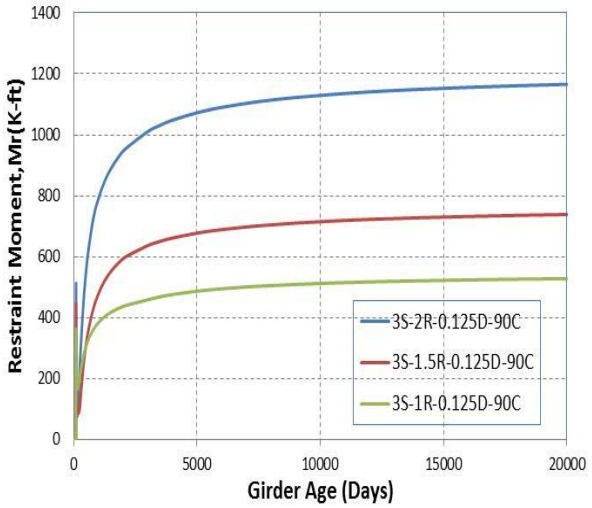

(n) Age = 90 days and $I_{dia} = 0.125*I_g$

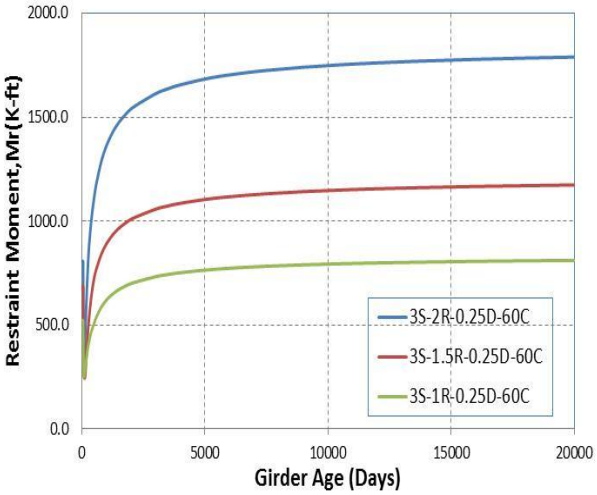

(k) Age = 60 days and $I_{dia} = 0.25*I_g$

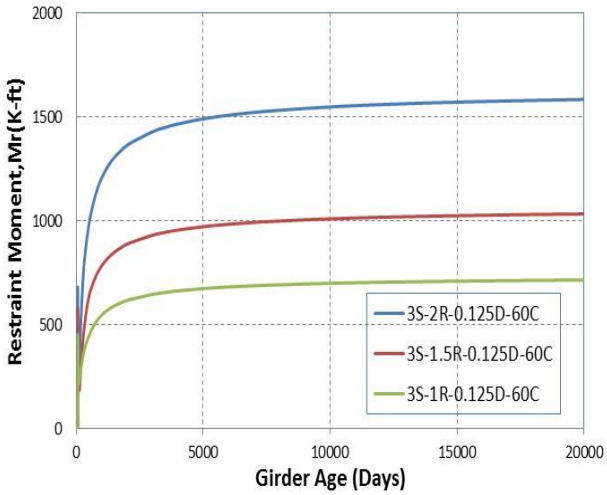

(o) Age = 60 days and $I_{dia} = 0.125*I_g$

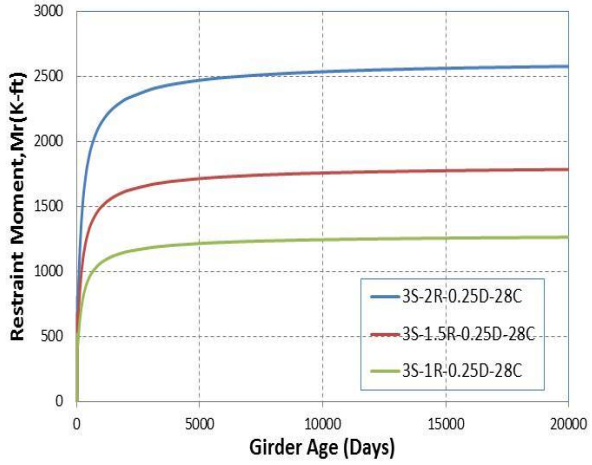

(l) Age = 28 days and $I_{dia} = 0.25*I_g$

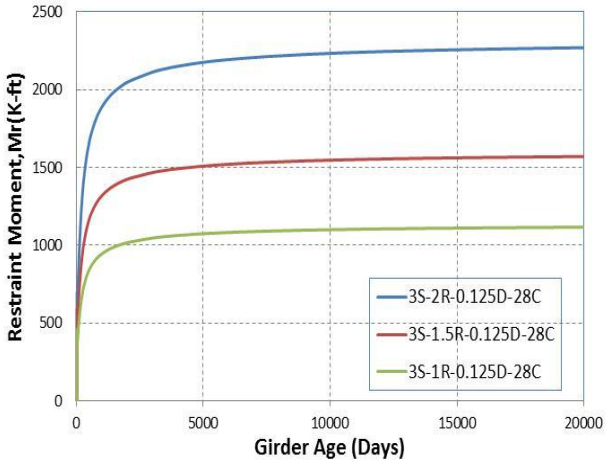

(p) Age = 28 days and $I_{dia} = 0.125*I_g$

Figure 5.7 continued

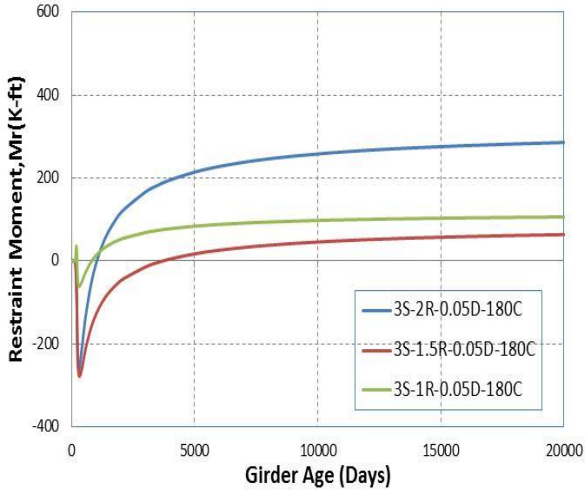

(q) Age = 180 days and $I_{dia} = 0.05*I_g$

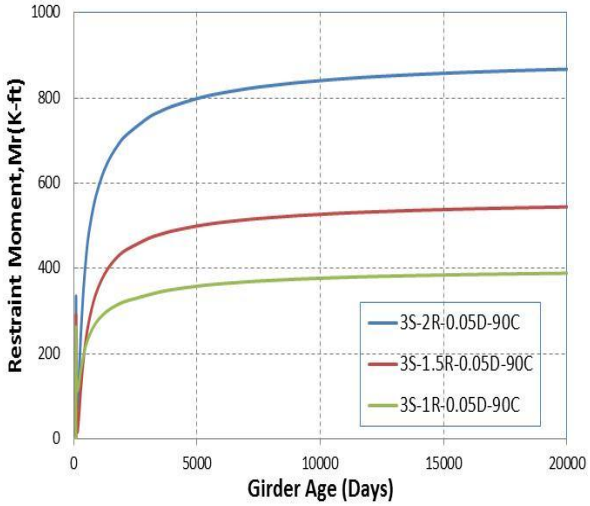

(r) Age = 90 days and $I_{dia} = 0.05*I_g$

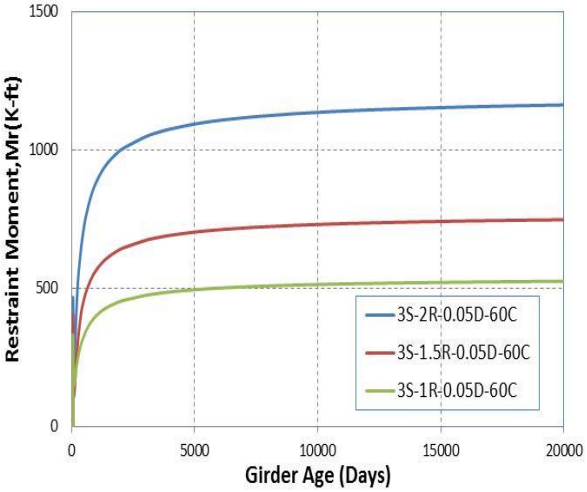

(s) Age = 60 days and $I_{dia} = 0.05*I_g$

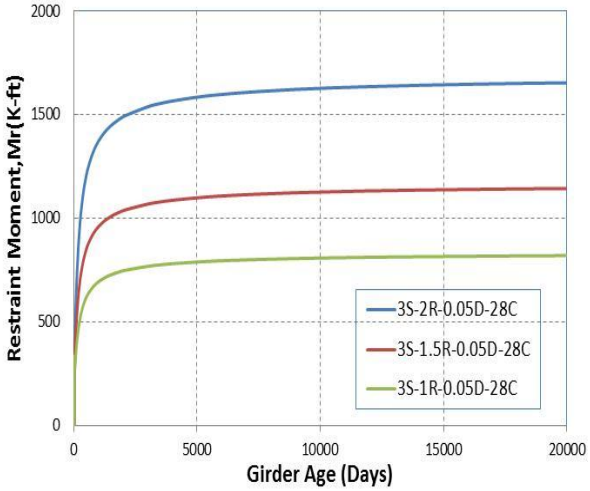

(t) Age = 28 days and $I_{dia} = 0.05*I_g$

From the plots presented in the Figure 5.7, it can be concluded that higher positive restraint moment develop when the span length ratios are the combination of the short and long span lengths. In other words the magnitudes of the restraint moment are affected by the span lengths ratio and its value increases or decreases depending upon the age of girder at continuity with the asymmetry of the span lengths ratio.

The magnitude of the final restraint moment value can be either positive or negative and it depends upon the bridge's configuration.

5.3.6 Effect of Diaphragm Stiffness Ratio on 3-span bridges

This section presents the effect of the diaphragm stiffness to girder stiffness ratio on the magnitude of the final restraint moment. There are twelve figures (Figure 5.8(a) – 5.8 (I)) which show how the diaphragm stiffness ratio affects the total restraint moments. The plots are grouped by the other parameters span lengths ratio and girder age at continuity thus, five plots can be seen in each figure corresponding to the five diaphragm stiffness ratios considered in this study.

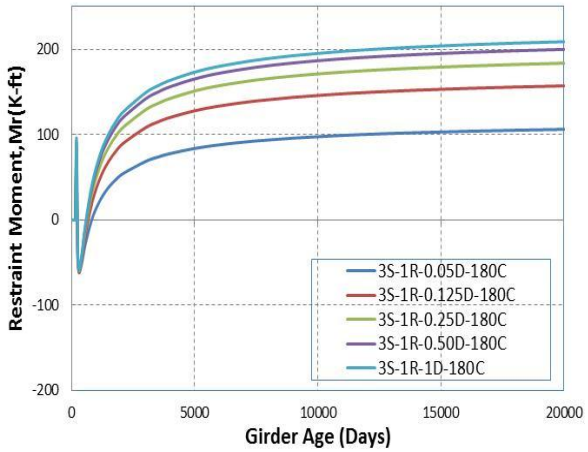

(a) $L_1 = L_2 = L_3$ and Age = 180 days

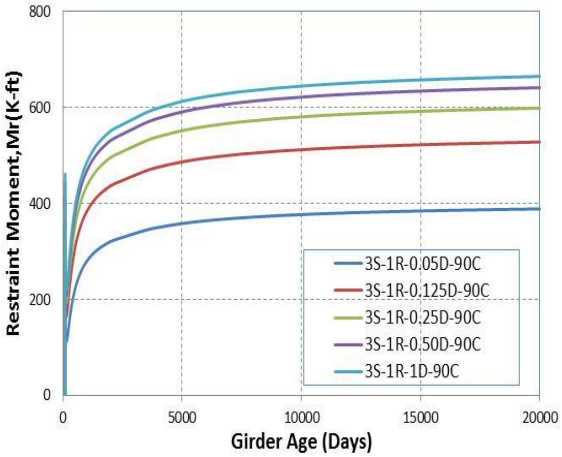

(d) $L_1 = L_2 = L_3$ and Age = 90 days

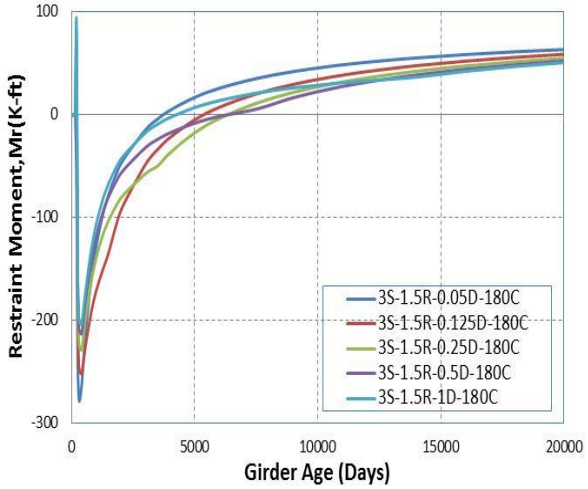

(b) $L_2 = 1.5*L_2 = 1.5*L_3$ and Age = 180 days

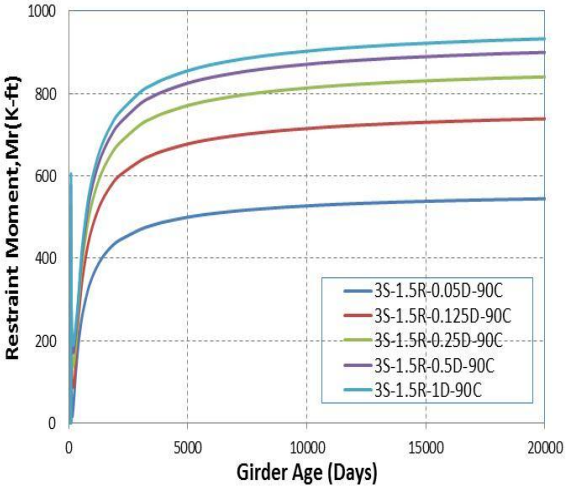

(e) $L_2 = 1.5*L_2 = 1.5*L_3$ and Age = 90 days

Figure 5.8 Effect of Diaphragm Stiffness Ratio on Restraint Moment (3-Span)

Figure 5.8 continued

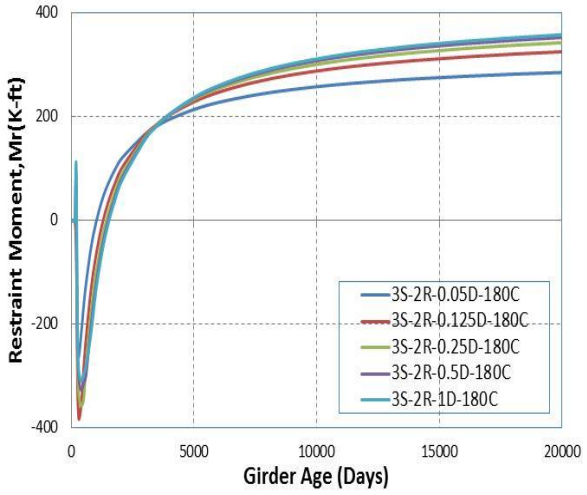

(c) $L_2 = 2.0*L_2 = 2.0*L_3$ and Age = 180 days

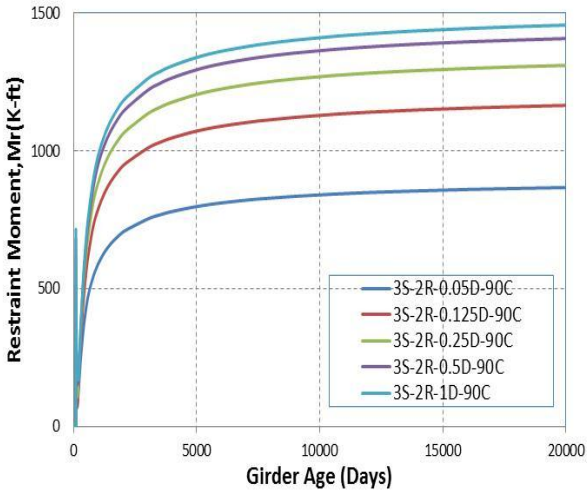

(f) $L_2 = 2.0*L_2 = 2.0*L_3$ and Age = 90 days

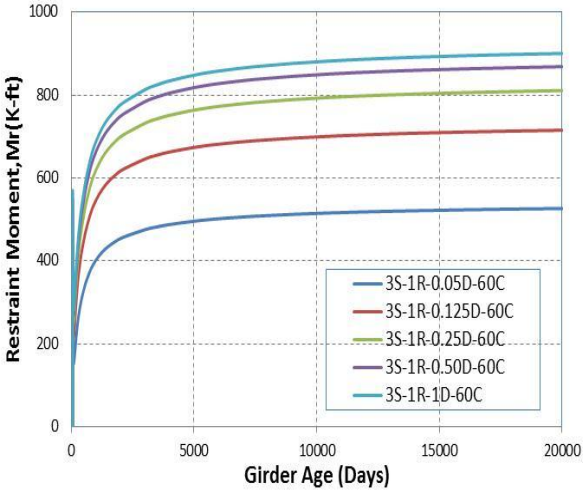

(g) $L_1 = L_2 = L_3$ and Age = 60 days

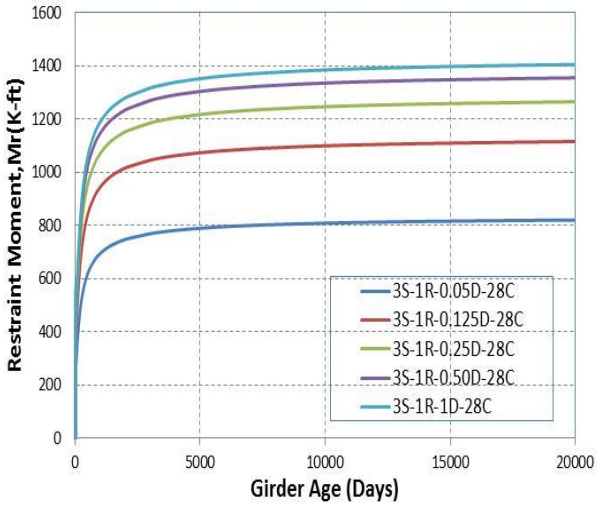

(j) $L_1 = L_2 = L_3$ and Age = 28 days

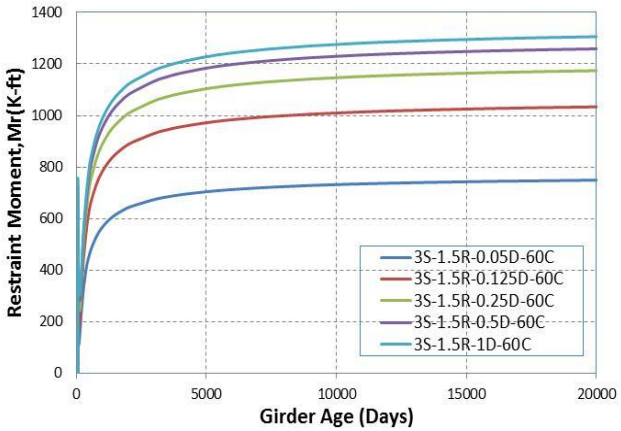

(h) $L_2 = 1.5L_1 = 1.5*L_3$ and Age = 60 days

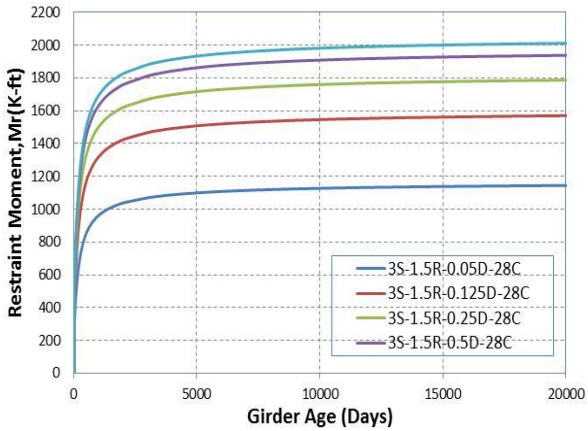

(k) $L_2 = 1.5L_1 = 1.5*L_3$ and Age = 28 days

Figure 5.8 continued

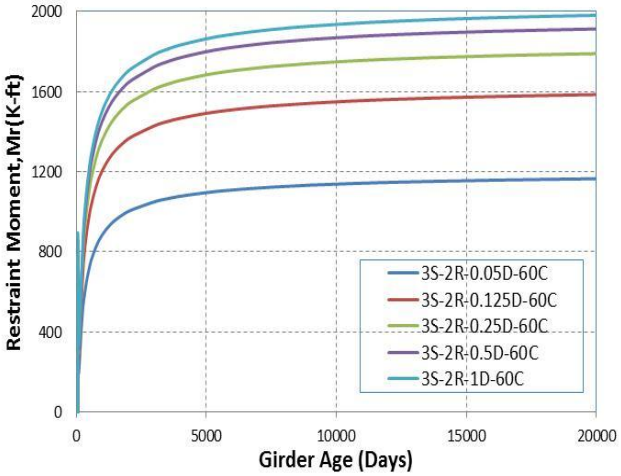

(i) $L_2 = 2.0L_1 = 2.0*L_3$ and Age = 60 days

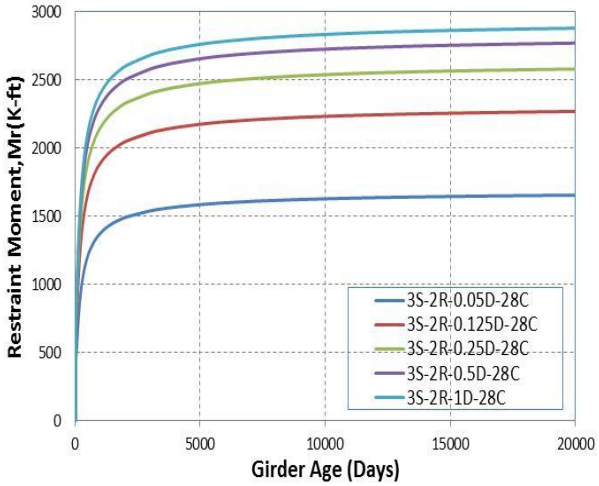

(l) $L_2 = 2.0L_1 = 2.0*L_3$ and Age = 28 days

From the twelve figures presented on the Figure 5.8, it can be seen that diaphragm stiffness ratio affects the final restraint moment values. It can be concluded that the lower negative restraint moment values are achieved when the diaphragm to girder stiffness ratio is 1.0 when the girder age at continuity is established at later ages. However, higher positive final restraint moment values can be achieved when the girder age at continuity is established at early ages when the diaphragm to girder stiffness ratio is 1.0. Therefore, it can be concluded that restraint moment increases if the diaphragm stiffness is increased.

5.4 Optimum Age at Continuity

As it was shown in the previous section, all studied parameters (span lengths ratio, diaphragm to girder stiffness ratio and the age of continuity) affect the magnitude of the final restraint moments that develop in continuous bridge girders. The girder's age when the continuity is established is the most influential in all these factors leading to high restraint moments for early girder ages (e.g. 28 days). Therefore, it was deemed that further investigation of age of continuity was needed

Results from the parametric study are used to determine an optimum girder age at time of establishing continuity such that an allowable restraining moment is exceeded. The portion of the calculated cracking moment of girder was considered as the allowable restraint moment.

The girder's age of continuity is determined by interpolation between results obtained for the for the corresponding desired or allowable restraint moment value obtained for the considered girder ages (28, 60, 90 and 180 days). This exercise was done for restraint moment values at a girder age of 7500 days and 20000 days. The allowable restraint moment values considered in this study was taken equal to 25%, 50%, 75% and 90% of the cracking moment. For example, the 2-span continuous bridge with a diaphragm to girder stiffness ratio equal to 0.05 and for all the considered span lengths ratio (0.5:1, 0.75:1 and 1:1) i.e., cases 2S-0.5R-0.05D, 2S-0.75R-0.05D and 2S-1R-0.05D, the calculated restraint moment value at 20000 days from the modified mRESTRAINT program are plotted in Figure 5.9 for allowable restraint moments. Optimum ages for continuity can be easily determined from the figure for the 2S-0.5R-0.05D, 2S-0.75R-0.05D and 2S-1R-0.05D.

This approach was used to determine the optimum age at continuity for all cases considered in the parametric study considering moment values at 20000 days and 7500 days. Figures 5.10 through 5.13 represent the plots created to calculate the target age at continuity for all cases.

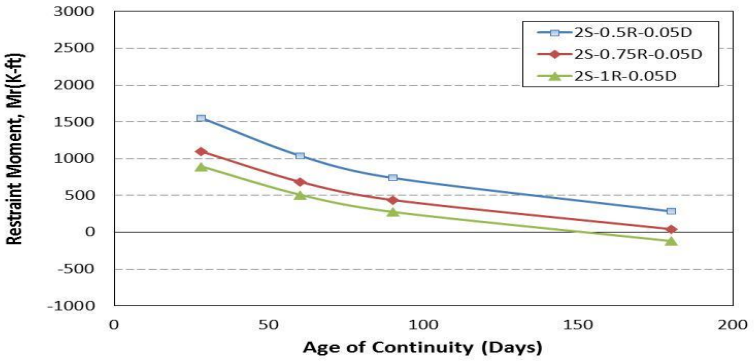

Figure 5.9 Restraint Moment vs. Target Age at Continuity for 2-Span Bridge (20000 days)

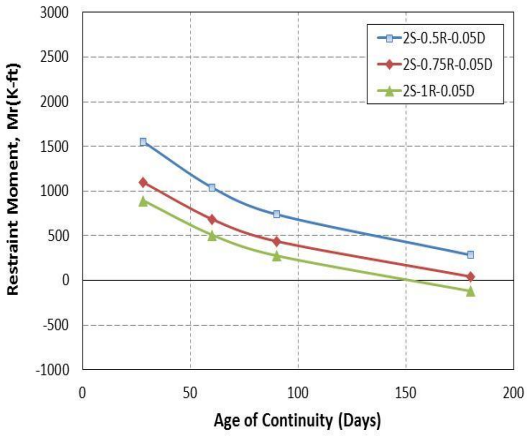

(a) $I_{dia} = 0.05 * I_g$

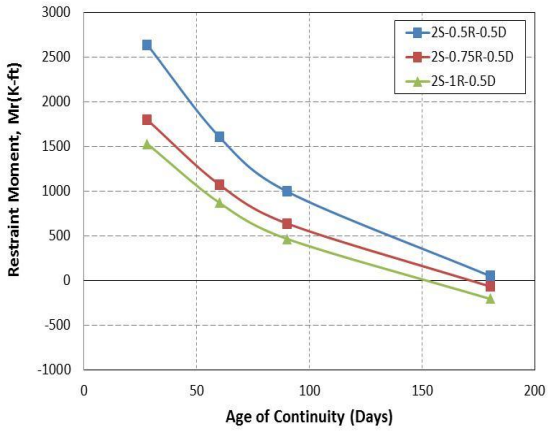

(b) $I_{dia} = 0.5 * I_g$

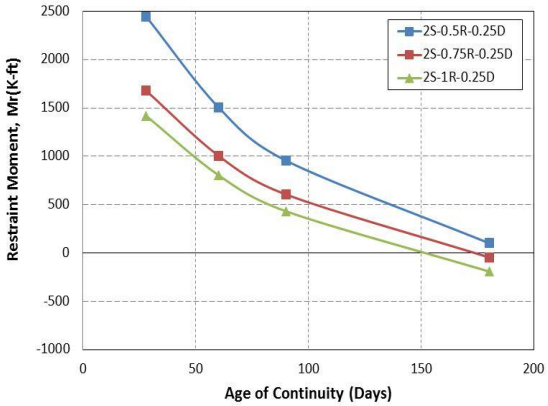

(c) $I_{dia} = 0.25 * I_g$

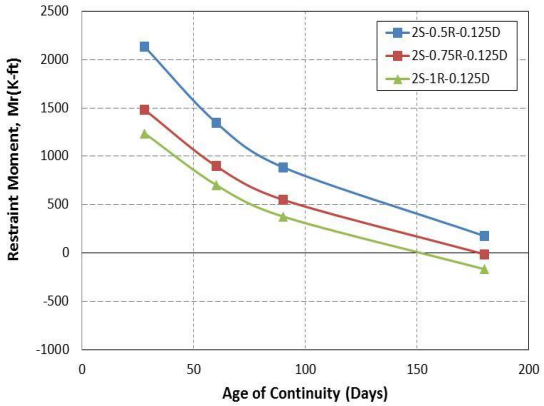

(d) $I_{dia} = 0.125 * I_g$

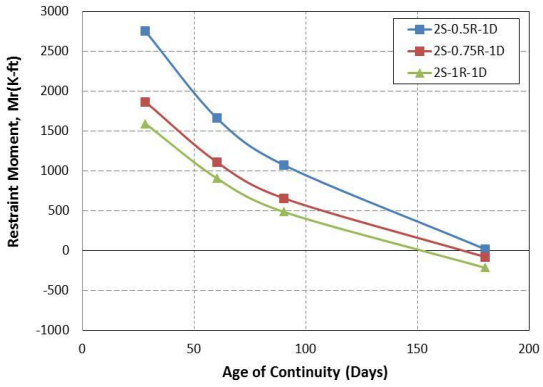

(e) $I_{dia} = I_g$

Figure 5.10 Restraint Moment vs Age at Continuity for 2-Span Bridge Cases (20000 days)

Figure 5.11 displays the plots drawn to calculate optimum age of two spans bridges girders when restraint moment is taken for 7500 days.

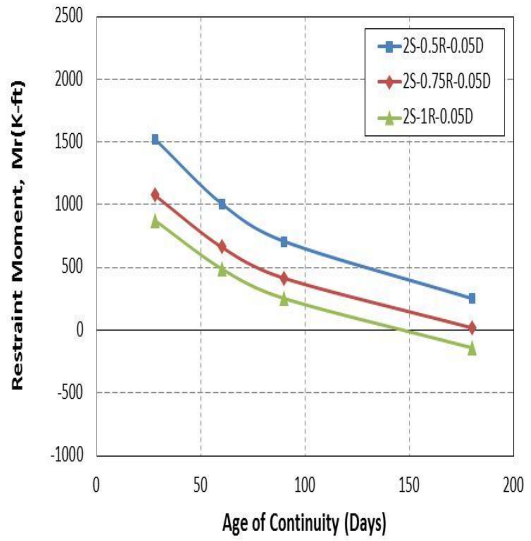

(a) $I_{dia} = 0.05 * I_g$

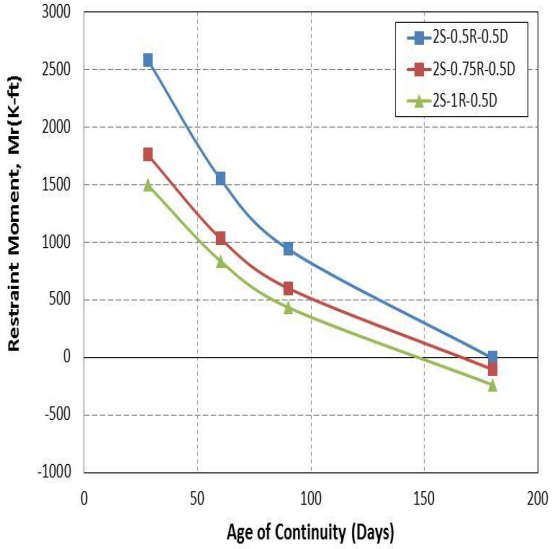

(b) $I_{dia} = 0.5 * I_g$

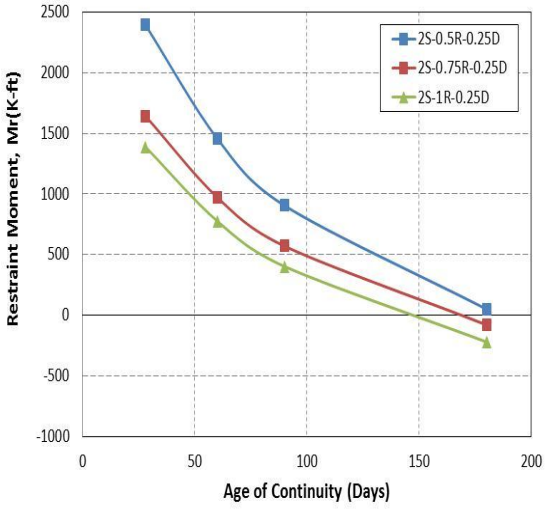

(c) $I_{dia} = 0.25 * I_g$

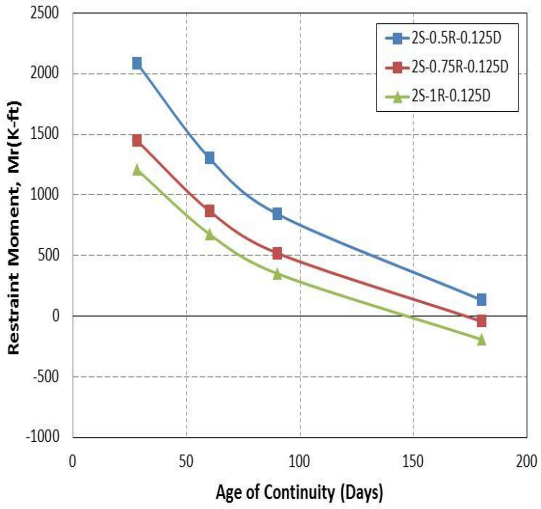

(d) $I_{dia} = 0.125 * I_g$

Figure 5.11 Restraint Moment vs Age at Continuity for 2-Span Bridge Cases (7500 days)

Figure 5.11 continued

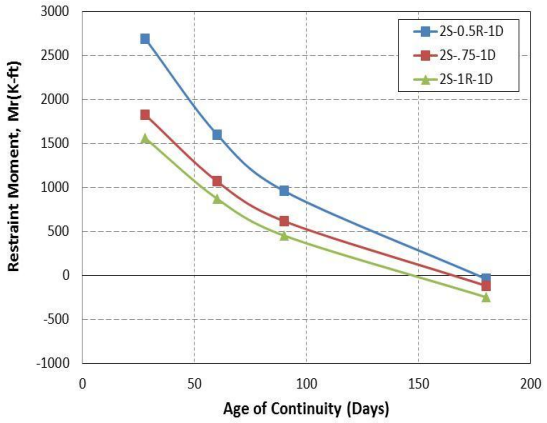

(e) $I_{dia} = 0.05 * I_g$

Figure 5.12 displays the plots drawn to calculate the optimum age of girder when restraint moment is taken from 20000 days for 3 span bridges girders.

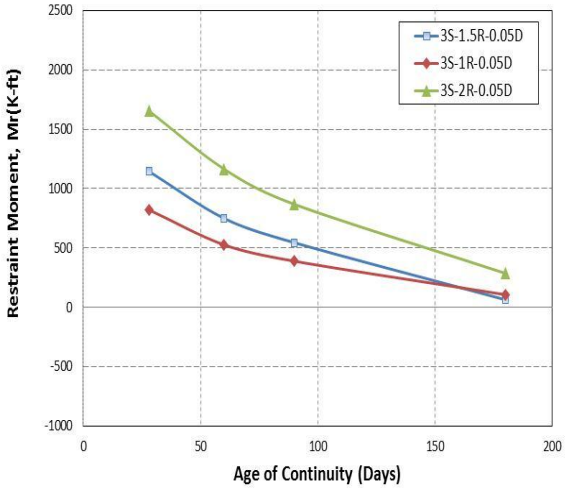

(a) $I_{dia} = 0.05 * I_g$

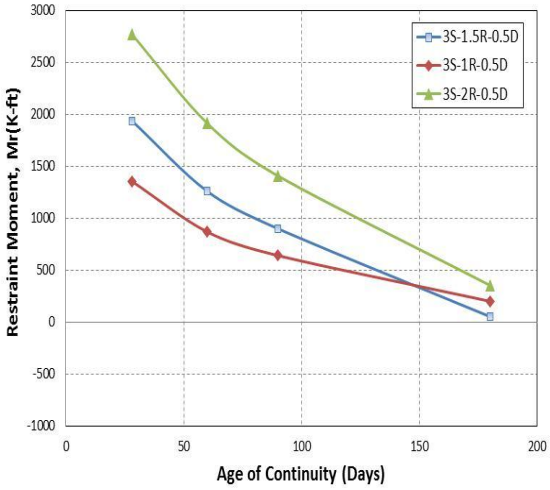

(b) $I_{dia} = 0.5 * I_g$

Figure 5.12 Restraint Moment vs Age at Continuity for 3-Span Bridge Cases (20000 days)

Figure 5.12 continued

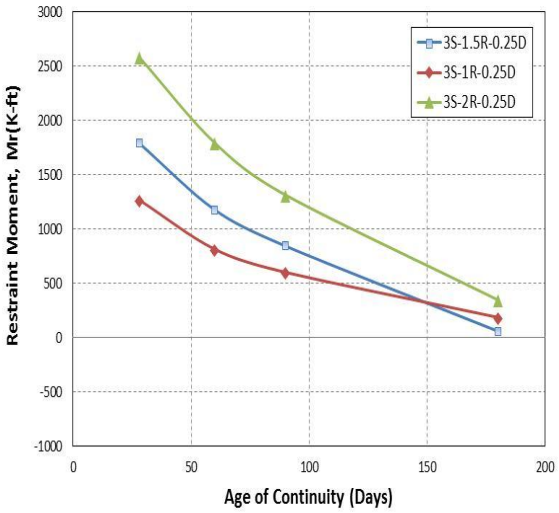

(c) $I_{dia} = 0.25 * I_g$

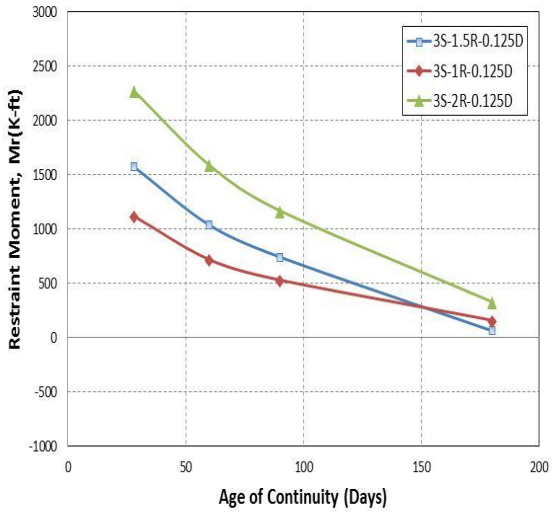

(d) $I_{dia} = 0.125 * I_g$

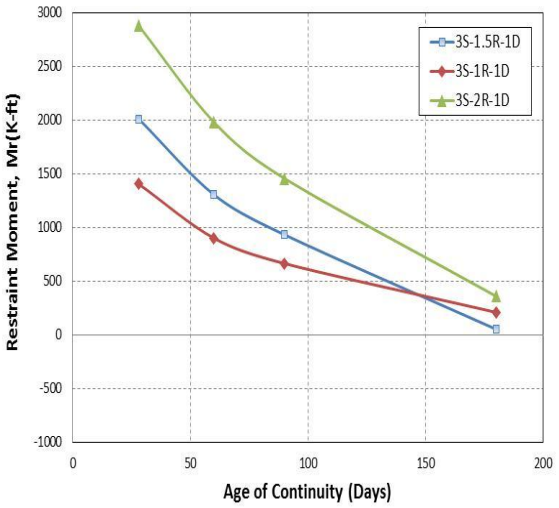

(e) $I_{dia} = I_g$

Figure 5.13 displays the plot drawn to calculate the optimum age of girder for 3 spans girders when restraint moment is taken from 7500 days.

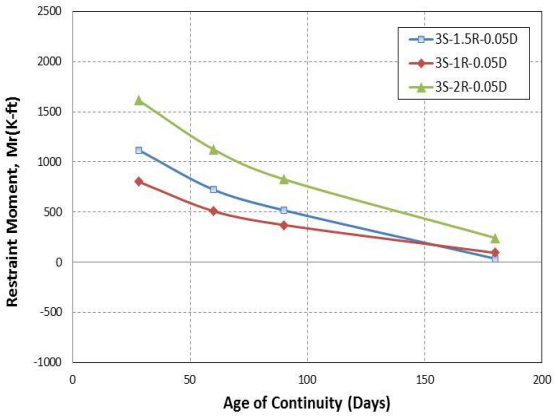

(a) $I_{dia} = 0.05 * I_g$

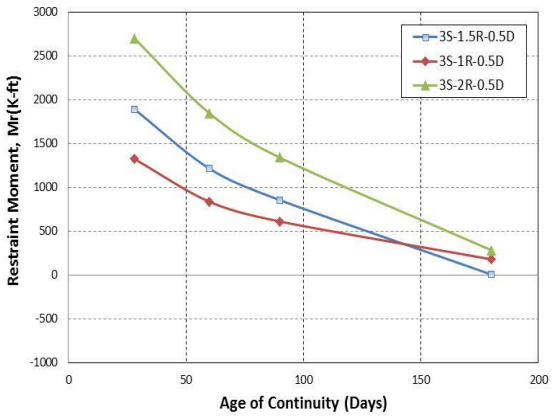

(b) $I_{dia} = 0.5 * I_g$

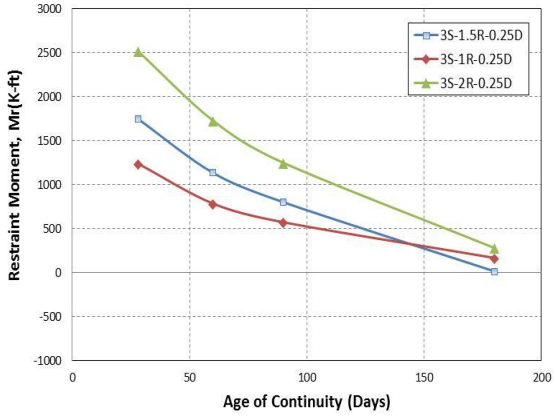

(c) $I_{dia} = 0.25 * I_g$

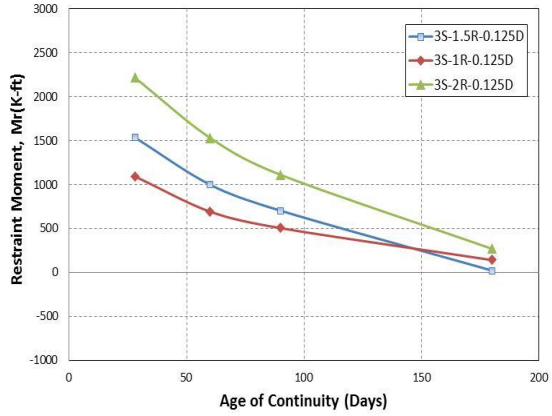

(d) $I_{dia} = 0.125 * I_g$

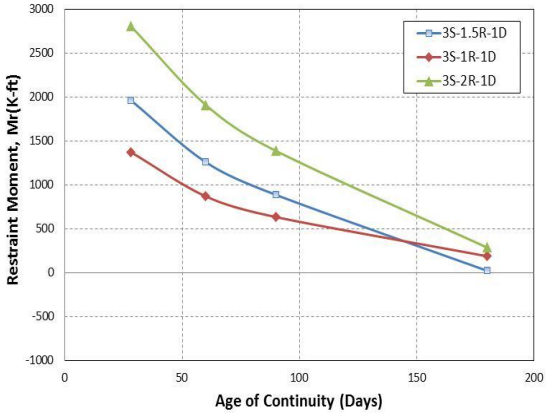

(e) $I_{dia} = I_g$

Figure 5.13 Restraint Moment vs Age at Continuity for 3-Span Bridge Cases (7500 days)

5.4.1 Cracking Moment

As stated earlier, the allowable restraint moment is taken as fraction (25%, 60%, 75% and 90%) of the girder's cracking moment.

The cracking moment (M_{cr}) is calculated by using the following equation (Nawy 2009).

$$M_{cr} = \frac{I_c}{y_{bc}}\left[\frac{P_e}{A_{nc}}\left(1 + \frac{e.c_b}{r^2}\right) + f_r\right] \quad (5.1)$$

where, f_r – Modulus of Rupture.
I_c – Moment of Inertia of the composite section.
y_{bc}- Distance from the bottom of the girder to the neutral axis of the composite section .
A_{nc} – Area of the non-composite section.
e – Eccentricity of the girder.
P_e – Prestressing force.
C_b – Distance from the bottom of the girder to the neutral axis of the non-composite section.

The modulus of rupture for a girder can be calculated by using the following equation.

$$f_r = 0.24 * \sqrt{f'_c} \quad (5.2)$$

where. f'_c – Girder Concrete Compressive Strength.

The effective prestress used in Eq. 5.1 for the calculation at a distance of 4 in from the girder's end. This distance is considered to be the most critical based on field observations (Okeil et al. 2011). The transfer of prestress is assumed to be linear as shown in the Figure 5.14 and the transfer length (l_t) for the girder is calculated using the following equation (Nilson 1987).

$$l_t = \left(\frac{f_{pe}}{3}\right) * d_b \quad (5.3)$$

where, d_b – diameter of prestressing strand
f_{pe} – effective prestress

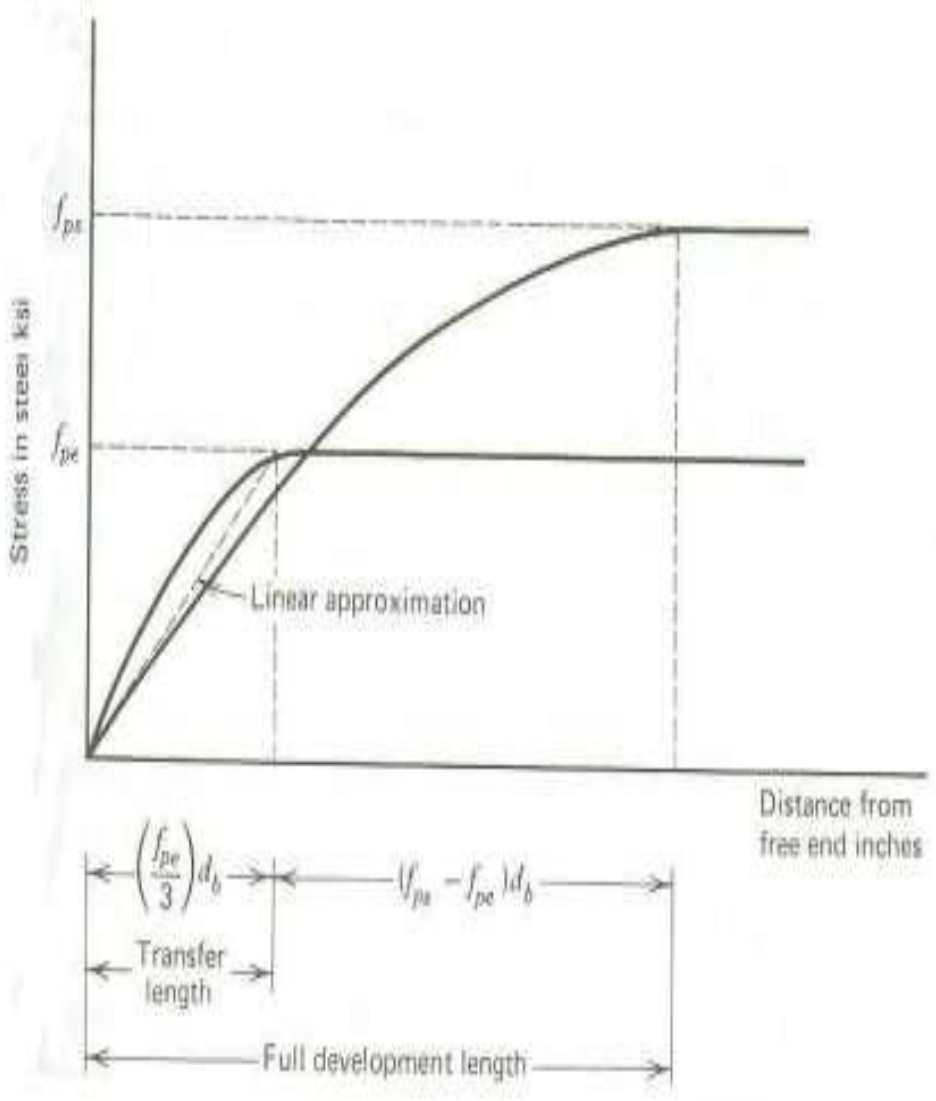

Figure 5.14 Transfer Length (Nilson 1987)

5.5 Target Age Results

The optimum ages were calculated for all 120 cases considered in the parametric study using the approach described in section 5.4. The results are presented in Table 5.3 and Table 5.4. These optimum ages are also plotted as a histogram and are shown in Figure 5.16 through 5.19. From the results it can be concluded that the 90 day recommended in NCHRP Report 519 for girder age should be reevaluated.

Table 5.3 Optimum Girder age Values in 2-Span Bridge Cases

CASE	Calculated Girder Age (20000 days)				Calculated Girder Age (7500 days)			
	0.25	**0.5**	**0.75**	**0.9**	**0.25**	**0.5**	**0.75**	**0.9**
2S-1R-1D	124	96	78	68	120	92	75	66
2S-0.75R-1D	143	116	90	81	139	112	87	78
2S-0.5R-1D	155	128	101	87	148	120	91	82
2S-1R-0.125D	116	84	64	55	112	82	62	53
2S-0.75R-0.125D	143	108	81	69	138	103	78	67
2S-0.5R-0.125D	162	122	86	74	157	117	83	71
2S-1R-0.50D	123	94	76	69	119	90	73	63
2S-0.75R-0.50D	143	115	89	79	139	111	86	77
2S-0.5R-0.50D	155	125	95	83	149	119	90	80
2S-1R-0.25D	121	89	72	61	116	87	69	59
2S-0.75R-0.25D	143	113	86	76	139	108	83	74
2S-0.5R-0.25D	157	124	91	80	152	119	88	77
2S-1R-0.05D	103	69	48	37	98	66	46	35
2S-0.75R-0.05D	140	90	63	52	135	87	60	50
2S-0.5R-0.05D	174	111	69	54	168	105	66	52
MEAN	**140**	**106**	**79**	**68**	**135**	**101**	**76**	**66**
STANDARD DEVIATION	**19**	**17**	**14**	**14**	**18**	**16**	**13**	**13**

Table 5.4 Optimum Girder age Values in 3-Span Bridge Cases

CASE	Calculated Girder Age (20000 days)				Calculated Girder Age (7500 days)			
	0.25	**0.5**	**0.75**	**0.9**	**0.25**	**0.5**	**0.75**	**0.9**
3S-1R-1D	178	135	91	74	173	129	87	70
3S-1.5R-1D	153	121	89	74	149	117	85	70
3S-2R-1D	176	142	108	88	170	136	102	84
3S-1R-0.5D	176	131	88	70	172	126	84	66
3S-1.5R-0.5D	152	119	86	70	147	114	82	67
3S-2R-0.5D	175	140	104	85	169	134	99	81
3S-1R-0.25D	172	125	82	63	168	119	78	59
3S-1.5R-0.25D	150	114	81	64	145	109	77	60
3S-2R-0.25D	174	135	97	79	167	129	91	75
3S-1R-0.125D	165	112	69	54	160	106	65	52
3S-1.5R-0.125D	146	104	69	54	141	99	65	52
3S-2R-0.125D	171	126	85	67	164	120	81	63
3S-1R-0.05D	144	79	46	74	139	75	44	70
3S-1.5R-0.05D	133	77	44	74	128	73	42	70
3S-2R-0.05D	160	97	55	88	154	90	52	84
MEAN	**162**	**117**	**80**	**72**	**156**	**112**	**76**	**68**
STANDARD DEVIATION	**14**	**20**	**19**	**11**	**14**	**20**	**18**	**10**

Figure 5.15 and Figure 5.16 shows the histogram for optimum girder age for 2-span bridge cases when restraint moment is taken from 20000 days and 7500 days respectively.

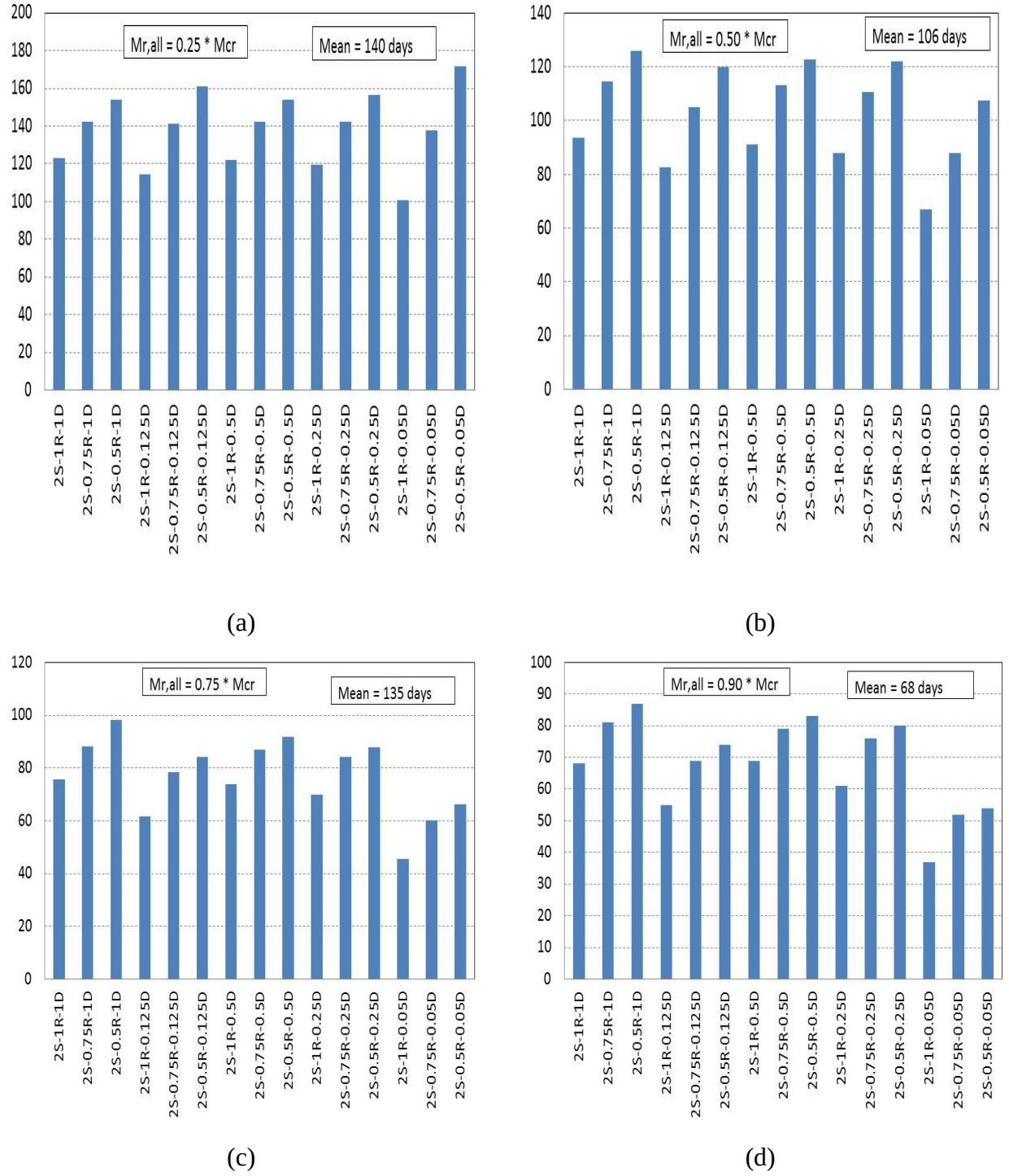

(a) (b)

(c) (d)

Figure 5.15 Histogram of optimum girder age for 2-Span Bridge Cases (20000 days)

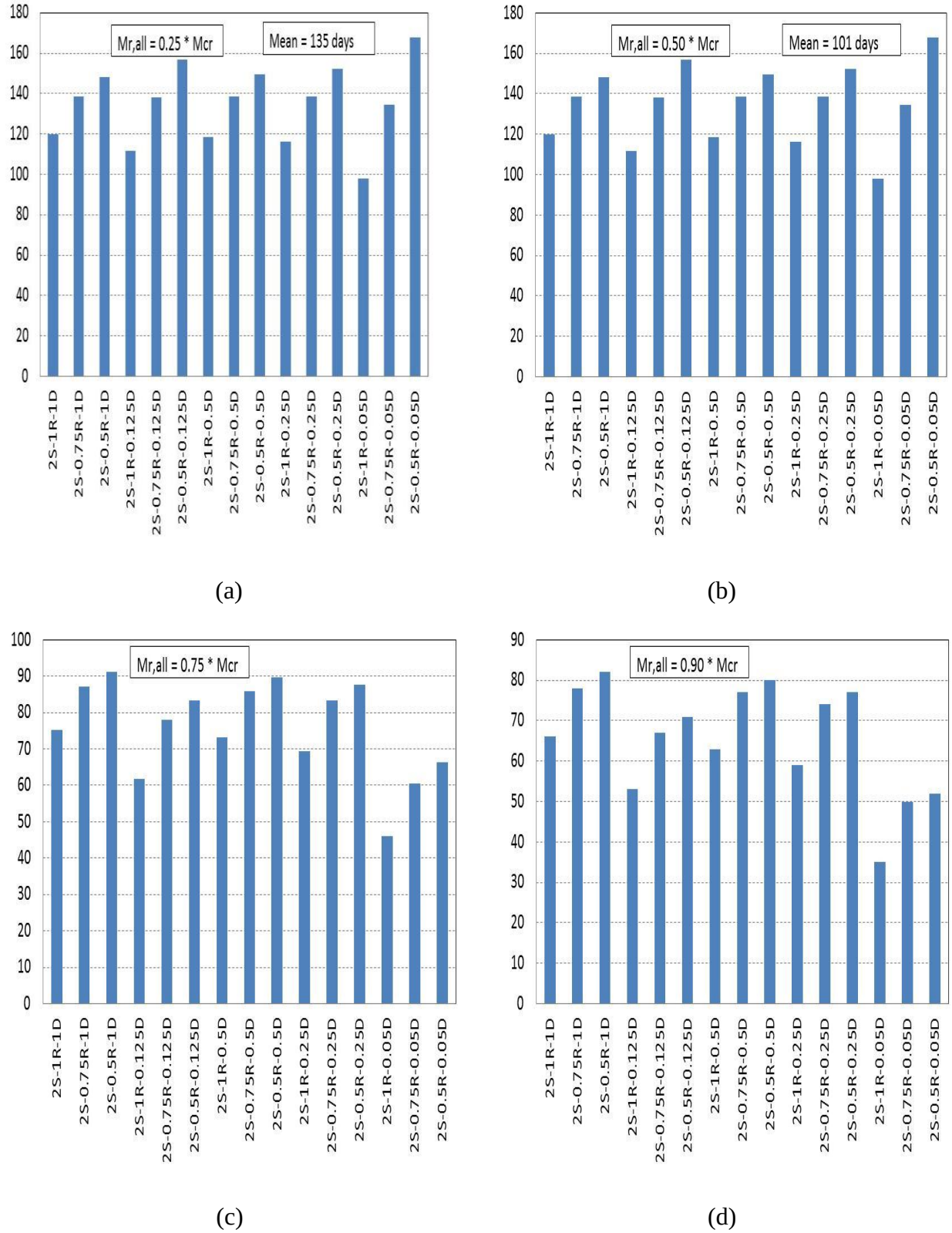

Figure 5.16 Histogram of optimum girder age for 2-Span Bridge Cases (7500 days)

Figure 5.17 and Figure 5.18 shows the histogram for optimum girder age for 3-span bridge cases when restraint moment is taken from 20000 days and 7500 days respectively.

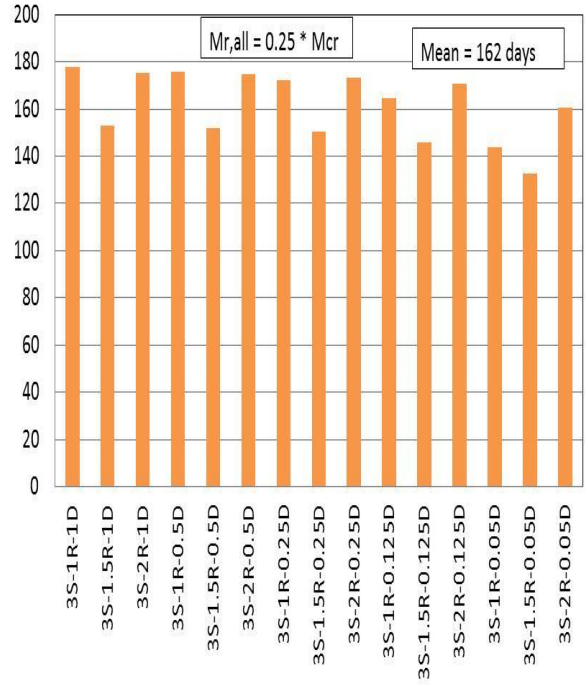

(a)

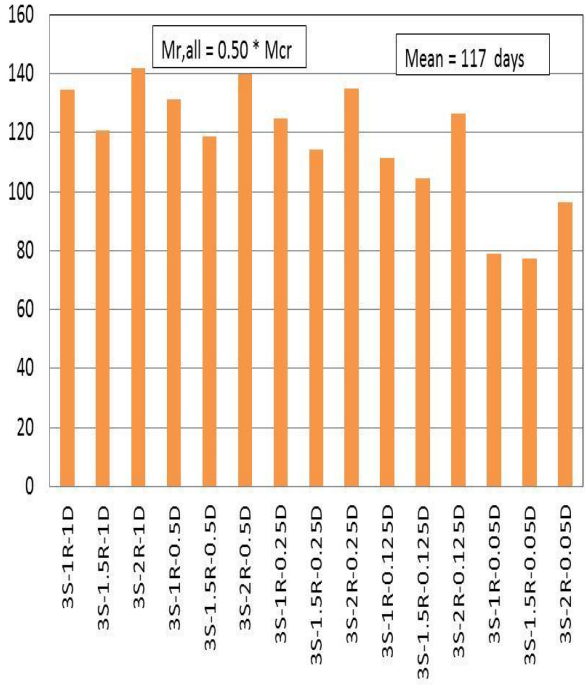

(b)

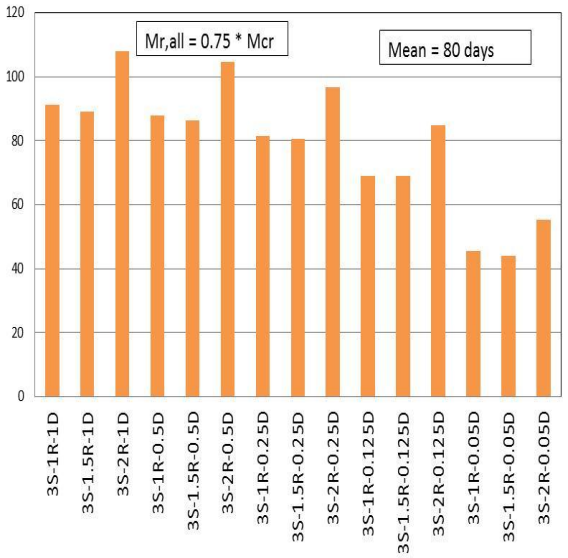

(c)

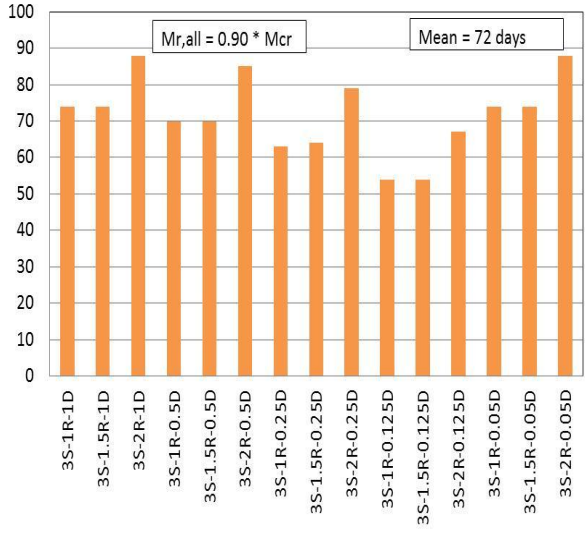

(d)

Figure 5.17 Histogram of optimum girder age for 3-Span Bridge Cases (20000 days)

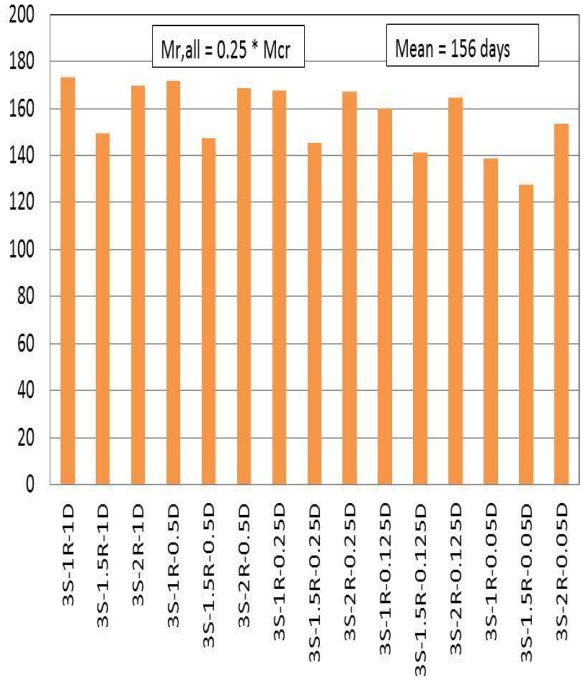

(a)

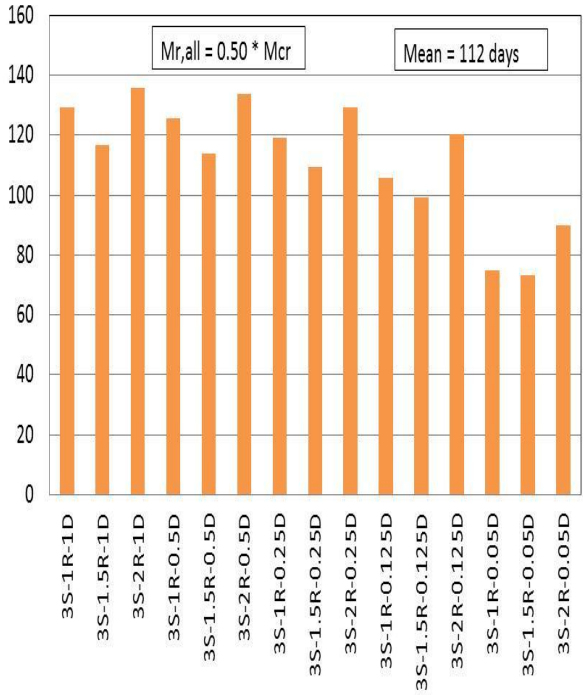

(b)

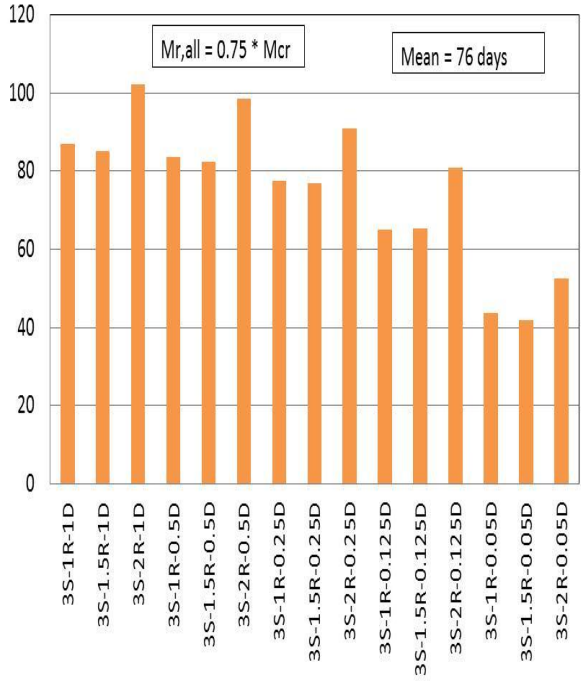

(c)

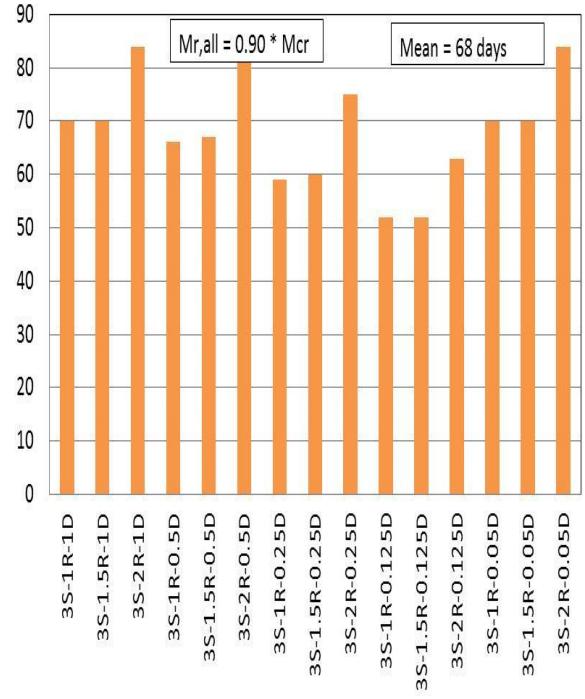

(d)

Figure 5.18 Histogram of optimum girder age for 3-Span Bridge Cases (7500 days)

5.6 Contribution of Thermal Gradient and Creep/Shrinkage on Total Restraint Moment

The study was extended to understand the contribution of the thermal gradient versus creep and shrinkage to the total restraint moment individually. This was necessary to emphasize to the designer the importance of thermal gradient effects. Considering a final girder age of 20000 days, the restraint moment was calculated due to effect of creep and shrinkage with and without thermal gradient effects for all the 120 cases. The results were then plotted in such a way to illustrate the contribution of each source (creep and shrinkage versus thermal gradient). Only positive restraint moments were considered; i.e., all the negative restraint moments were excluded since they do not impose girder cracking dangers. Figure 5.19 shows a sample plot case 2S-0.5R-0.05D at a final girder age of 20,000 days. The blue area represents the restraint moment at 20000 days due to the creep, shrinkage and thermal gradient combine and the red area represents the restraint moment at girder age of 20000 days due to creep and shrinkage alone. The corresponding percentage is calculated for each case when the bridge is made continuous at 28 days, 60 days, 90 days and 180 days respectively. As it can be seen in the figure when the girder age at continuity is 28 days, the total restraint moment was 1552.6 kips-ft at 20000 days due to creep, shrinkage and thermal gradient combined and the total restraint moment was 1024.6 kips-ft at 20000 days due to the creep and shrinkage only. Therefore, percentage or contribution of thermal gradient to total restraint moment is 34% and percentage or contribution of creep and shrinkage to total restraint moment is 66%. Similarly, the corresponding percentages were determined for other girder ages at time of establishing continuity. Figure 5.20 shows the area plots for 2 spans cases.

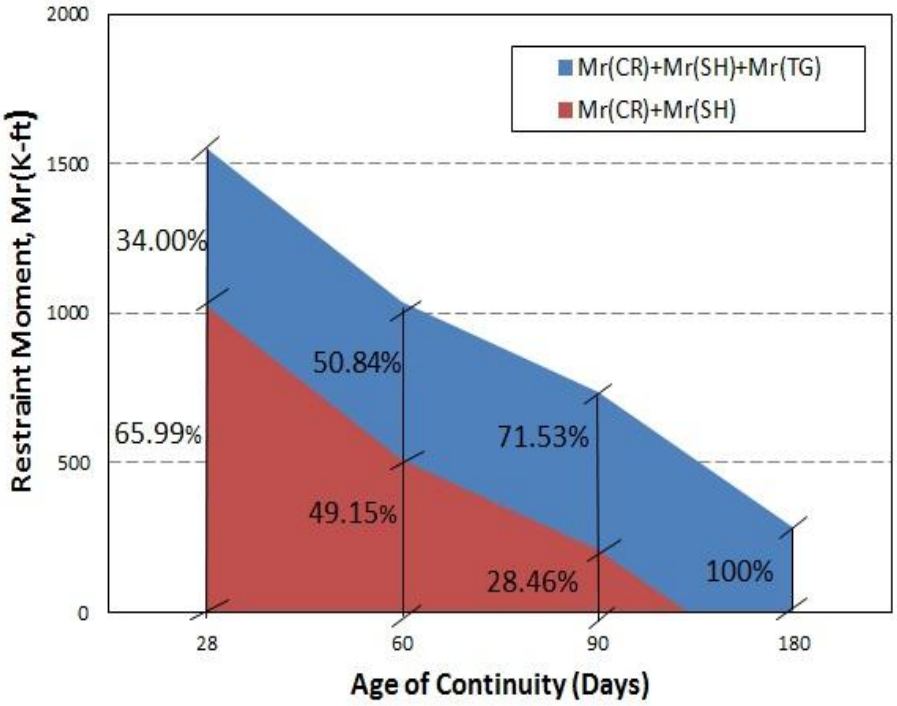

Figure 5.19 Area plot for 2S-0.5R-0.05 D

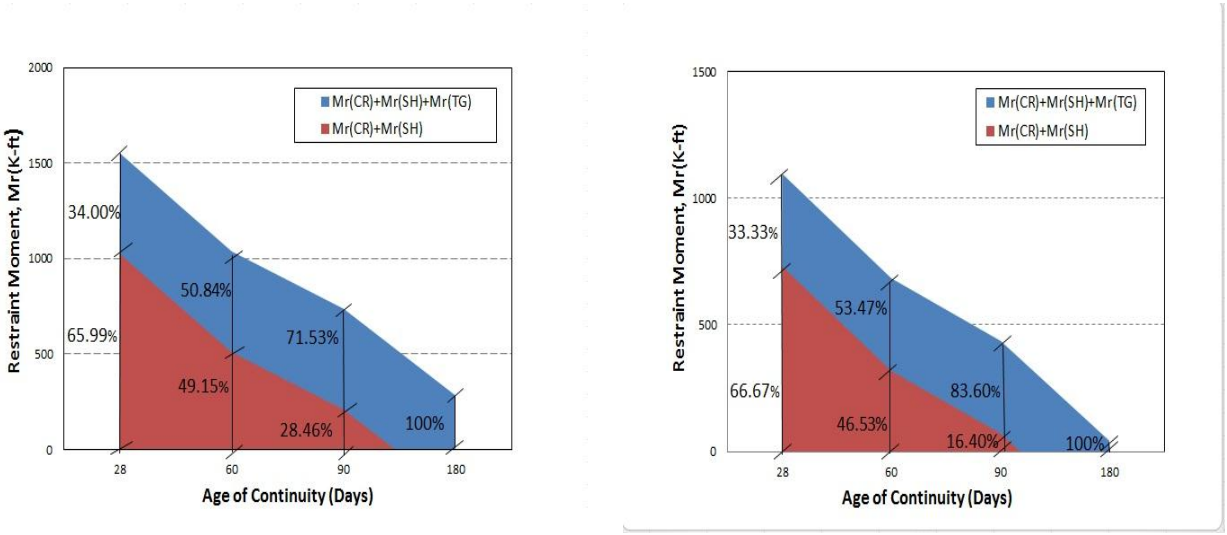

(a) 2S-0.5R-0.05D (b) 2S-0.75R-0.05D

Figure 5.20 Area plot for all 2 spans cases

Figure 5.20 continued

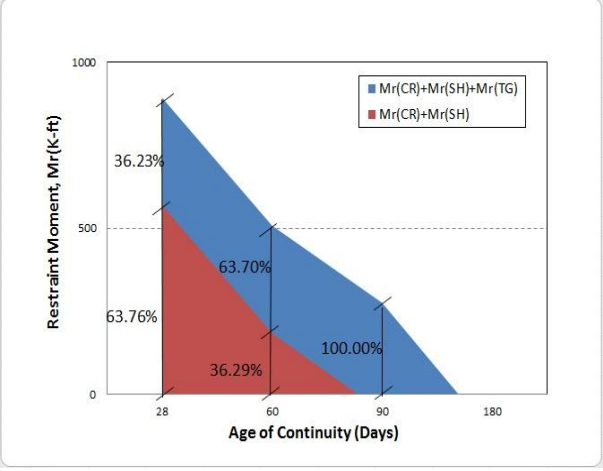

(c) 2S-1R-0.05D

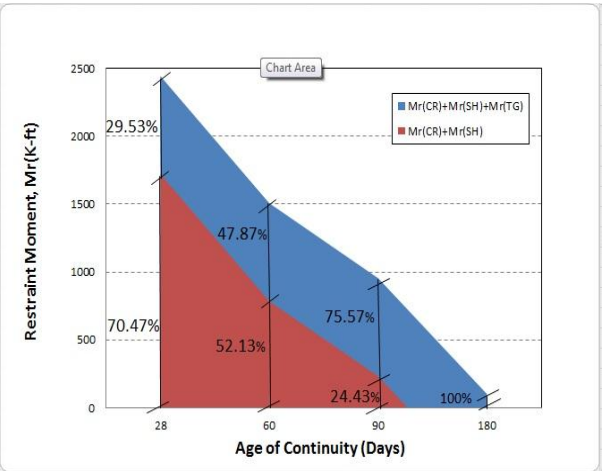

(d) 2S-0.5R-0.25D

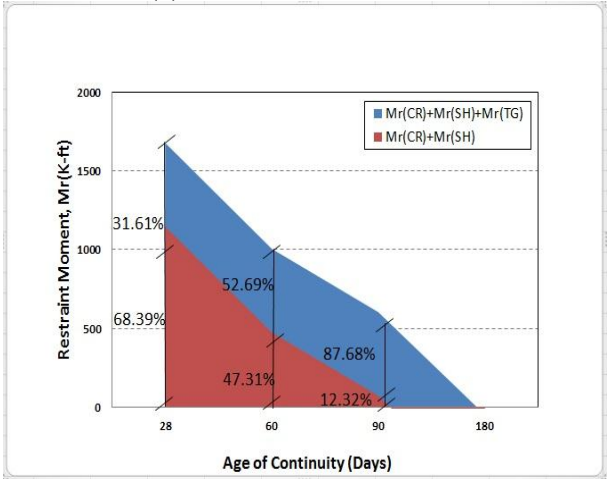

(e) 2S-0.75R-0.25D

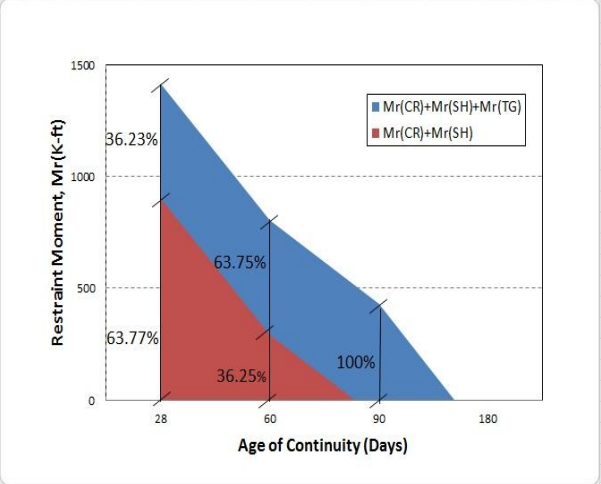

(f) 2S-1R-0.25D

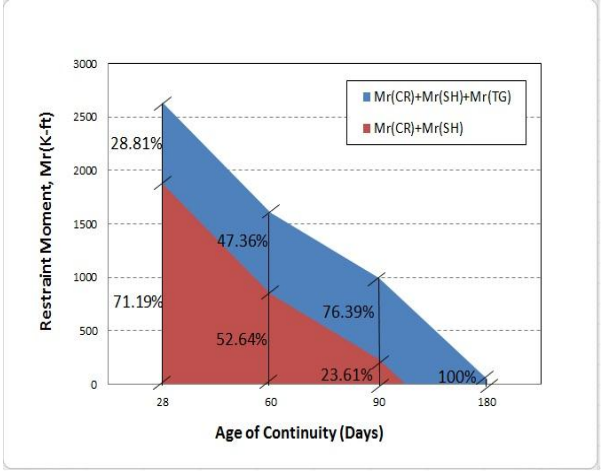

(g) 2S-0.5R-0.5D

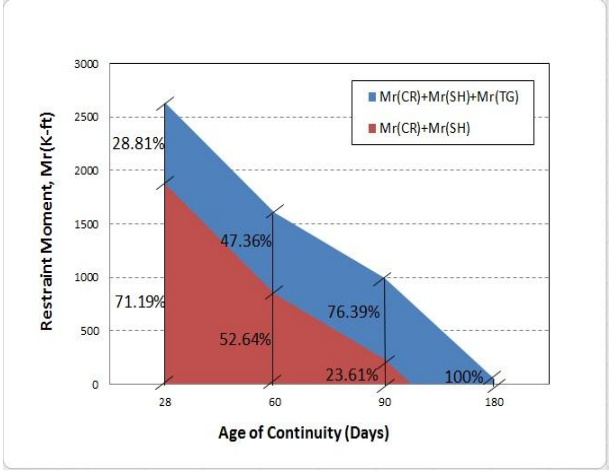

(h) 2S-0.75R-0.5D

Figure 5.20 continued

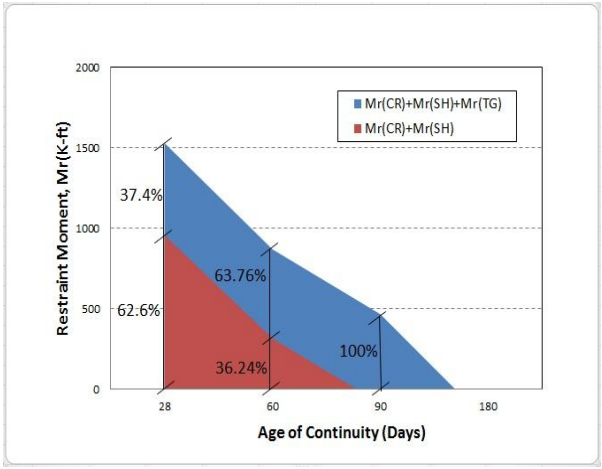

(i) 2S-1R-0.5D

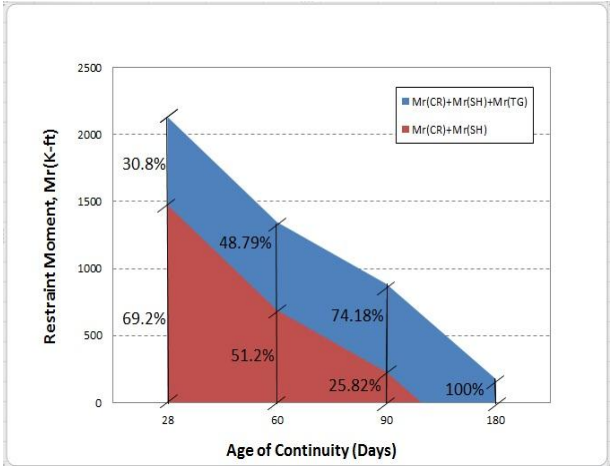

(j) 2S-0.5R-0.125D

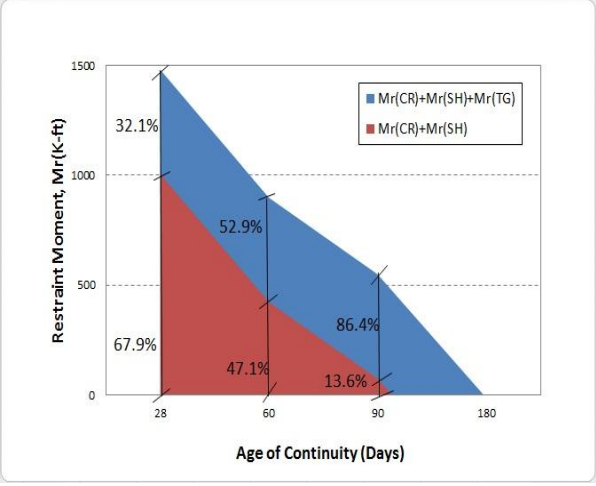

(k) 2S-0.75R-0.125D

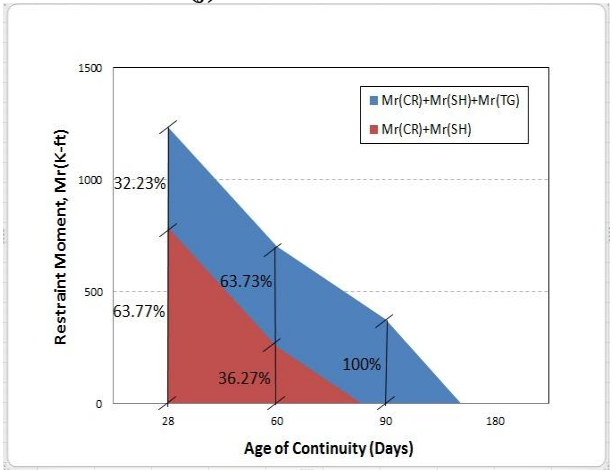

(l) 2S-1R-0.125D

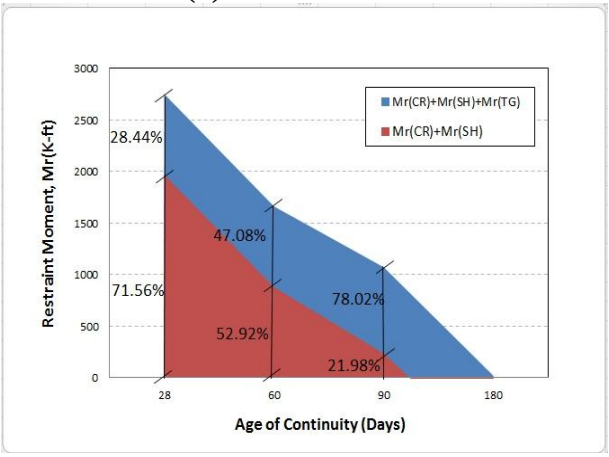

(m) 2S-0.5R-1D

Figure 5.20 continued

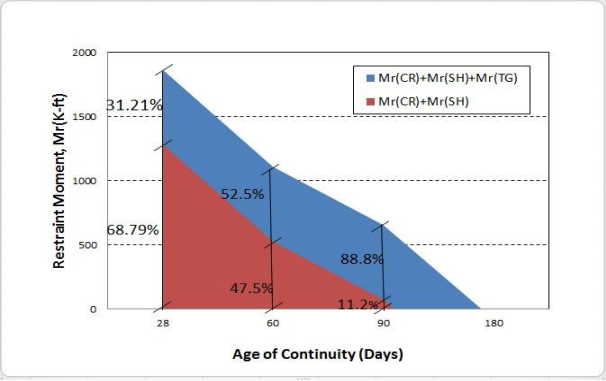

(n) 2S-0.75R-1D

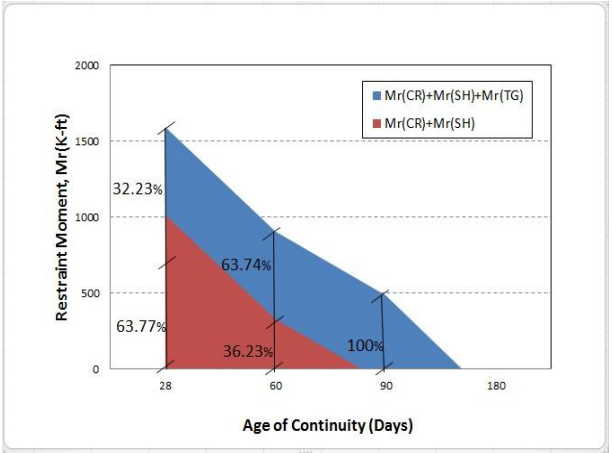

(o) 2S-1R-1D

Figure 5.21 shows the area plots for 3 spans cases.

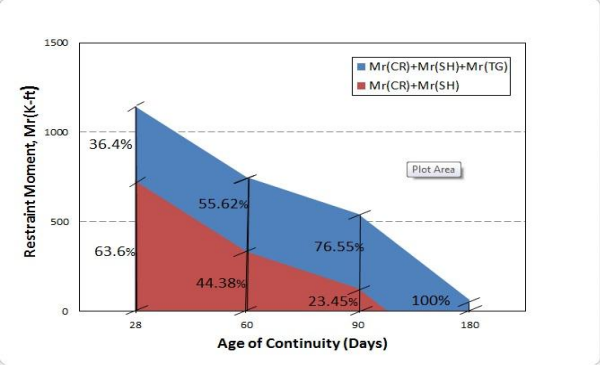

(a) 3S-1.5R-0.05D

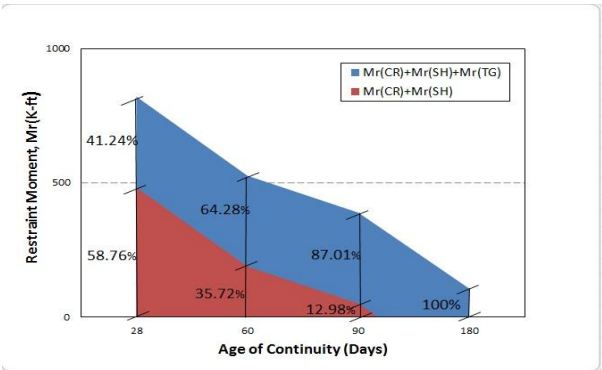

(b) 3S-1R-0.05D

Figure 5.21 Area plots for all 3 spans cases

Figure 5.21 continued

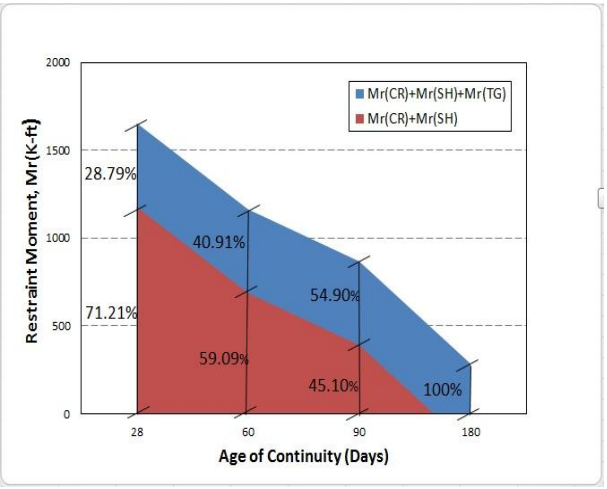

(c) 3S-2R-0.05D

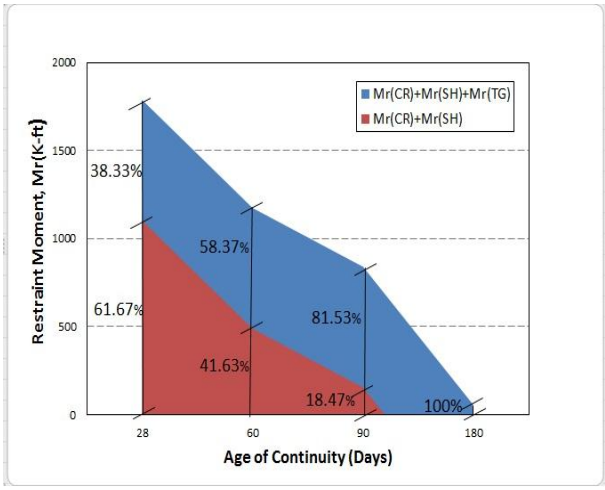

(d) 3S-1.5R-0.25D

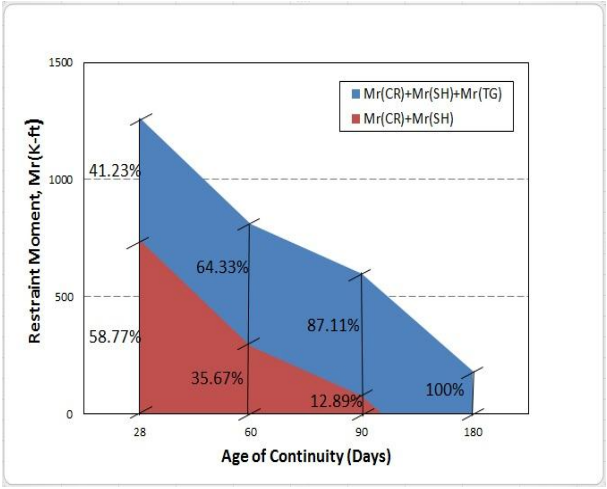

(e) 3S-1R-0.25D

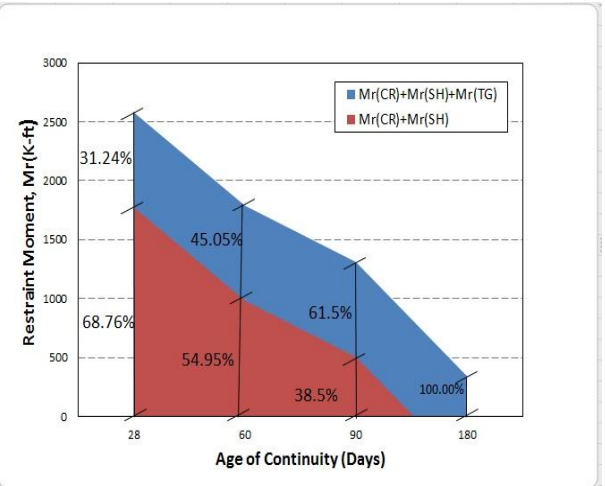

(f) 3S-2R-0.25D

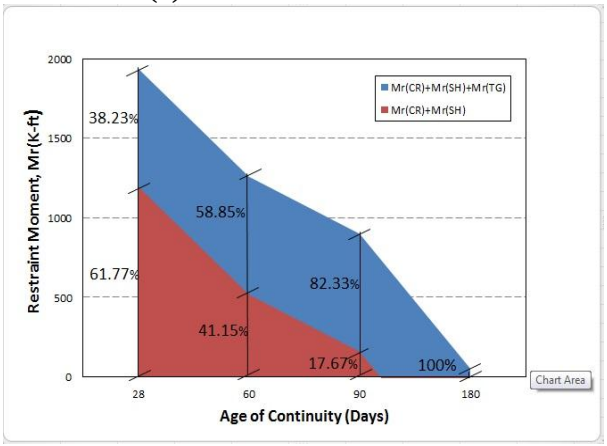

(g) 3S-1.5R-0.5D

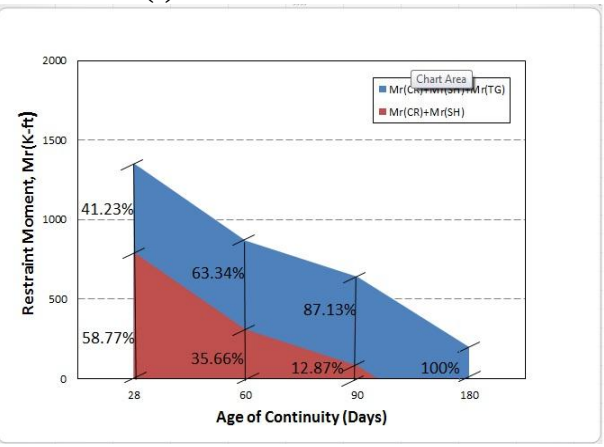

(h) 3S-1R-0.5D

Figure 5.21 continued

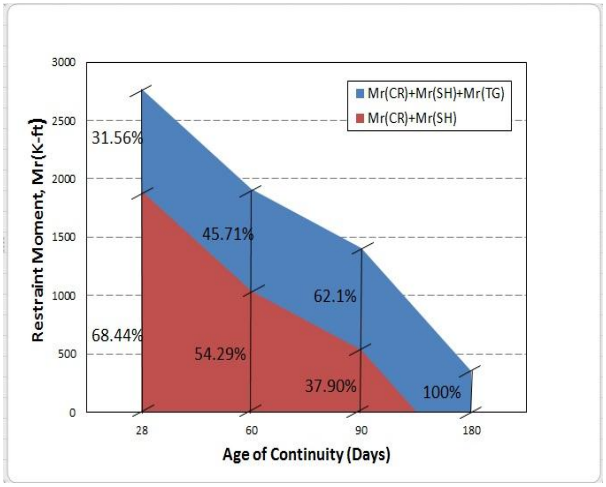

(i) 3S-2R-0.5D

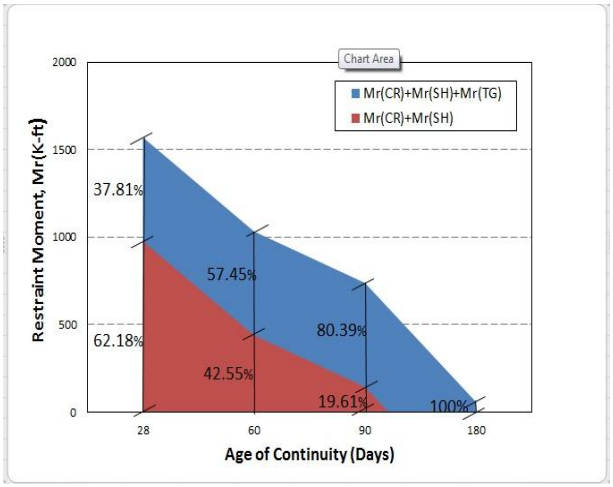

(j) 3S-1.5R-0.125D

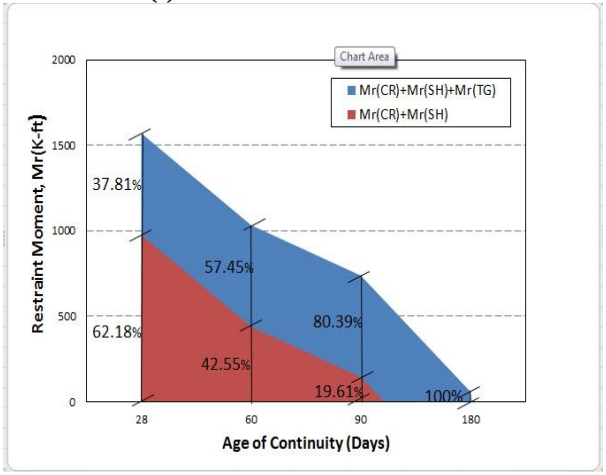

(k) 3S-1R-0.125D

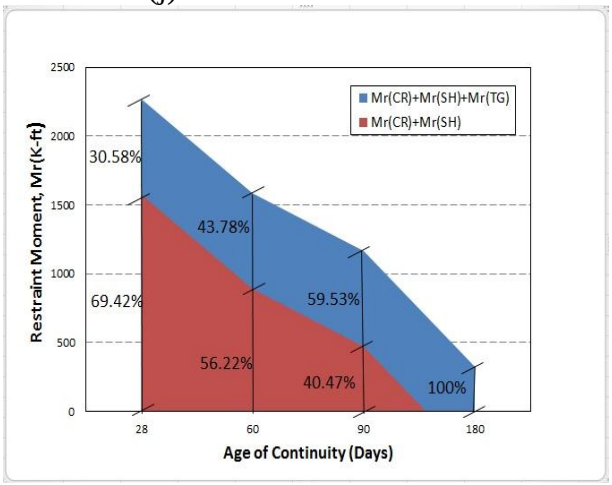

(l) 3S-2R-0.125D

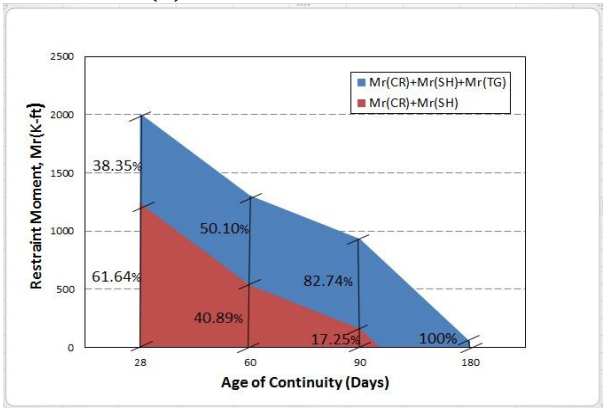

(l) 3S-1.5R-1D

Figure 5.21 continued

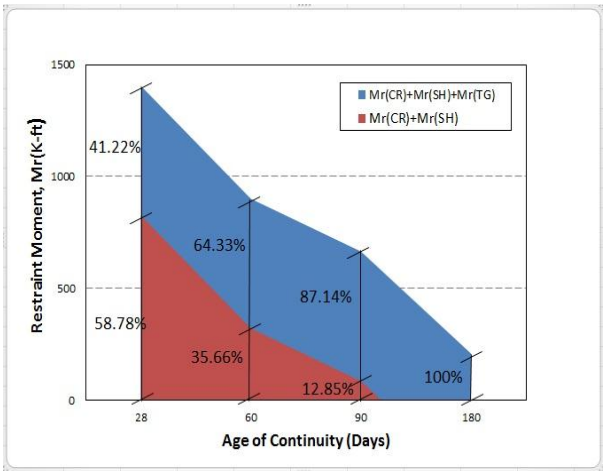

(m) 3S-1R-1D

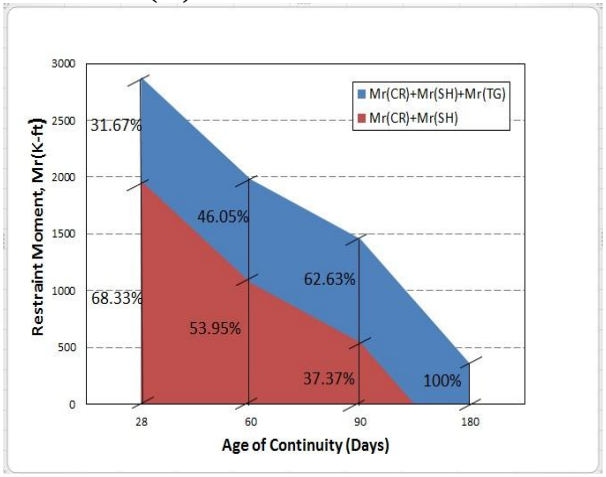

(n) 3S-2R-1D

5.7 Summary

In this chapter, a detailed parametric study was carried out to study the effect of different factors on the total restraint moment. A total of 120 cases were studied which included 60 2-Span bridges and 60 number of 3-Span bridges. The considered parameters were span lengths ratio, girder age at continuity and the ratio of diaphragm stiffness to girder stiffness. The study was then extended to investigate the effect of the age of continuity in detail and to determine the optimum age for girder for all 120 cases in such a way that the restraint moment does not exceed

the allowable restraint moment taken as a fraction of girder's cracking moment. Another study was also carried out to understand the contribution of thermal gradient, creep and shrinkage to the total restraint moment combined and the thermal gradient alone.

The results that were achieved from this study suggested that the final restraint moment values are affected by the parameters which are span lengths ratio, girder age at continuity and the diaphragm to girder stiffness ratio. It was confirmed that whenever the continuity is established at the early ages then the restraint moment are larger than the restraint moments when the continuity is established at later ages. It was also found that as the asymmetry of the span lengths ratio increases, restraint moment values increases as well and lastly if the diaphragm stiffness is increased then the restraint moment increases as well.

The optimum girder ages calculated in the study to sustain an allowable restraint moment values after 20000 days vary from 68 da0ys to 140 days and to sustain an allowable restraint moment values after 7500 days vary from 66 days to 135 days from 2-span bridge case. Similarly, the optimum girder ages calculated for an allowable restraint moment values after 20000 days vary from 72 to 162 days and 68 to 156 days after 7500 days for 3-span bridge case.

The area plots which were created to study the contribution of thermal gradient and creep and shrinkage individually suggested that the effect of the thermal gradient will increase as the girder age is established at later ages. This is because the effect due to creep and shrinkage decreases as the girder age at continuity increases but the thermal gradient remains same for the corresponding girder.

6 RELIABILITY ANALYSIS OF CONTINUOUS PRESTRESSED CONCRETE GIRDERS

6.1 Introduction

In this chapter, the probability of girder end cracking in continuous prestressed concrete bridges is assessed using theory of structural reliability. Recent studies suggest that, one in nine of the bridges in United States are rated as structurally deficient and that the average bridge is about older than 42 years (The Federal Highway Administration). The Federal Highway Administration also claims that United States should invest $20.5 billion annually to rehabitate and renovate those structurally deficient bridges to eliminate the deficient backlog by 2028. It is also evident that the traffic flow on these bridges is increasing day by day in United States and around the world which makes structures like roads and bridges become deficient earlier than what they are designed for.

A deterministic approach for assessing the vulnerability of concrete girders to cracking is straight forward. However, practice has shown that cracking took place in situation when it is not expected (Nowak and Collins 2000). Many parameters used in structural design are not deterministic quantities. Such parameters can be treated as random variables, which imply that absolute safety or zero probability of failure cannot be achieved (Nowak and Collins 2000). Therefore, structures must be designed in such a way that they serve their function in relation with an acceptable low probability of failure which translates into a reasonable safety level.

Safety levels differ based on many factors, but in all cases have to meet societal expectations of safety. In our modern society, these safety levels are achieved by using or following code requirements. Design codes set minimum design requirements that must be met such as minimum strength and maximum allowable deflection. Modern design codes have

evolved to include the sources of uncertainty in design (Nowak and Collins 2000), in what is known as reliability-based design criteria.

6.2 Historical Background

The approaches used in structural designs in present days for safety evolved over many centuries. All design codes that engineers and other designers currently use have been modified and revised many times. Even in ancient societies there were some rules and regulations to ensure the safety of the citizens. There were severe punishments to ensure the minimum safety requirements were being followed by the designers and workers (Nowak and Collins 2000). The earliest known building code known to mankind was used in Mesopotamia and it was issued by Hamurabi, the King of Babylonia (Nowak and Collins 2000). Figure 6.1 shows the picture of the stone which has codes carved into it.

The knowledge and idea of designing and constructing structures were passed on for one generation or society to another over time. A builder used to copy previously constructed successful design and re-design it in his or her own way to increase the height or span of structure using intuition of designer (Nowak and Collins 2000). Failure of a particular structure led to the modification of the design for that structure of its abandonment.

As time passed by, science and math began to evolve and laws of nature were better understood. These developments had a direct effect on structural designs because these theories provided missing framework that could be applied to improve structural safety and reliability. For the structural safety problem, the first mathematical formulations were from Mayer (1926), Streletzki (1947) and Wierzbicki (1936). They were the ones who first recognized that there is some finite amount of probability of failure on every design and that load and resistance parameters are random variables. Their ideas and concepts were later used by many

mathematicians and scientists, but the major pioneering work done on the practical applications of reliability analysis was done by Cornell and Lind in the late 1960s and early 1970s (Nowak and Collins 2000). The second moment reliability index was proposed by Cornell and later an efficient method for determining the reliability index was introduced by Rackwitz and Fiessler in 1978 (Nowak and Collins 2000).

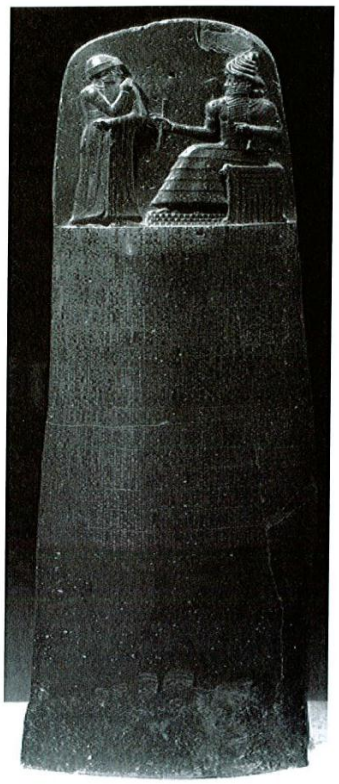

Figure 6.1 The code of Hammurabi (Nowa and Collins 2000)

6.3 Objective

The objective of this part of the research is to understand the probability of the prestressed concrete girder cracking due to positive restraint moment that develops as a result of long-term effects. The goal is to have a better understanding of probability of cracking at girder ends, which should be avoided or at least minimized since it may lead to adverse effects.

6.4 Random Variables

A random variable can be defined as a function which assigns a real number to each possible outcome (Chao 2014). Random variables are important for estimating the reliability of a structure because there are many factors on the design and construction of structure whose outcomes are unpredictable. Material strength, live loads and dimensions are only a few examples of outcomes that are unpredictable. Therefore, estimating the random variables play a vital role in determining the reliability of any structures. Random variable can be divided into types, namely discrete random variable and continuous random variable

In this study, only continuous random variables were used to model design parameters such as dimensions, modulus of elasticity, modulus of rupture, area of prestressing steel and temperature gradient.

There are many types of random variables but the most important random variable types used in structural reliability analyses are uniform, normal, lognormal, extreme type I, extreme type II, extreme type III and gamma. More details about the random variables used in this study are discussed later.

6.5 Limit State Function

As stated earlier, all structures are prone to failure, albeit with a small or large probability of failure. The definition of failure in this context does not imply collapse or loss of capacity but rather implies that the demands (load effect) exceed the structure's capacity (resistance).This definition of failure goes beyond structural applications. For example, in transportation engineering, failure of a highway happens when the traffic volume exceeds its capacity. This is considered a temporary failure because a traffic jam will go back to normal after the rush hour.

Permanent failure occurs when a bridge fails because of being subjected to loads that exceeds its resistance. The first step in calculating a probability of failure is to establish a limit state function.

A limit state can be defined as a boundary of a desired and undesired performance of any structure (Nowak and Collins 2000). These boundaries are represented by mathematical equation which is known as limit state function. In general, limit state function can be seen as difference between the structure's capacity to resist applied loads (R) and the applied load effects (L). The equation can be written as:

$$g(R,L) = R-L$$

where, g(R,L) is the limit state function

If g() is greater than zero, it can be said that the structure did not fail, conversely, if g() is less than zero it can be said that the structure did fail since it means that structure's resistance (capacity) is less than the load it is subjected to. Limit state functions can be written to describe (Nowak and Collins 2000):

1) Ultimate limit states
2) Serviceability limit states
3) Fatigue limit states

Ultimate limit states describe the load-carrying capacity of a structural element. Some examples of modes of failure are formation of plastic hinge, loads exceeding the structure's capacity, load buckling of both flanges or a web and loss of stability (Nowak and Collins 2000). Serviceability limit states are related to the daily operation of a structure, which can lead to slow deterioration over time. Some of the modes of failure for this limit states are excessive deflection, excessive vibration and deformations (permanent) (Nowak and Collins 2000). Lastly, fatigue

limit states are the limit states which are related to loss of strength under constant cyclic loads, when the structure fails due to the repeated loads.

Since the aim of this study is to calculate the probability of cracking of continuous prestressed concrete girder bridges caused by positive restraint moments that develop due to thermal gradient, the limit state function for this study is taken as follows:

$$g() = M_{cr} - M_{TG} \quad (6.1)$$

where M_{cr} is cracking moment of the girder, and M_{TG} is restraint moment due to thermal gradient.

Positive restraint moment caused by creep/shrinkage is not considered in this study, but will be discussed later.

It should be noted that the effective primary stress occurs due to the thermal gradient in concrete, which should be accounted for in estimating the probability of cracking even though it does not generate additional moments.

$g()=M_{cr}-M_{TG}$-effective primary stress effect

M_{cr} is expressed as,

$$Mcr = \frac{I_c}{y_{bc}}\left[\frac{P_e}{A_{nc}}\left(1 + \frac{e.c_b}{r^2}\right) + f_r\right] \quad (6.2)$$

where, f_r – Modulus of Rupture.
I_c– Moment of Inertia of the composite section.
y_{bc}- Distance from the bottom of the girder to the neutral axis of the composite section .
A_{nc} – Area of the non-composite section.
e – Eccentricity of the girder.
P_e – Prestressing force.
C_b – Distance from the bottom of the girder to the neutral axis of the non-composite section.

$$M_{TG}=E_c*I_c*\psi \quad (6.3)$$

where, E_c= Modulus of elasticity of concrete
ψ = final curvature of the girder

$$\psi = \frac{\alpha_c}{I}\sum_{i=1}^{n}\theta_i(y_i - n)dA_i \quad (6.4)$$

where, α_c=coefiecient of thermal expansion

y_i = Distance from centroid of the section to arbitrary datum

A_i= Area of the section where the y_i is taken.

n= Distance from NA (composite section) to arbitrary datum.

As stated earlier, the effect of the primary stress due to thermal gradient must be incorporated in the limit state function; therefore modulus of rupture is reduced by the magnitude of the final primary stress, which implies superposition of combined effects.

And primary effective stress is given by

$$Fp = Ec*(\epsilon_o + \psi*yi - \alpha_c*\theta_i) \quad (6.5)$$

where, ϵ_o= final strain of the girder

Now, Mcr becomes

$$Mcr = \frac{I_c}{y_{bc}}\left[\frac{P_e}{A_{nc}}\left(1 + \frac{e.c_b}{r^2}\right) + (f_r - f_p)\right] \quad (6.6)$$

It can be seen from the M_{cr} and M_{TG} equations that the random quantities involved in this study are geometrical variability (e.g. height. length) and material properties like (e.g. modulus of elasticity and modulus of rupture of concrete). The geometrical random variables for the height, length are required to calculate moment of inertia, non-composite area, distance from bottom of girder to N-A and composite section area. Few papers were reviewed to garner the information about these variables regarding their bias values, coefficient of variation, mean, standard deviation and distribution types. Table 6.1 lists the statistical characteristics of random variables used in this study. The statistical distribution type for each variable is also given in Table 6.1. This information was compiled from the cited papers in the literature.

Table 6.1 Random Variable Summary Form

SUMMARY OF RANDOM VARIABLES						
RV		BIAS	COV	MEAN	STD	DISTRIBUTION TYPES
Okeil et al. (2002)	Dimensions of girder	1.00	0.03			Normal
Hueste et al. 2004	Modulus of elasticity of concrete ($f_c' = 8 \pm 1$) ksi	1.13	0.043			Lognormal
Hueste et al. 2004	Modulus of elasticity of concrete ($f_c' = 6 \pm 1$) ksi	1.31	0.043			Lognormal
Hueste et al. 2004	Modulus of rupture of concrete	1.54	.1			Lognormal
Orton et al. 2012	Area of Prestressing steel	1	0.0125			Normal
Tanesi et al. 2007	Thermal expansion Coefficient			$5.54*10^{-6}$ (^oF)	$0.43*10^{-6}$ (^oF)	Normal
Kim 2008	Temperature Gradient			11.8F (TOP)	5.9F (TOP)	Normal
				1.7F (BOT)	0.9 (BOT)	

It should be also noted that the probability of cracking for the girder was calculated with the consideration of web and without the consideration of web. It was necessary to calculate the probability of failure for both conditions because the stress distribution was found to be concentrated around the hairpin bars at the girder ends rather than the entire cross section as shown in Figure 6.2 (Hossain and Okeil 2014). Hossain and Okeil 2012 did a study on force transfer mechanism for prestressed concrete girder bridges. 3-D finite element model of the girder was created to study the mechanism. In the model 180^0 hairpin bars as recommended by National Cooperative Highway Research Program Report No 519 was used for the positive moment reinforcement. The 3-D finite model was then subjected to the positive moment that would develop over the service life of the bridge. From this study, it was found that asymmetric stress distribution develops at the continuity diaphragms due to the asymmetric configuration of the hairpin bars. It was also observed that the tensile force is transferred through the positive moment reinforcement between the girder end and the continuity diaphragm when the joint is subjected to a positive moment. As a result the stress distribution was found to be concentrated around the bottom flanges at the girder ends rather than be resisted by the entire girder composite section.

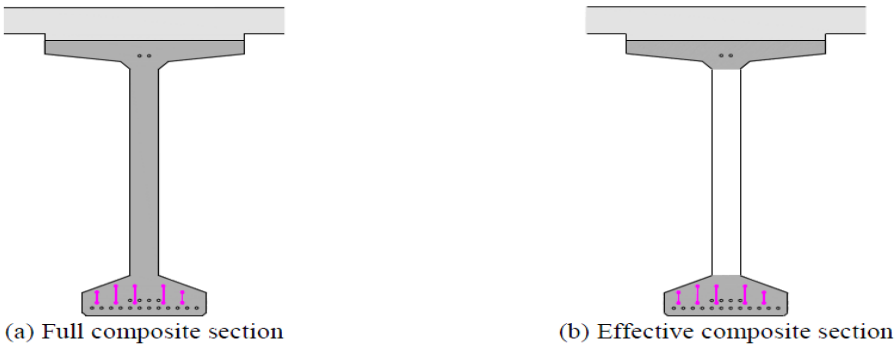

Figure 6.2 Full and effective section geometry for calculation of moment of inertia at girder ends (Hossain and Okeil 2014).

6.6 Methodology

Monte Carlo simulation was used for calculating the probability of cracking due to positive restrained moment developed by thermal gradient. A two span bridge with span lengths ratio 1:1 and AASHTO Type - IV girder was chosen for this study. Figure 6.3 and Figure 6.4 shows the dimensions for AASHTO TYPE – IV girder with the web part and without the web part respectively. The lengths of two spans of the girder are 100 ft.

A second bridge with a larger cross section was also evaluated for cracking probability. The reason for calculating this probability was to understand the changes in probabilities of failure due to change in size. AASHTO BT-72 girder is larger than AASHTO Type-IV girder in size and is the largest girder among the other AASHTO girders. A two span bridge was assumed with 120 ft long spans. Figure 6.5 and 6.6 show the dimensions for AASHTO BT-72 girder with and without the web part respectively.

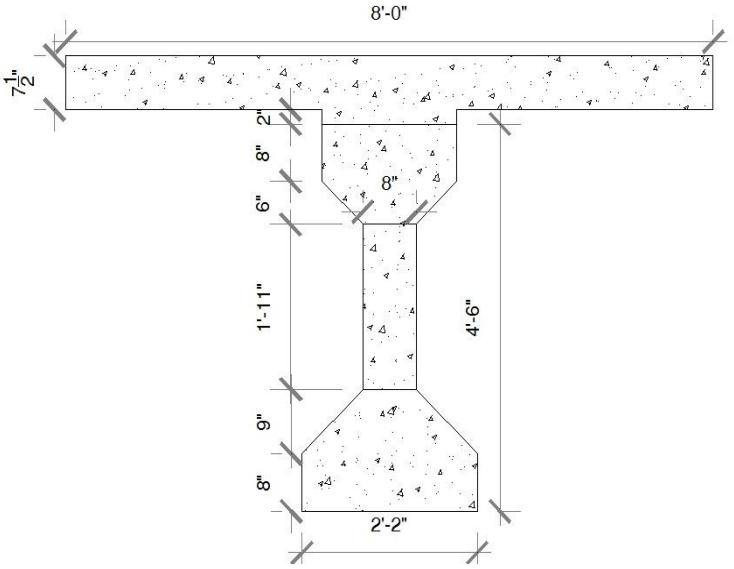

Figure 6.3 AASHTO Type IV girder dimensions (with web)

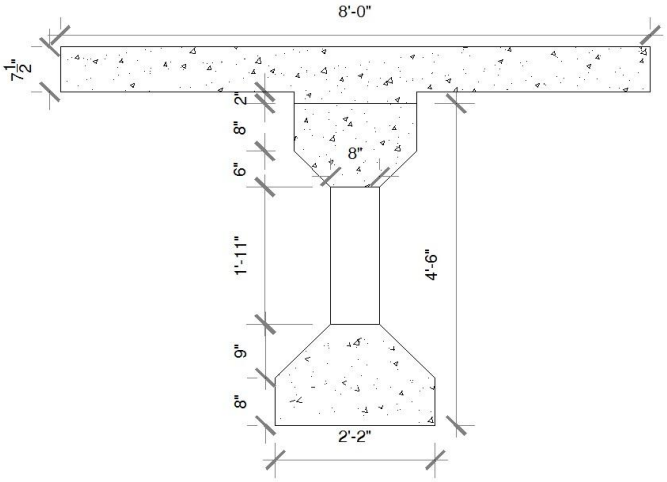

Figure 6.4 AASHTO Type IV girder dimensions (without web)

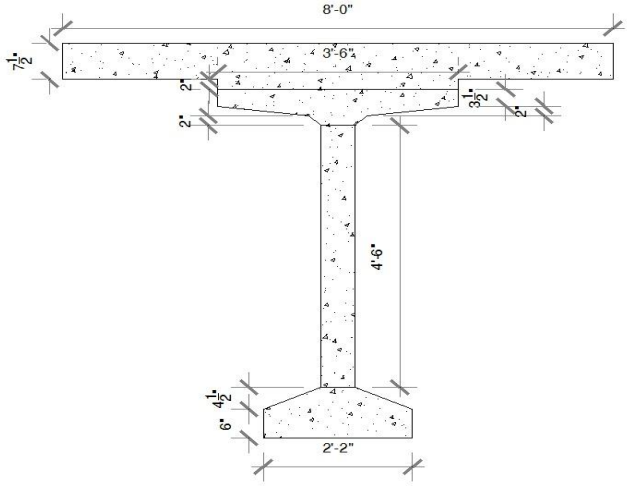

Figure 6.5 AASHTO BT-72 girder dimensions (with web)

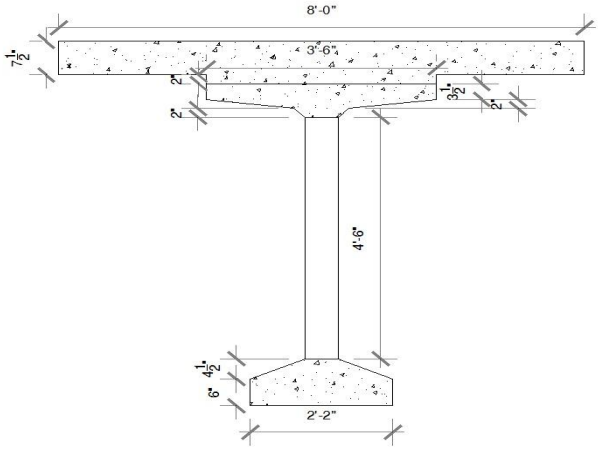

Figure 6.6 AASHTO BT-72 girder dimensions (without web)

The composite section including deck and haunch was divided into seven and eleven elements for AASHTOP Type IV and AASHTO BT-72 girders for calculations of composite area, moment of inertia, non-composite area and temperature variations. The nominal values taken for modulus of elasticity of girder and deck are 5422 ksi and 3834 ksi respectively. The nominal value taken for modulus of rupture is 0.678 ksi and the nominal value taken for area of prestressing steel is 0.217 in^2.

Using AASHTO temperature gradient's mean and standard deviation change in temperatures for each section were also generated. The commercially available software MATLAB was used to generate the random variables with the appropriate distribution types; i.e., normal or lognormal. Monte Carlo simulation was then conducted using the generated random values to calculate probability of cracking of the girder based on the limit state function (Eq. 6.6). Algorithm used for this study on MATLAB is as shown in Figure 6.7.

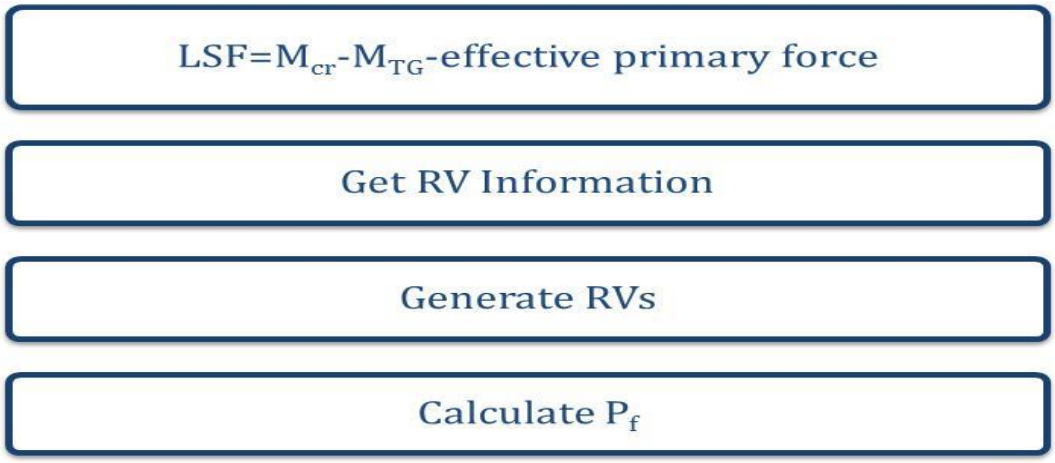

Figure 6.7 Flow-Chart for Monte-Carlo Simulation

Matlab code was first written without introducing the random variables to check the validity of the code for both conditions i.e. with web and without web. The results from this code were compared with mRESTRAINT results, which turn out to be identical. Hence, the code was

validated. Table 6.2 and Table 6.3 shows the calculated values for the variables from the Matlab code. After the validation of the Matlab code, it was then modified to generate the random variables and to calculate the probability of cracking. Figure 6.8 shows the temperature profile generated from Matlab.

Table 6.2 AASHTO Type IV girder properties (With Web and wihout web)

Properties	With Web	Without Web
Area of non-composite section	789 in^2	605 in^2
Area of composite section	1326.4 in^2	1142.4 in^2
Moment of inertia of non-composite section	258110 in^4	246430 in^4
Moment of inertia of composite section	649530 in^4	618900 in^4
Cracking Moment	1313.1 kips-ft	1226.8 kips-ft
Restraint Moment due to Thermal gradient	538.87 kips-ft	538.87 kips-ft
Final Moment	784.76 kips-ft	784.76 kips-ft

Table 6.3 AASHTO BT-72 girder properties (With Web and Without web)

Properties	With Web	Without Web
Area of non-composite section	767 in^2	443 in^2
Area of composite section	1335 in^2	1011.5 in^2
Moment of inertia of non-composite section	544890 in^4	465730 in^4
Moment of inertia of composite section	1087500 in^4	893410 in^4
Cracking Moment	1610.80 kips-ft	1327.8 kips-ft
Restraint Moment due to Thermal gradient	612.22 kips-ft	612.22 kips-ft
Final Moment	896 kips-ft	896 kips-ft

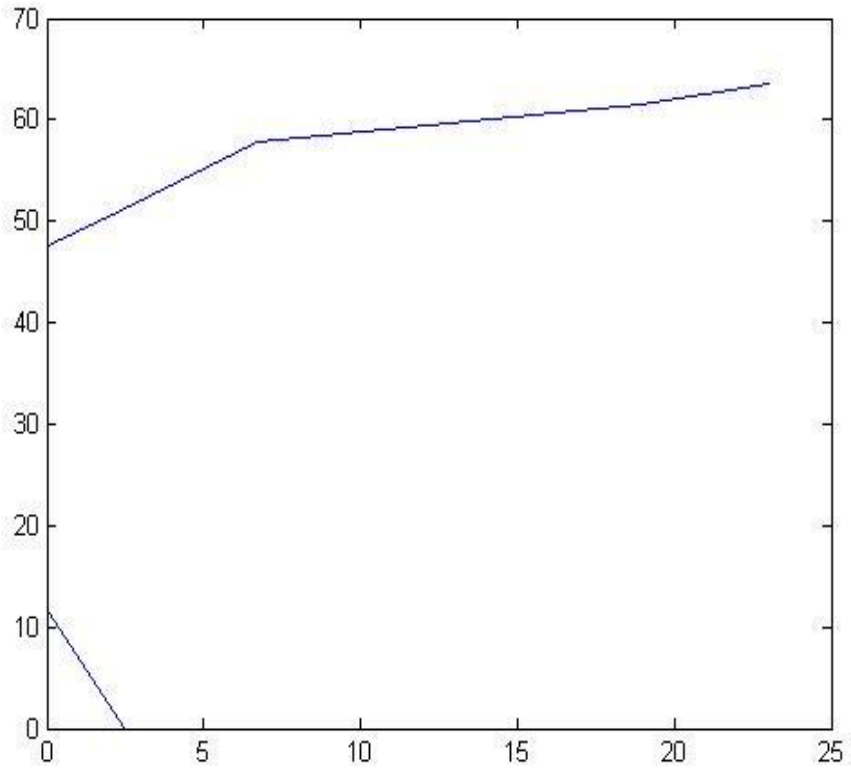

Figure 6.8 Temperature profile generated from Matlab

6.7 Results

First different numbers of simulations were used to calculate the probability of cracking. The numbers used for calculating the probability of cracking are 1000, 10000, 100000 and 1000000. Histograms for random variables were plotted when the maximum number of simulations was used i.e. 1000000. Figure 6.7 shows the histograms. Table 6.6 through Table 6.9 present the results that were obtained from the Monte-Carlo simulations for different number of simulations with the consideration of web and without the consideration of web respectively for AASHTO Type IV and AASHTO BT-72 girders.

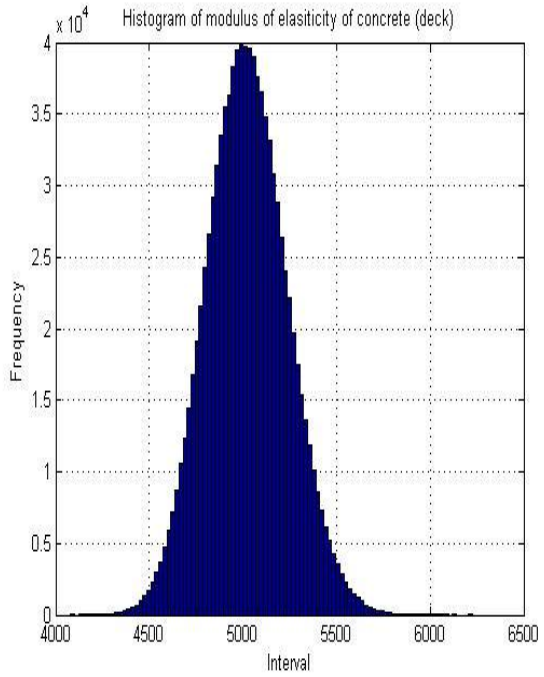

(a) Modulus of elasticity of concrete (deck)

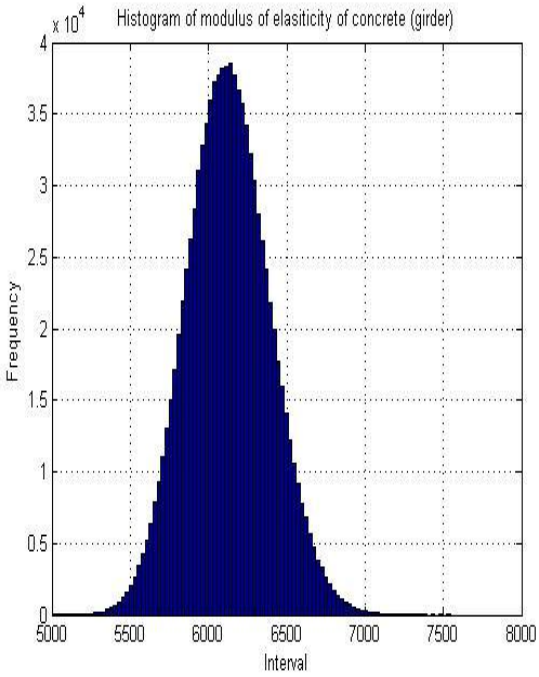

(b) Modulus of elasticity of concrete (girder)

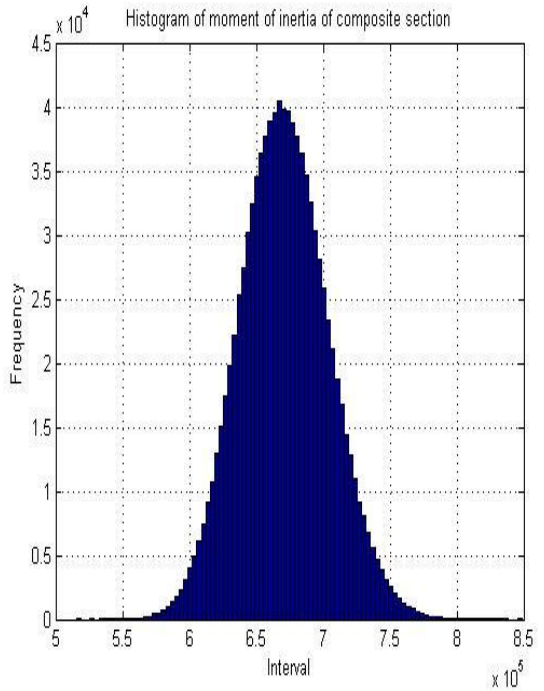

(d) Moment of inertia of composite section

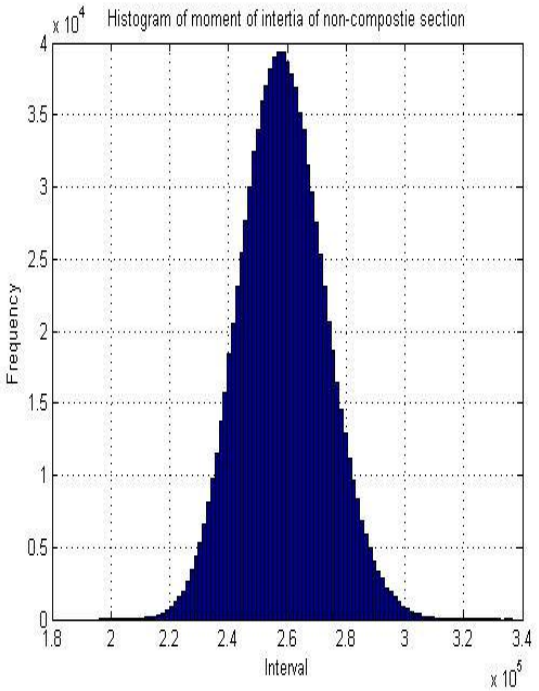

(e) Moment of inertia of non-composite section

Figure 6.9 Histogram of Random Variables

Figure 6.9 continued

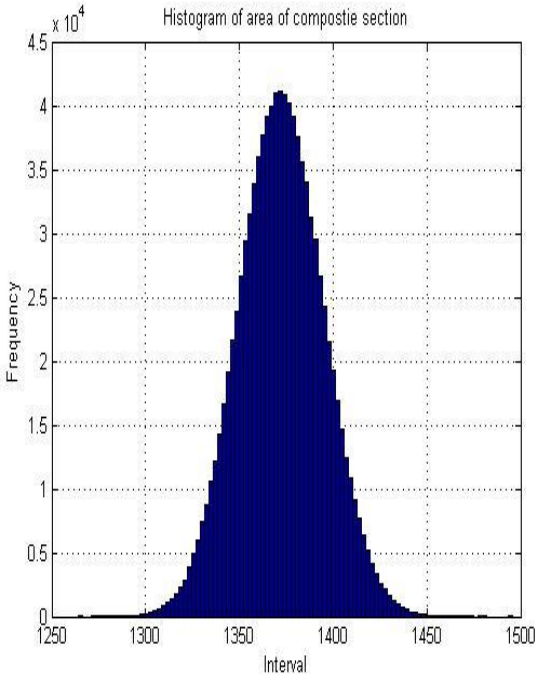

(f) Area of composite section

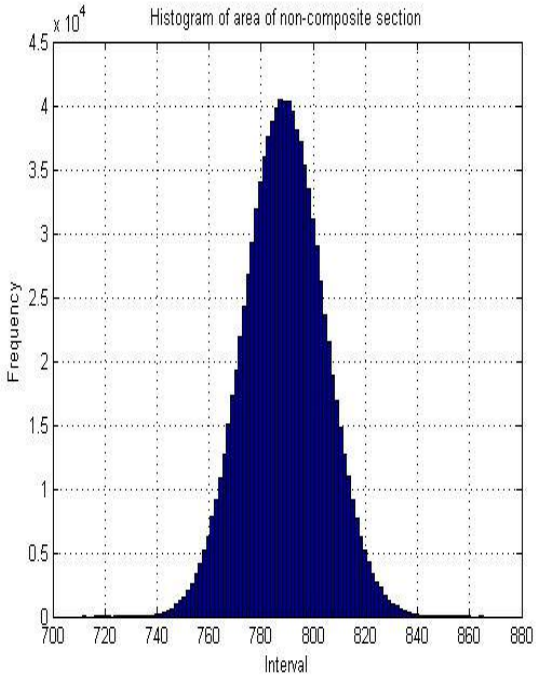

(g) Area of non-composite section

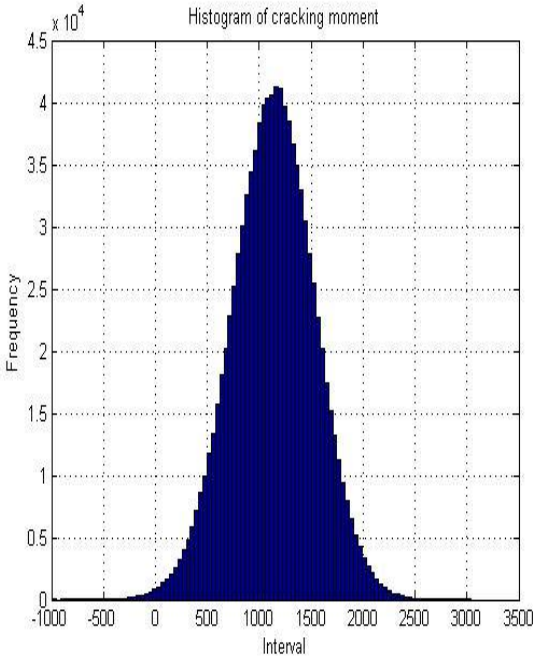

(h) Cracking Moment

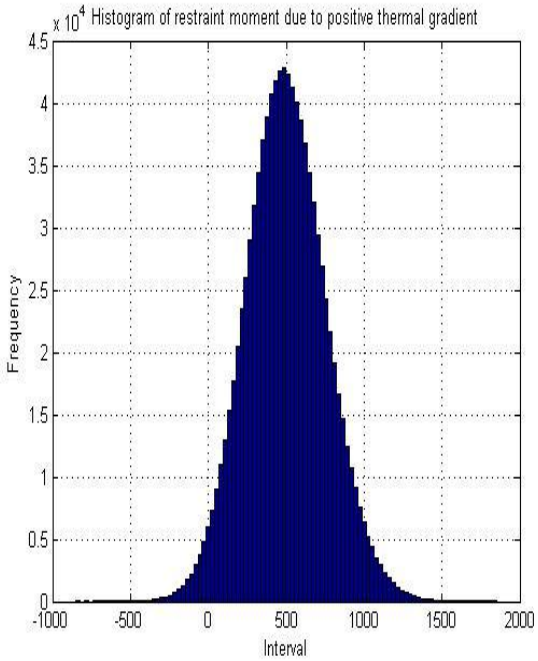

(i)Restraint moment due to thermal gradient

Table 6.4 shows the probability of cracking for AASHTO Type – IV girders with the consideration of web and without the consideration of web.

Table 6.4 Results from Monte-Carlo Simulation for AASHTO TYPE - IV(With and WithotWeb)

Number of simulation	Probability of Cracking (With Web)	Probability of Cracking (Without Web)
1,000	0.1450	0.2660
10,000	0.1460	0.2670
100,000	0.1510	0.2753
1,000000	0.1586	0.2850

From Table 6.4, it can be seen that the probabilities of cracking of girder when the number of simulations are 1,000, 10,000, 100,000 and 1,000000 are 14.5%, 14.6%, 15.1% and 15.86% respectively. From these results, it can be analyzed that the probabilities obtained from different number of the selected number of simulations are close to each other. Therefore, it can be concluded that the probability of failure of AASHTO girder Type IV is somewhere around 14.5% to 15.86% when the web part is considered.

If the web is ignored, the probabilities of cracking of girder increase by about 67% to 26.6%, 26.7%, 27.53% and 28.5% from 1,000, 10,000, 100,000 and 1,000000 simulations respectively.

It can be observed from Table 6.4 that the probabilities of failure of AASHTO girder Type IV increased when the web part is not considered. This is because of the fact that the size of the girder has been reduced when the web part is not considered. This means the variables like area, moment of inertia, and cracking moment also get reduced thus increasing the change of cracking.

Therefore, the probability of cracking of girder gets increased when the web part is not considered. Table 6.5 presents the results for AASHTO BT-72 girders.

Table 6.5 Results from Monte-Carlo Simulation for AASHTO BT-72 (With and without web)

Number of simulations	Probability of Cracking (With Web)	Probability of Cracking (Without Web)
1,000	0 .229	0 .474
10,000	0 .2354	0 .4743
100,000	0.2383	0.479
1,000000	0 .2395	0 .4797

Table 6.5 presents the probabilities of cracking of AASHTO BT-72 girder when the numbers of simulations for Monte-Carlo simulations are 1,000, 10,000, 100,000 and 1,000000. As seen it table, the probabilities of cracking are 22.9%, 23.54%, 23.83% and 23.95% for the respective number of simulations.

The probabilities of cracking of AASHTO Type BT-72 girder without considering its web part is presented in Table 6.5 as well. If the web is ignored, the probabilities of cracking of girder are 47.4%, 47.43%, 47.9% and 47.97% from 1,000, 10,000, 100,000 and 1,000000 simulations respectively. Therefore, it can be concluded that the probability of cracking for AASHTO BT072 is somewhere around 47.4% to 48%.

From Table 6.5, it can be noticed that the probabilities of cracking for AASHTO BT-72 increased when the web part is not considered like AASHTO Type-IV girder.

It can be seen from the results for both girders that probabilities of cracking increases when there is increase in size of girder. From Table 6.4 – Table 6.5, it can be seen the rise in probabilities of cracking when AASHTO BT-72 girder is used rather than AASHTO Type-IV

girder. Therefore, it can be concluded that AASHTO BT-72 is more critical to cracking than AASHTO Type-I. From, the results it can also be concluded that the girders like AASHTO Type I, II and III which are smaller in size than AASHTO Type IV and AASHTO BT-72 will probably have less probabilities of cracking than both girders. Other girders like AASHTO Type V and VI whose size are later than AASHTO Type IV and smaller than AASHTO BT-72 will have probabilities of cracking more than AASHTO Type IV and smaller than AASHTO BT-72.

The results presented in Table 6.4 and Table 6.5 are the probabilities of cracking of the girder when only the restraint moment developed due to the thermal gradient is considered. If restraint moment developed due to creep and shrinkage is also added then the probability of cracking should be higher than the value it is observed in Table 6.4 and Table 6.5 because of the increase in the positive restraint moment.

The probabilities of cracking were also calculated for aforementioned bridges with the same girders and same span lengths and properties. It should be noted that the study was done including the effect of creep, shrinkage and thermal gradient combined. This study was done to get an idea about the probabilities of failure when the effect of creep and shrinkage are combined. Since there will be increase in final restraint moment when the effect of creep and shrinkage is added to the thermal gradient. Thus, an increase in probabilities of cracking was already expected.

It should be noted that this study is not done in details rather it is done assuming that restraint moment due to creep and shrinkage follows a normal distribution. Nominal value for restraint moment due to creep and shrinkage is taken from the mRESTRAINT program for the 2 span bridge case with AASHTO Type-IV and AASHTO BT-72 girders respectively. It was assumed that girder age was 28 days when the continuity was established and ratio of diaphragm to girder

stiffness is taken as 1:1. The nominal values are 944.8 kips-ft and 1348.3 kips-ft for AASHTO Type-IV and AASHTO BT-72 respectively.

The value of bias for restraint moment due to creep and shrinkage was assumed to be 1.0 and coefficient of variation as assumed to be 10%, 20%, 30%, 40% and 50%. Probabilities was cracking was calculated for 1000, 10000, 100000 and 1000000 number of simulations for all five coefficient of variation.

Since there is an addition of a new term in the calculation so now the limit state function becomes:

$$g() = M_{cr} - M_{TG} - \text{effective primary stress effect} - M_{(CR+SH)} \quad (6.7)$$

where, $M_{(CR+SH)}$ is the restraint moment due to creep and shrinkage.

Table 6.6 and Table 6.7 shows the probabilities of cracking of AASHTO Type-IV girder with and without web when restraint moment due to creep, shrinkage and thermal gradient is considered and when the coefficient of variance is equal to 0.1, 0.2, 0.3, 0.4 and 0.5 respectively.

Table 6.6 Results from Monte-Carlo simulations for AASHTO Type-IV (with web)

Number of simulations	Probability of cracking (with web)				
	Coefficient of variation				
	0.1	0.2	0.3	0.4	0.5
1000	0.6750	0.6680	0.6520	0.6420	0.6350
10000	0.6831	0.6768	0.6651	0.6647	0.6549
100000	0.6866	0.6737	0.6641	0.6507	0.6497
1000000	0.6817	0.6712	0.6609	0.6468	0.6412

Table 6.7 Results from Monte-Carlo simulations for AASHTO Type-IV (without web)

Number of simulations	Probability of cracking (without web)				
	Coefficient of variation				
	0.1	0.2	0.3	0.4	0.5
1000	0.8090	0.7840	0.7780	0.7550	0.7430
10000	0.7912	0.7755	0.7623	0.7603	0.7511
100000	0.7906	0.7833	0.7619	0.7544	0.7475
1000000	0.7902	0.7772	0.7585	0.7476	0.7398

It can be noticed the rise in probability of failure if compared to the probabilities when only effect of thermal gradient was considered.

If the web is ignored then the probability of cracking is ranges from 73.98% to 80.90% for when the coefficient of variation ranges from 10% to 20%.

Similarly, Table 6.8 and Table 6.9 shows the probabilities of cracking of AASHTO Type BT-72 girder when the effect due to creep, shrinkage and thermal gradient is considered. Table 6.8 shows the probability when the web is considered and Table 6.9 shows when web is not considered.

Table 6.8 Results from Monte-Carlo simulations for AASHTO Type BT-72 (with web)

Number of simulations	Probability of cracking (with web)				
	Coefficient of variation				
	10%	20%	30%	40%	50%
1000	0.8100	0.7950	0.7860	0.7760	0.7520
10000	0.8090	0.7905	0.7834	0.7680	0.7494
100000	0.8029	0.7951	0.7813	0.7658	0.7433
1000000	0.8030	0.7945	0.7820	0.7644	0.7429

Table 6.9 Results from Monte-Carlo simulations for AASHTO Type BT-72 (without web)

Number of simulations	Probability of cracking (with web)				
	Coefficient of variation				
	10%	20%	30%	40%	50%
1000	0.9320	0.9180	0.8960	0.8730	0.8670
10000	0.9261	0.9181	0.9040	0.8897	0.8797
100000	0.9260	0.9176	0.9023	0.8856	0.8781
1000000	0.6817	0.6712	0.6609	0.6468	0.6412

7 CONCLUSIONS AND RECOMMENDATIONS

7.1 Summary

In this research the methods for calculating restraint moments are first presented. A modified version of the program RESTRAINT was developed and used to calculate the restraint moments in representative bridges. RESTRAINT was developed as a part of NCHRP project 12-53 (Miller et al. 2004). Originally, the software was limited only to symmetric span length configurations and was not capable of accounting for existence of continuity diaphragm. The program also used the same prestressing strand data for all spans regardless of span length. Chebole (2011) modified the software to add these capabilities and eliminate the aforementioned limitations. The new version of RESTRAINT was called mRESTRAINT. The modifications included the following:

1) Numbers of span was increased to five.
2) Modeling of diaphragm (length and stiffness) was added.
3) Prestressing strand data can be changed for each span length.
4) Custom girder dimensions were added.

For this research, mRESTRAINT was further modified to include the effect of the thermal gradient on the final restraint moment resulting in the current version of mRESTRAINT-TG. Previously, mRESTRAINT calculated the restraint moment due to creep and shrinkage only. The new version can calculate the restraint moment due to creep, shrinkage and thermal gradient combined. The modified version of the mRESTRAINT program can calculate the restraint moment up to 5 spans including or excluding the effect of the diaphragm length and stiffness. The new set of modifications for mRESTRAINT are:

1) The haunch was not accounted for in either RESTRAINT or mRESTRAINT while calculating the composite girder properties. Therefore, it was added in mRESTRAINT-TG.
2) The effect of thermal gradient implemented in the modified version of mRESTRAINT-TG. Users can choose whether they would like to include thermal gradient in the final restraint moment calculations or not. Both positive thermal gradient and negative thermal gradient can be calculated for standard AASHTO LRFD gradients or user defined gradients.
3) New user forms and modules were added to make the software more user friendly and easy to use.
4) The graphical output of results was modified to show the effect of the positive and negative thermal gradient on the plot.

A parametric study was carried out for 120 bridge girder (cases) using the mRESTRAINT-TG. The parametric study was carried out to understand the effect of wide range of variables (number of spans, span lengths ratio, diaphragm stiffness ratios and age of continuity) on the development of the restraint moments in continuous prestressed bridges. Results from the parametric study were used to study the girder age at continuity and to calculate the optimum age of the girder such that an allowable restraint moment is not exceeded.

Finally, a reliability study was carried out on two sample bridges and the probability of cracking for those girders was calculated. For both girders, probability of cracking was calculated with the web and without the web. This study was done based on the cracking of the girders due to thermal gradient only.

7.2 Conclusion Drawn From the Study

Based on results from this study the following conclusions are made:

1) Temperature gradients can cause large restraint moments in continuous bridges.
2) Positive restraint moment may cause cracking in the diaphragm and/or girder ends.
3) The development of the restraint moment is directly affected by the span lengths ratio, girder age at continuity and the diaphragm to girder stiffness ratio.
4) It was found that restraint moment when the girder age at continuity is early (e.g. 28 days) is comparatively higher than the restraint moment when the girder age at continuity is later like 180 days. For example, 1552.6 kips-ft of restraint moment was observed for 2S-0.5R-0.05D-28C when the girder age was 20,000 days and for same girder age 283.9 kips-ft of restraint moment was observed for 2S-0.5R-0.05D-28C.
5) A single value for girder age such as the 90-day recommended in NCHRP Report 519 is not suitable for all bridge configurations. Therefore, the recommended 90-day girder age should be reevaluated.
6) The optimum girder ages calculated in this research to sustain an allowable restraint moment value after 20000 days vary from 68 days to 140 days. The corresponding numbers after 7500 days vary from 66 days to 135 days. Similarly, the optimum girder ages calculated for an allowable restraint moment values after 20000 days vary from 72 to 162 days and 68 to 156 days after 7500 days for 3-span bridge case.
7) The contribution of thermal gradient and creep and shrinkage individually to the total restraint moment show that the effect of the thermal gradient is as high as that of creep and shrinkage and should not be ignored.

8) The reliability study showed that the probability of cracking at girder ends is high (68% - 93%). Therefore, thermal gradient effects should be considered in the design.
9) The reliability also showed that the probability of cracking is affected by girder size i.e., probability of cracking increases with increase in size. This may be due to the fact that larger girders are more susceptible to thermal gradient effects.

7.3 Recommendations

From this study, it was found that the thermal gradient can cause the development of large restraint moments in continuous bridges which may lead to cracking in the diaphragm and girder ends. Therefore, it is recommended that the temperature gradient effects be considered in the design of continuous bridges.

The new mRESTRAINT-TG program is capable of calculating primary and secondary thermal stresses in continuous girder bridges. Therefore, it is recommended that thermal effects to be studied using this program or any other structural analysis tools with thermal analysis capabilities. It is recommended that the reliability study be further developed to account for the uncertainties in creep and shrinkage based on data from the literature rather than the assumed values.

REFERENCES

1. American Association of State Highway and Transportation Officials (AASHTO), (2004). "AASHTO LRFD Bridge Design Specifications – Third Edition w/ 2005 & 2006 Interims". Washington, D.C.

2. American Association of State Highway and Transportation Officials (AASHTO), (1994). "AASHTO LRFD Bridge Design Specifications – First Edition". Washington, D.C.

3. American Association of State Highway and Transportation Officials (AASHTO), (1998). "AASHTO Guide Specifications for Design and Construction of Segmental Concrete Bridges". Washington, D.C.

4. American Concrete Institute (ACI) (2002). "Prediction of Creep, Shrinkage, and Temperature Effects in Concrete Structures" *ACI 209R-92.* Farmington Hills, Michigan.

5. American Concrete Institute (ACI) (2002). "Report on Factors Affecting Shrinkage and Creep of hardened Concrete" *ACI 209R-05.* Farmington Hills, Michigan.

6. Bazant, Z. P. (1975). "Theory of Creep and Shrinkage in Concrete Structures: A précis of recent development." *Mechanics Today.* American Academy of Mechanics, 2. Pergamon, New York.

7. Bellevue, L., and Towell, P. J. (2000). "Creep and shrinkage effects in segmental bridges." ASCE, Advanced Technology in Structural Engineering. 1-8.

8. Benboudjema, F., Meftah, F., Sellier, A., Heinfling, G. and Torrenti, J.M. (2001), "A Basic Creep Model for Concrete Subjected to Multiaxial Loads." 1, 161-168.

9. Chao, P. (2014). "Random Variables." *Introduction to Random Variables*, < http://www.stat.purdue.edu/~panc/teaching/2014spring/slides/08_Random_Variables_slide.pdf > (April 04, 2014).

10. Collins, M., Mitchell, D., Felber, A., and Kuchma, D. *RESPONSE V 1.0*, (computer software), Provided with Prestressed Concrete Strucutures. Prentice Hall: Englewood Cliffs, NJ.

11. Chebole, V.S.M. (2011). "Long-Term Continuity Moment Assessment in Prestressed Concrete Girder Bridges." M.S. thesis, Louisiana State Univ., Baton Rouge, LA.

12. Dimmerling, A., Miller, R. A., Reid, C., Mirmiran, A., Hastak, M., and Baseheart, T. M. (2005). "Connections Between Simply Supported Concrete Beams Made Continuous – Results of NCHRP Project 12-53." *Transportation Research Record*: *Journal of the TransportationResearch Board*, No. 1928. Transportation Research Board of the National Academies,Washington, D.C.

13. Elbadry, M., Ghali, A. (1986). “Thermal Stresses and Cracking of Concrete Bridges.” *Journal of ACI,* 83(6), 1001-1009.

14. Fanourakis, G.C., and Ballim, Y. (2006). “An assessment of the accuracy of nine design models for predicting creep in concrete.” *Journal of the South African Institution of Civil Engineerig*, 48(4), 2-8.

15. Freyermuth, C.L., (1969), “Design of Continuous Highway Bridges with Precast, Prestressed Concrete Girders.” *Journal of Prestressed Concrete Institute,* 14(2).

16. Fu, Y.F., Wong, Y.L., Poon, C.S., and Tang, C.A. (2006). “Numerical tests of thermal cracking induced by temperature gradient in cement-based composites under thermal loads.” *Journal of Cement & Concrete Composites,* 29(2007), 103-116.

17. Gopalakrishnan, K. S., Neville, A. M., and Ghali, A. (1969). "Creep Poisson's ratio of concrete under multiaxial compression.” *Journal of American Concrete Institute*, 66(12), 1008-1019.

18. Hossain, T. (2012). “Global and Local Performance of Prestressed Girder Bridges with Positive Moment Continuity Detail.” Doctoral dissertation, Louisiana State Univ., Baton Rouge, LA.

19. Hossain, T., and Okeil, A. (2014). “Force Transfer Mechanism in Positive Moment Continuity Details for Prestressed Concrete Girder Bridges.”

20. Hueste, M.B.D., Chompreda, P., Trejo, D., Cline, D.B.H., and Keating, P.B. (2004). “Mechanical Properties of High-Strength Concrete for Prestressed Members.” *Journal of American Concrete Institute,* 101(4), 457-466.

21. Imbsen, A., Vandershaf, D.E., Schamber, R. A., and Nutt, R.V. (1985). “Thermal Effects in Concrete Bridge Superstructures.” National Cooperative Highway Research Program Report276, Washington, D.C.

22. Kim, W.S. (2008). “Load and Resistance Factor Design for Integral Abutment Bridges.” Doctoral dissertation, The Pennsylvania State Univ., University Park, PA.

23. Krauss, P.D., and Rogalla, E.A. (1996). “Transverse Cracking in Newly Constructed Bridge Decks.” *NationalCooperative Highway Research Program.*

24. Mattock, A.H., and Kaar, P.H. (1960). “Continuous Precast-Prestressed Concrete Bridges.” *Journal of PCA Research and Development Laboratories,* 2(5), 51-78.

25. Mattock, A.H. (1961). “Precast-Prestressed Concrete Bridges 5: Creep and Shrinkage Studies.” *Journal of PCA Research and Development Laboratories,* 3(2), 32-66.

26. Ma, Z., Huo, X., Tadros, M. K., and Baishya, M. (1998) "Restraint Moments in Precast/Prestressed Concrete Continuous Bridges," *Journal of Prestressed Concrete Institute*, 43(6), 40-57.

27. MacGregor, J. G., and Wright, J. K. (2005). Reinforced Concrete: Mechanics and Design 4th Edition. Pearson Prentice Hall, New Jersey.

28. Menn, C. (1986). "Prestressed Concrete Bridges." Springer-Berlag, Wein. Vienna. Austria.

29. McDonagh, M.D., and Hinkley, K.B. (2003). "Resolving Restraint Moments: Designing for Continuity in Precast Prestressed Concrete Girder Bridges." *Journal of Prestressed Concrete Institute*, July-Aug 2003, 104-119.

30. Miller, R. A., Castrodale, R., Mirmiran, A., and Hastak, M. (2004). "NCHRP Report 519:Connection of simple-span precast concrete girders for continuity." *NCHRP REPORT 519.* Transportation Research Board of The National Academies.

31. Mirmiran, A., Kulkarni, S., Castrodale, R., Miller, R., and Hastak, M. (2001). "Nonlinear continuity analysis of precast, prestressed concrete girders with cast-in-place decks and diaphragms." *Journal of Prestressed Concrete Institute*, 46(5), 60-64.

32. Nawy G. E. (2009). "Prestressd Concrete - A Fundamental Approach – Fifth Edition." Pearson. Upper Saddle River, NJ.

33. Nilson, A. H. (1987). "Design of Prestressed Concrete – Second Edition." John Wiley and Sons. New York, NY.

34. NBI. (2014). "Deficient Bridges by State and Highway System." URL= http://www.fhwa.dot.gov/bridge/nbi.cfm (July 10, 2014).

35. Nowak, A.S., and Collins, K.R. (2000). "Reliability of Structures." The McGraw-Hill Companies, Inc. USA.

36. Oesterle, R. G., Glikin, J. D., and Larson, S. C. (1989). "NCHRP Report 322: Design of Precast Prestressed Bridge Girders Made Continuous." National Cooperative Highway Research Program Report 322, National Research Council, Washington, D.C.

37. Okeil, A. M., El-Tawil, S., and Shahawy, M. (2002) "Flexural Reliability of RC Bridge Girders Strengthened with CFRP Laminates," *Journal of Bridge Engineering*, ASCE, 7(5), 290-299.

38. Orton, S.L., Kwon, O.S., and Hazlett, T. (2012). "Statistical Distribution of Bridge Resistance Using Updated Material Parameters." *Journal of Bridge Engineering*, 17(3), 462-469.

39. Ozbolt, J., and Reinhardt, H.W. (2001). "Sustained Loading Strength of Concrete Modelled by Creep-Cracking Interaction." *Otto-Graf-Journal,* 12, 9-20.

40. Priestley, M. J. N. (1984). "Analysis of Temperature Gradient Effects." *Proceedings of RILEM-ACI Symposium on LTO of Structure Budapest.*

41. Priestley, M. J. N. (1978). "Design of Concrete Bridges for Temperature Gradients." *Journal of American Concrete Institute,* 75(5), 209-217.

42. Peterman, R. J., and Ramirez, J. A. (1998). "Restraint moments in bridges with full-span prestressed concrete form panels." *Journal of Prestressed Concrete Institute,* 43(1), 54-73.

43. Seth Segura, Thermal Stresses Induced by Temperature Gradient in Concrete Structures, 2011.

44. Shushkewich, K.W. (1998). "Design of Segmental Bridges for Thermal Gradient." *Journal of Prestressed Concrete Institute,* August 2008, 120-137.

45. Tanesi, J., Kutay, M.E., Abbas, A., and Meininger, R. (2007). "Effect of Coefficient of Thermal Expansion Test Variability on Concrete Pavement Performance as Predicted by Mechanistic-Empirical Pavement Design Guide" *Journal of the Transportation Research Board,* 2020, 40-44.

46. Wollman, R., Carin, L., Breen, J.E. and Cawrse, J. (2002). "Measurement of Thermal Gradients and their Effects on Segmental Concrete Bridge." *Journal of Bridge Engineering,* 43(4), 120-137.

VITA

Sushovan Ghimire was born in March, 1987, in Lalitpur, Nepal. He completed his high school and undergraduate from Kathmandu, Nepal. He graduated from Purbanchal University Biratanagar, Nepal in 2009 earning his Bachelor of Science in Civil Engineering discipline. He was admitted to Louisiana State University Agriculture and Mechanical College, Department of Civil and Environmental Engineering in August 2012. He worked as a graduate research assistant under Dr. Ayman Okeil and completed his research successfully in May 2014. He is expected to receive a Master of Science in Civil Engineering degree in summer of 2014.